

**SEISMIC RESPONSE OF RC BUILDINGS
INCORPORATING EFFECTIVE SOIL ISOLATION WITH
SUSTAINABLE MATERIALS**

Thesis

Submitted in partial fulfilment of the requirements for the degree of
DOCTOR OF PHILOSOPHY

by

SREYA M V



DEPARTMENT OF CIVIL ENGINEERING
NATIONAL INSTITUTE OF TECHNOLOGY KARNATAKA
SURATHKAL, MANGALORE - 575 025

August, 2022

**SEISMIC RESPONSE OF RC BUILDINGS
INCORPORATING EFFECTIVE SOIL ISOLATION WITH
SUSTAINABLE MATERIALS**

Thesis

Submitted in partial fulfilment of the requirements for the degree of

DOCTOR OF PHILOSOPHY

By

SREYA M V

Reg.No. 187031CV011

Research Supervisors

Prof. B.R. JAYALEKSHMI

&

Prof. KATTA VENKATARAMANA



DEPARTMENT OF CIVIL ENGINEERING
NATIONAL INSTITUTE OF TECHNOLOGY KARNATAKA
SURATHKAL, MANGALORE – 575025

August, 2022

DECLARATION

by the Ph.D. Research Scholar

I hereby *declare* that the Research Thesis entitled “**Seismic Response of RC Buildings Incorporating Effective Soil Isolation with Sustainable Materials**” which is being submitted to the **National Institute of Technology Karnataka, Surathkal** in partial fulfilment of the requirements for the award of the Degree of **Doctor of Philosophy in Civil Engineering**, is a *bonafide report of the research work carried out by me*. The material contained in this Research Thesis has not been submitted to any University or Institution for the award of any degree.

Sreya
12/08/22

SREYA M V

(Register No: 187031CV011)

Department of Civil Engineering

Place: NITK Surathkal

Date: 12-08-2022

CERTIFICATE

This is to *certify* that the Research Thesis entitled “**Seismic Response of RC Buildings Incorporating Effective Soil Isolation with Sustainable Materials**” submitted by **SREYA M V**, (Register Number: **187031CV011**) as the record of the research work carried out by her, is *accepted as the Research Thesis submission* in partial fulfilment of the requirements for the award of the degree of **Doctor of Philosophy**.


10/08/2022

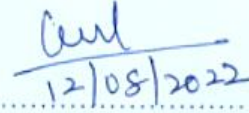
Prof. B.R. Jayalekshmi

Research Guide

Professor

Department of Civil Engineering

NITK, Surathkal


12/08/2022

Prof. Katta Venkataramana

Research Guide

Professor

Department of Civil Engineering

NITK, Surathkal



Chairman-DRPC

Department of Civil Engineering

NITK, Surathkal



Chairman (DRPC)
Department of Civil Engineering
National Institute of Technology Karnataka, Surathkal
Mangalore - 575 025, Karnataka, INDIA

Thank You God Almighty for Everything

Dedicated to My Family

ACKNOWLEDGEMENT

It gives me immense pleasure and a great sense of satisfaction to express my heartfelt gratitude to those who made this dissertation possible.

I would like to express my sincere gratitude to my research supervisor Dr. B.R. Jayalekshmi, Professor, Department of Civil Engineering, National Institute of Technology Karnataka for her guidance, patience, encouragement and support. She has been a constant source of inspiration throughout this journey. I take this great opportunity to express my sincere gratitude and heartfelt thanks to my guide Dr. Katta Venkataramana, Professor, Department of Civil Engineering, National Institute of Technology Karnataka, Surathkal also for his advice, support, expert guidance and constant encouragement for the successful completion of the research work. I am deeply indebted to my guides for their warmth, care, affection, and meaningful life lessons. I feel proud to have worked under their guidance.

I wish to thank my research progress assessment committee (RPAC) members Dr. A U Ravishankar, Professor, Dept. of Civil Engineering and Dr. Varija K, Assistant Professor, Dept. of Water Resources and Ocean Engineering for their constructive feedback and guidance.

I am grateful to the Head of Department of Civil Engineering, Dr. B R Jayalekshmi, who is also my research supervisor for all the support and help in spite of her busy schedule. I am thankful to Dr. Swaminathan K, former Head of the Department of Civil Engineering, for his timely help. I also take this opportunity to thank Prof. Varghese George, former Head of Department during my coursework term for his kind support.

I take this opportunity to thank all the faculty and staff of the Department of Civil Engineering, NITK, Surathkal. I thank National Institute of Technology Karnataka

(NITK), Surathkal for giving me an opportunity for undertaking research and the Ministry of Education, Government of India for awarding research scholarship.

I would like to express my gratitude to Dr. Sankar N, Professor, Department of Civil Engineering, NIT Calicut for the constant support and guidance during the period of research work.

I wish to thank all my dear friends for their care, support, valuable input and constant encouragement. My stay at NITK, Surathkal was delightful and memorable in the company of my fellow researchers who never let me know that I am away from home. I am indebted to all of them.

I thank my parents for their affection, love, care, constant support, and encouragement in the successful completion of my research work.

Sreya M V

Abstract

Seismic isolation is a technique that has been adopted worldwide to protect building structures, non-structural components, and content from the damaging effects of earthquake-induced ground shaking. Geotechnical seismic isolation is a kind of isolation technique that has recently emerged as a possible solution to reduce the effects of earthquakes. The present research investigates the effectiveness of different materials such as natural material (coir mat), elastomeric material (rubber mat) and polymer material (epoxy polystyrene, polyethylene foam) as a medium for soil isolation to limit seismic energy transfer and thus the dynamic response of buildings. Finite element analysis is carried out on low-rise reinforced concrete buildings, resting on raft foundation over reinforced soil subjected to various earthquake motions. Two kinds of soil, namely soft and stiff soil, are considered based on their flexibility to study the dynamic soil-structure interaction (DSSI) effects. The linear elastic as well as non-linear inelastic behavior have been assumed for the analysis of the integrated building-foundation-soil system. The nonlinear analysis is carried out by incorporating the material non-linearity in the soil and isolation materials. The response of SSI system subjected to ground motions corresponding to the elastic design spectrum for Zone III as per the IS code, El Centro earthquake (1940), Northridge earthquake (1994) and Chi-Chi earthquake (1999) is analysed. The results indicate that soil isolation provided by the coir mat substantially reduces the earthquake energy transmission to the superstructure compared to other isolation mats. The optimum values for the depth of embedment, width and thickness of the coir mat were analysed and identified as $B/18$, B and $B/36$ respectively from the parametric analysis of the soil-structure system, where, B is the width of foundation. The coir composites such as coir-rubber and coir-polymer foam are proposed to increase the durability of the coir mat by preventing coir mat from biodegradation.

Further, a pore water pressure analysis of soil bed also has been carried out in Cyclic 1D software and PLAXIS 3D software to study the efficacy of these materials to reduce

the excess pore water pressure generated in soil under earthquake loading. The isolation efficiency of reinforcement materials in reducing the excess pore water pressure generated in soil under different earthquake motions obtained is 75-82%, 71-80% and 67-72% with coir, coir-polymer and coir-rubber composites respectively. Among various isolation mats, the coir mat and coir-polymer foam composite mat are recommended as the efficient soilisolation medium, especially at soft soil sites.

Keywords: Finite element simulation, soil reinforcement, raft-foundation, seismic soil isolation-building system, soil-structure interaction, pore water pressure analysis

Contents

ABSTRACT	i
NOMENCLATURE	vii
LIST OF FIGURES	x
LIST OF TABLES	xiii
CHAPTER 1	1
INTRODUCTION	1
1.1 SEISMIC ISOLATION SYSTEMS.....	1
1.2 CLASSIFICATION OF SEISMIC ISOLATION SYSTEMS	2
1.2.1 Passive Control Systems	3
1.2.2 Active Control Systems	4
1.3 NEW SEISMIC ISOLATION METHODS	4
1.4 SIGNIFICANCE OF THE PRESENT WORK	5
1.4.1 Tyre chips.....	5
1.4.2 Polyethylene Foam.....	7
1.4.3 Epoxy Polystyrene Geofoam	7
1.4.4 Coir Mat	8
1.5 ORGANIZATION OF THESIS.....	9
CHAPTER 2	11
LITERATURE REVIEW	11
2.1 INTRODUCTION	11
2.2 EFFECT OF SOIL ISOLATION ON SEISMIC RESPONSES	11

2.2.1 Isolation Using Geosynthetic Materials.....	12
2.2.2 Isolation Using Tyres.....	12
2.2.3 Isolation using Geofoams.....	13
2.2.4 Isolation Using Coirs.....	14
2.2.5 Durability of Isolation Materials.....	16
2.2.6 Effects of Isolation Materials on Pore Water Pressure.....	17
2.2.7 Effects of Soil-Structure Interaction.....	18
2.3 LITERATURE SUMMARY.....	20
2.4 RESEARCH GAPS IDENTIFIED.....	21
2.5 OBJECTIVES.....	21
CHAPTER 3.....	23
METHODOLOGY.....	23
3.1 DESCRIPTION OF THE PROBLEM.....	23
3.2 PARAMETRIC STUDIES ON PLACEMENT OF COIR MAT IN SOIL.....	24
3.3 LINEAR AND NONLINEAR ANALYSIS OF ISOLATED SOIL-STRUCTURE SYSTEM.....	26
3.3.1 Idealization of Structure.....	26
3.3.2 Idealization of Infinite Soil.....	27
3.3.4 Idealization of Isolation Layer.....	29
3.3.5 Damping.....	31
3.3.6 Finite Element Modeling of The Soil-Structure System in ANSYS.....	31
3.3.7 Seismic Analysis.....	33

3.4 FINITE ELEMENT MODELING OF THE SOIL-STRUCTURE SYSTEM IN PLAXIS 3D.....	37
3.4.1 Calculation of Pore Water Pressure	38
CHAPTER 4	41
PARAMETRIC STUDIES ON THE PLACEMENT OF ISOLATION MATERIAL IN SOIL.....	41
4.1 PARAMETRIC STUDY ON PLACEMENT OF COIR MAT	41
4.1.1 Depth of Embedment of Coir Mat	41
4.1.2 Width of Coir mat	44
4.1.3 Thickness of Coir Mat.....	45
4.2 SUMMARY	47
CHAPTER 5	48
EFFECT OF SOIL FLEXIBILITY ON ISOLATED SOIL-STRUCTURE SYSTEM	48
5.1 GENERAL.....	48
5.2 EFFECT OF SOIL FLEXIBILITY	48
5.2.1 Roof Acceleration of Building.....	49
5.2.2 Contact Pressure at Raft-Soil Interface	55
5.2.3 Total and Differential Settlement at Soil-Raft Foundation Interface.....	59
5.2.4 Seismic Base Shear of Building.....	61
5.3 SUMMARY	63
CHAPTER 6	65
NONLINEAR ANALYSIS OF ISOLATED SOIL-STRUCTURE SYSTEM.....	65

6.1 GENERAL	65
6.2 ROOF ACCELERATION AND ROOF DEFLECTION OF BUILDING	65
6.3 INTERSTOREY DRIFT OF BUILDING	69
6.4 SEISMIC BASE SHEAR OF BUILDING	71
6.5 SHEAR FORCE OF BUILDING	72
6.6 SUMMARY	75
CHAPTER 7	77
PORE WATER PRESSURE ANALYSIS	77
7.1 GENERAL	77
7.2 MODELLING IN CYCLIC 1D	77
7.2.2 Pore Water Pressure Analysis in Cyclic 1D.....	78
7.3 PORE WATER PRESSURE ANALYSIS IN PLAXIS 3D.....	81
7.3.1 Excess Pore Water Pressure in Soil (P_{excess})	81
7.3.2 Shear Strain and Mobilized Shear Strength	86
7.3.3 Effective Confining Stress	93
7.4 SUMMARY	95
CHAPTER 8	97
CONCLUSION	97
PUBLICATIONS	99
REFERENCES	101

Nomenclature

3D-FEM	Three Dimensional Finite Element Method
A	Area of element on which the wave component acts
aARF	Acceleration amplitude reduction factor
b	Width of beam/column
B	Width of raft foundation
BCR	Bearing Capacity Ratio
C	Coir mat
CONTA	Contact element
C_p	Damping coefficient for perpendicular wave
C-PE₁	Coir-Polyethylene ₁ composite
C-PE₂	Coir-Polyethylene ₂ composite
C-RU	Coir-Rubber composite
C_s	Damping coefficient for shear wave
C-S_b	Coir-stiff soil
D	Depth of beam/column
dAPR	Deflection amplitude percentage reduction
E_c	Modulus of elasticity
EPS	Epoxy Polystyrene
EQ-1	IS Earthquake motions
EQ-2	Northridge Earthquake motions
EQ-3	El Centro Earthquake motions
EQ-4	Chi-Chi Earthquake motions
F'	Base shear ratio of building
F	Shear force at the base of the building
f_{ck}	Characteristic compressive strength of concrete
Fe 415	Grade of High Strength Deformed Steel Bar
FFT	Fast Fourier Transform

GRMs	Gravel Rubber Mixtures
HDPE	High Density Poly Ethylene
h_w	Groundwater head
IF	Improvement factor
IS	Indian Standard
l	Length of beam/column
L	Length of the raft foundation.
M25	Grade of concrete
NEHRP	National Earthquake Hazards Reduction Program
P_{active}	Active pore pressure
PE	Polyethylene
PE₁	Polyethylene foam with low stiffness
PE₂	Polyethylene foam with high stiffness
P_{excess}	Excess Pore Water Pressure in Soil
PGA	Peak Ground Acceleration
PP	Polypropylene
P_{steady}	Steady-state pore pressure
P_w	Pore water pressure
RC	Reinforced Concrete
RFc	Contact pressure reduction factor
RFs	Settlement reduction factors
RSM	Rubber Soil Mixtures
RU	Rubber mat
S₁	Soft soil
S₂	Stiff soil
S_{eff}	Effective saturation
SMC	Strong Motion CD-ROM
SOLSH190	Solid shell 190 element
SRC	Seismic response of conventional soil-structure system

SRI	Seismic response of isolated soil-structure system
SRMs	Sand Rubber Mixtures
SSI	Soil-Structure Interaction
t	Thickness of isolation mat
UR	Unreinforced soil
V_p	Perpendicular wave velocity
V_s	Shear wave velocity
W	Total weight of the building
w	Width of coir mat
z	Depth of embedment of coir mat
ρ	Mass density of the soil system
σ	Total stresses
σ'	Effective stress

List of Figures

Figure 1.1	Schematic description of a seismic isolation system (Ho 2011)	1
Figure 1.2	A typical laminated rubber bearing (Ho 2011).....	2
Figure 1.3	Seismic isolation by (a) mechanical devices (b) hydraulic dampers (Ho 2011)	3
Figure 1.4	(a) Active system used in Taipei 101 (b) Golden Globe of Taipei 101 (Ho 2011)	4
Figure 1.5	(a) Polyethylene foam (b) Tyre Chips	6
Figure 1.6	(a) EPS geofom (b) Coir mat	8
Figure 3. 1	Configuration of the soil-structure system	26
Figure 3. 2	Photographic view of; (a) coir mat (b) rubber mat (c) polyethylene foam and (d) polystyrene foam	32
Figure 3.3	Input acceleration time history of (a) IS (EQ-1) (b) Northridge (EQ-2) (c) El Centro (EQ-3) and (d) Chi-chi (EQ-4) earthquake motions	34
Figure 4. 1	The effect of variation in the depth of embedment of coir mat	43
Figure 4.2	The effect of variation in the width of embedment of coir mat.....	45
Figure 4.3	The effect of variation in the thickness of embedment of coir mat	46
Figure 5.1	Time history of roof acceleration in building with fixed base and building on (a) soft soil (S_1) and (b) stiff soil (S_2)	50
Figure 5.2	Roof acceleration for soil reinforced with different isolation mats (a) El Centro- soft soil (b) El Centro-stiff soil (c) IS-soft soil (d) IS-stiff soil.....	51
Figure 5.3	Roof acceleration time history plot of the soil-structure system for unreinforced and reinforced cases of S_1 and S_2 type soil with coir mat	53

Figure 5.4	Reduction factor for contact pressure distribution along the length of raft foundation under different input motions.....	57
Figure 5.5	Vertical settlement along the length of raft foundation in soft soil	58
Figure 5.6	Reduction factor for total settlement along the length of raft foundation under (a) El Centro-soft soil (b) El Centro-stiff soil (c) IS-soft soil (d) IS-stiff soil.	61
Figure 5.7	Seismic base shear of building on reinforced soil with various isolation mats	63
Figure 6.1	(a) Slip deformation of isolation mats under different earthquake input motions (b) roof acceleration (c) roof deflection (soil reinforced with different isolation mats) under different earthquake input motions	67
Figure 6.2	Roof acceleration time history plot of the soil-structure system for the rigid base, unreinforced and coir mat reinforced soil bases; (a) EQ-1 (b) EQ-2 (c) EQ-3 (d) EQ-4 input motions.....	68
Figure 6.3	Roof deflection time history plot of the soil-structure system for the rigid base, unreinforced and coir mat reinforced soil base under (a) EQ-1 (a) EQ-2 (b) EQ-3 (c) EQ-4 input motions.....	69
Figure 6.4	Interstorey drift of the building for the rigid, unreinforced and reinforced soil base under (a) EQ-1 (b) EQ-2 (c) EQ-3 (d) EQ-4 input motions.....	70
Figure 6.5	(a) Seismic base shear ratio of building on soil reinforced with various mats (b) Percentage reduction in the seismic base shear ratio (c) percentage reduction in seismic shear force of building on reinforced soil with various mats	71
Figure 6.6	Storey shear force of the building for the rigid, unreinforced and reinforced soil base under (a) EQ-1 (b) EQ-2 (c) EQ-3 (d) EQ-4 input motions.....	73
Figure 6.7	Shear force-time history plot of the building for the unreinforced and coir mat reinforced soil base under (a) EQ-1 (b) EQ-2 (c) EQ-3 (d) EQ-4 input motions	74
Figure 7.1	Variation in excess pore water pressure with the depth of soil domain for unreinforced (UR) and soil reinforcement with C, C-PE ₃ and C-RU mats....	79

Figure 7.2 Excess pore pressure-time history plot of the soil domain at different depths below the ground level under El Centro input motion	80
Figure 7.3 Excess pore pressure-time history plot of the soil domain at different depths below the ground level under Northridge input motion.....	81
Figure 7.4 Percentage reduction in excess pore pressure in the soil domain near the ground surface for isolated soil base under El Centro and Northridge input motion. 81	
Figure 7.5 Excess pore water pressure-time history in soil for reinforced and unreinforced cases under different earthquake input motions; (a) EQ-1, (b) EQ-2, (c) EQ-3, (d) EQ-4	83
Figure 7.6 Excess pore water pressure distribution in the soil at its central portion below the superstructure for coir mat reinforced and unreinforced cases of soil excited under; (a)-(b) EQ-1 (c)-(d) EQ-2 (e)-(f) EQ-3 (g)-(h) EQ-4.....	85
Figure 7.7 Shear strain time history in the soil for reinforced and unreinforced cases under different earthquake input motions; (a) EQ-1, (b) EQ-2, (c) EQ-3, (d) EQ-4.	87
Figure 7.8 Mobilized shear strength in the soil at its central portion below the superstructure excited under EQ-1 input motion.....	89
Figure 7.9 Mobilized shear strength in the soil at its central portion below the superstructure excited under EQ-2 input motion.....	90
Figure 7.10 Mobilised shear strength in the soil at its central portion below the superstructure excited under EQ-3 input motion.....	92
Figure 7.11 Mobilized shear strength in the soil at its central portion below the superstructure excited under EQ-4 input motion.....	93
Figure 7.12 Effective confining stress time history in the soil for reinforced and unreinforced cases under; (a) EQ-1, (b) EQ-2, (c) EQ-3, (d) EQ-4	95

List of Tables

Table 3. 1 Details of parametric study on placement of coir mat	26
Table 3. 2 Properties of soil for linear analysis to study the effect of soil flexibility.....	28
Table 3. 3 Properties of building components and isolation materials for linear analysis	29
Table 3. 4 Properties of soil and reinforcement materials for nonlinear analysis.....	30
Table 3. 5 Fourier amplitude and specific energy density of input motion	35
Table 5.1 Natural frequencies of the soil-structure system.....	49
Table 5.2 Percentage reduction in differential settlement of raft foundation	60
Table 5.3 Base shear ratio for buildings on a fixed base and flexible base	62

Chapter 1

INTRODUCTION

1.1 SEISMIC ISOLATION SYSTEMS

A seismic isolation system is defined as a flexible or sliding interface placed between a structure and its foundation to decouple horizontal ground motions from horizontal structure motions, hence limiting earthquake damage to the structure and its contents (Fig 1.1). Various mechanisms for seismic isolation, such as rollers and sand layers, have been developed over the past century.

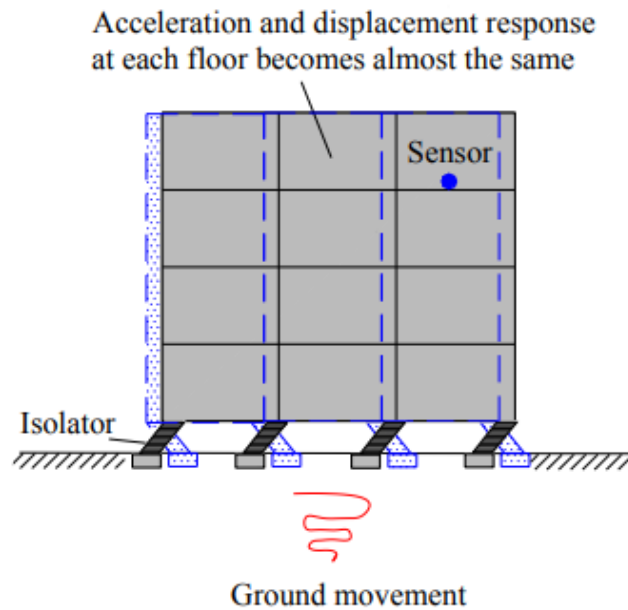


Figure 1.1 Schematic description of a seismic isolation system (Ho 2011)

Rubber material has been employed as an isolation device over the last few decades. Laminated rubber bearings (Fig. 1.2) are presently the most widely used system due to the strength necessary in the vertical direction to support the full weight of the structure.

Another form of seismic isolation approach is a sliding system (Fig. 1.2), such as the friction-pendulum system, which limits the transfer of shear across the isolation interface. Because of the considerable implementation costs, these basic isolation approaches are now only used in structures with critical or expensive contents.

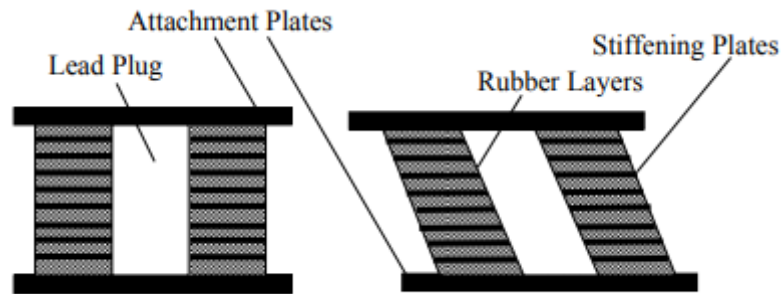


Figure 1.2 A typical laminated rubber bearing (Ho 2011)

1.2 CLASSIFICATION OF SEISMIC ISOLATION SYSTEMS

The seismic isolation devices that are installed in buildings are typically energy dissipation mechanisms. The devices can be classified in two ways: according to their position in the building or according to their working principles. Isolators can be classified into two kinds based on their location in the building. These are external and internal isolators. External devices are positioned outside the building and are typically inserted into the foundations. The mechanisms that dissipate energy are the internal type devices. All response control systems are classed as active or passive based on their functioning principles.

1.2.1 Passive Control Systems

Passive control systems do not need extra energy to work and are merely activated by earthquake motion. The system is intended to dissipate a major percentage of the seismic energy in unique components. There are two types of passive control systems as below:

Seismic Isolation Systems

These systems decouple ground motion and prevent the structure from earthquake energy absorption. The entire superstructure should be supported by discrete isolators, with seismic energy released by their sliding (along with damping for some specialised devices). The superstructures isolated by this system function more like rigid bodies. An example of using mechanical devices for seismic isolation is shown in Fig. 1.3(a).



(a)



(b)

Figure 1.3 Seismic isolation by (a) mechanical devices (b) hydraulic dampers (Ho 2011)

Passive Energy Dissipation Systems

This type of system provides additional damping to the structure, reducing the structural responses under earthquake vibrations significantly. This can be achieved by using viscous dampers such as visco-elastic dampers, hydraulic dampers, or lead extrusion systems, as well as hysteretic dampers such as metallic yielding or shape-memory alloy devices. When this method is deployed, deformations concentrated in the energy

dissipation equipment will dampen much of the earthquake energy. The illustration in Fig. 1.3(b) depicts a structure isolated by hydraulic dampers.

1.2.2 Active Control Systems

This type of system protects the structure against the destructive impacts of earthquakes by exerting forces on the structure to counter-balance the earthquake-induced forces. These are "active" systems as they require an energy supply and computer-controlled actuators to operate customised braces and/or tuned mass dampers. This approach was used in the construction of Taiwan's Taipei101, one of the world's highest skyscrapers. A schematic explanation for the application of active control system is shown in Fig. 1.4(a), along with a representation of the weight employed to counter-balance the earthquake-induced forces in Fig. 1.4(b).

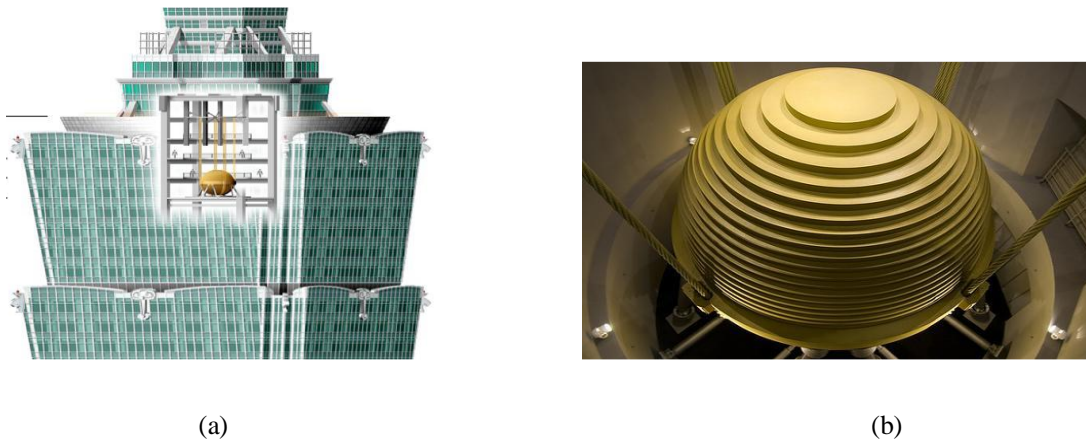


Figure 1.4 (a) Active system used in Taipei 101 (b) Golden Globe of Taipei 101 (Ho 2011)

1.3 NEW SEISMIC ISOLATION METHODS

In past few years, novel seismic isolation methods have been presented in which the flexible or sliding interface comes into direct contact with geological sediments and the isolation mechanism is primarily based on geotechnics. There are two distinct but

promising approaches. Smooth synthetic liners have been suggested beneath foundations or between soil layers to dissipate seismic energy through sliding (Yegian and Catan 2004; Yegian and Kadakal 2004), and rubber-soil mixes (RSM) have been proposed around building foundations to absorb seismic energy and perform a function similar to that of a cushion (Tsang 2007). The low cost of these seismic isolation methods may benefit countries where resources and technology are insufficient to mitigate earthquakes using well-developed but costly procedures.

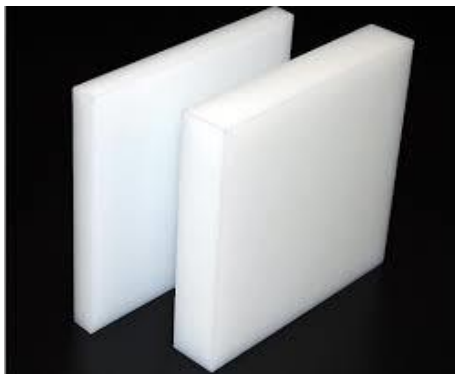
1.4 SIGNIFICANCE OF THE PRESENT WORK

Finding high-quality alternative geomaterials is a difficult task in geotechnical engineering. Non-traditional lightweight materials are the solution in such cases. The geomaterials used in this study for the soil isolation technique are polymer foam, natural rubber mat coir mat and composites of coir mat.

1.4.1 Tyre chips

Tyre usage has increased significantly in recent decades as the number of automobiles has increased drastically. Since the disposal of scrap tyres has become a serious matter, finding an effective way to reuse these discarded scrap tyres has become a difficult task. Tyre chips commonly range in size from 25mm x 50mm to 100mm x 450mm, with 50mm x 75mm being the most common. Many academics have explored the index and engineering properties of tyre chips, and study in this subject is still ongoing. However, the work of Tatlısoz et al. (1998), among others, provides more in-depth and fundamental knowledge about the engineering properties of tyre chips-soil mixes for a variety of mixing ratios. The compression characteristic of tyre chips-soil mixes under cyclic loading for seismic isolation is the most important result given in the cited article. Because of their high porosity and rubber content, they claim that tyre chips are extremely compressive. The majority of plastic deformation occurs during the first cycle of cyclic loading, and the rate of plastic strain accumulation decreases with each load cycle without a substantial change in the ultimate strain corresponding to the ultimate stress. Tsang (2011) proposes

an earthquake mitigation strategy that includes the use of rubber-soil mixes (RSM) provided around the foundation of low-to-medium-rise buildings to dissipate seismic energy and function as a cushion. A variety of numerical simulations using various recorded ground motions have shown that the proposed method is valid. The performance indicators such as peak and RMS values of the horizontal acceleration at the roof and foundation, as well as the first-floor inter-story drift were examined. On average, a 40-60% reduction in seismic response was obtained, and the findings were demonstrated to be particularly sensitive to variations in RSM layer thickness (Tsang 2011). The new idea of soil isolation is to reinforce the rubber mat as a vibration isolation material by considering the benefits of rubber shown by the previous studies.



(a)



(b)

Figure 1.5 (a) Polyethylene foam (b) Tyre Chips

The combination of sand and tyre chips helps strengthen the soil, both under static and dynamic loads. Shear strength is a significant parameter in certain studies (Tatlisoz et al. 1998) at the soil-tyre interface. The research on the compressive strength of tyre chips (Pincus et al. 1994) reveals that it is very compressible because of the porosity and rubber content. Further, rubber has been used as mats under railway embankment ballast for isolation (Indraratna et al. 1998). They observed that the rubber-stabilized (reinforced with a rubber mat), highly rigid substratum ballast can significantly reduce the settlement and degradation in the ballast. A reduction of 5-10% in the lateral plastic strain and a reduction

of 10-20% in the vertical plastic strain is observed in this study (Indraratna et al. 1998). Due to its high damping efficiency, the mat of rubber substantially absorbs the vibration energy to protect the structure above it.

1.4.2 Polyethylene Foam

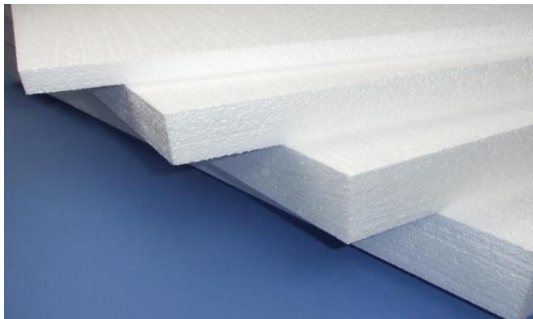
Several researchers have investigated the feasibility of the use of polyethylene fibers or strips in soil (Orman 1994; Abu-Hejleh et al. 2000; Piva et al. 2014; Meguid and Khan 2019). Polyethylene is made up of extremely long chains of ethylene, which all align in the same direction and derives strength largely from the length of each molecule (chain). The extremely long polymer chains enable load transfer by strengthening intermolecular interactions. Polyethylene fibers are manufactured in a gel spinning process. The high molecular weight gives polyethylene a unique combination of high impact strength, low coefficient of friction, and abrasion resistance. The results of a building model placed on a polyethylene liner demonstrate the proper capacity of the liner to act as an energy-absorbing medium, with which the seismic response of building can be significantly reduced (Narjabadifam and Chavoshi 2018).

1.4.3 Epoxy Polystyrene Geofam

Rather than replacing soil fill, the goal of epoxy polystyrene (EPS) geofam is to overcome technical issues. The block weight ranges from 0.11 kN/m³ to 0.40 kN/m³. When compared to traditional fill materials in geotechnical engineering, its density is very less (approximately 100 times less) (Fig. 1.6). Geofam has a lifespan of 70 to 100 years. Clay or silt has a bearing capacity equal to the compressive strength of EPS, that is 100 kPa. The use of EPS saves overall construction costs since it is simple to handle during construction, frequently without the need for special equipment, and is not affected by weather conditions. Furthermore, EPS geofam can be easily cut and moulded on the work place, controlling work requirements. Manufacturers and suppliers of EPS geofam can be found all around, mostly in North America. Expanded polystyrene is produced in two stages using a moulded bead method. To fulfil the needs of particular works, EPS geofam

is manufactured in blocks that may be carved into a number of shapes and sizes, as well as a range of compressive resistances. It can be produced as a material to offer the appropriate compressive resistance. The density of EPS geof foam is adjusted during the manufacturing process, giving it an excellent, ultra-lightweight fill material that considerably lowers stress on supporting subgrade layer. The smaller load can help to prevent settlements and increase stability against bearing and slope failures. The physical property criteria of EPS Geof foam are specified in ASTM D6817.

The application of geof foam in various construction activities is in high demand in India due to the rapid development of the construction sector and the ongoing need for eco-friendly and cost-effective building materials.



(a)



(b)

Figure 1.6 (a) EPS geof foam (b) Coir mat

1.4.4 Coir Mat

Coir is a natural fibre also known as coconut fibre, made from a coconut's husk and is used to make a variety of products, including brushes, mattresses, doormats, and floor mats. The fibrous layer coir is present between hard interior shell and its outer covering of coir. Brown coir (produced from ripe coconut) is also used in upholstery padding, sacking, and horticulture. White coir is extracted from unripe coconuts and used to make finer brushes, string, rope, and fishing nets. Coir characteristics are less affected by wet conditions than those of other rigid fibers. Since coconut fibre is a natural source,

several researchers have been studying it. Furthermore, coconut debris is discarded in landfills, causing environmental issues because this substance, although natural, takes time to decompose. Natural fibres, such as coconut fibers, have become industrially appealing because to its low cost, wide availability, and desired mechanical characteristics for particular applications, such as panels, ceilings, partition boards, and automobile components.

The total global coir fibre production is approximately 250,000 tonnes. The coir fibre sector is very important in several poor countries. In India, mostly the coastal region of Kerala state, 60% of the entire world supply of white coir fibre is produced. Sri Lanka accounts for 36% of global brown fibre output. Over 50% of the coir fibre produced around the world each year is used in the countries of origin, primarily India. Every year, India and Sri Lanka manufacture 90% of the world coir production. Sri Lanka continues to be the world's leading exporter of coir fibre and coir fiber-based products.

The current study intends to utilise the abovementioned materials as seismic isolators to reduce seismic energy transferred to the superstructure. The background and concepts of geotechnical soil isolation techniques will be presented in the following sections.

1.5 ORGANIZATION OF THESIS

The research outcome of the set objectives with the overall content is presented into eight chapters of the thesis. The content of each chapter is described as follows:

Chapter 1: This chapter gives general introduction and a brief overview of the different types of seismic isolation techniques existing in detail.

Chapter 2: A brief summary of literature focusing on research carried out related to soil isolation techniques for multistorey buildings is presented. An attempt has been made to identify the improvements made in isolation materials adopted for the soil isolation and study of isolation efficiency of soil reinforcement materials to reduce the seismic response

of buildings through the years. The research gaps have been identified. The research objectives are listed here.

Chapter 3: This chapter deals with the methodology followed in the study towards the fulfillment of the objectives set forth. It gives the details of the idealization of the soil-structure models and the analysis carried out.

Chapter 4: The chapter discusses various parameters affecting the placement of coir mat in soil by considering four-bay five storey buildings.

Chapter 5: Linear analysis of the soil-structure system is carried out and explained in this chapter.

Chapter 6: This chapter is devoted to nonlinear analysis of soil-structure system.

Chapter 7: This chapter explains the studies carried out on pore water pressure generated in soil under seismic loading as well as the seismic responses of building from the analysis carried out in PLAXIS software.

Chapter 8: This chapter summarizes main outcomes of this research. The significant conclusions are listed, highlighting the importance of consideration of natural material for soil isolation.

Chapter 2

LITERATURE REVIEW

2.1 INTRODUCTION

While conducting a detailed literature survey regarding the soil isolation techniques, it is found that different materials like tyre chips, geosynthetics, etc are used as vibration-isolating materials. Initially, researchers (Yegian et al. 1995; Yegian and Catan 2004) examined the benefit of using a geosynthetic reinforced soil isolation device to lower seismic responses of the superstructure. Yegian and Lahlaf (1994) investigated the dynamic shear strength property of nonwoven geotextile and geomembrane materials. Dynamic friction coefficients at the geomembrane and soil interfaces were also analyzed by Yegian and Lahlaf (1994). An experimental test on synthetic materials interfaces while those placed below the foundation to act as foundation isolation was performed by Yegian and Kadakal (2004). And from the information collected from the literature survey, it is possible to conclude that the existing materials like rubber chips, polymer foam and geosynthetics as well as the newly introduced material coir mat have a common character i.e., good vibration damping capacity. This chapter deals with an overview of the major research work carried out in this particular area where the detail of materials used in the previous studies, the analysis of the main parameters, findings obtained and finally the gap in literature is also added.

2.2 EFFECT OF SOIL ISOLATION ON SEISMIC RESPONSES

Soil isolation is a method of strengthening the soil with certain vibration-isolating materials (geotechnical isolation) or providing vibration isolators in the construction (structural isolation). The beginning and early improvement of seismic isolation have been given by researchers (Makris and Chang 2000). Different soil isolation materials in

different forms were used for soil isolation techniques. The scrap tyres are good isolation materials used in numerous civil engineering applications such as slope stabilization, vibration isolation, retaining structures, road construction, ground erosion control, etc.

2.2.1 Isolation Using Geosynthetic Materials

The basic strategies of isolation with particular emphasis and a summary of other innovations developed worldwide for structural mitigation of earthquake forces were reported in 'the state of the art review of base structure isolation systems' (Negusseyio 2008). The geotechnical base isolation system has been defined earlier by some researchers (Guler and Enunlu 2009; Nanda et al. 2012; Patil and Reddy 2012; Srilatha et al. 2016; Kolathayar 2019). They proposed the use of mixtures for low-cost seismic isolation by means of geosynthetic materials. Several soil reinforcement studies with geosynthetics for static and dynamic loads were reported (Nanda et al. 2017; Kou and Shukla 2019). The concept of geotechnical isolation includes a sliding mechanism with a low frictional coefficient by providing seismic isolation materials to dissipate seismic energy before it enters the superstructures. From the numerical analysis carried out (Nanda et al. 2017) to evaluate the efficacy of the seismic isolation system based on geosynthetic reinforcement below the foundation, it was reported that the absolute acceleration at roof level was reduced by up to 40%. The experimental studies by the shake table test have also been done (Nanda et al. 2017) by providing geotextiles and geomembranes as a base isolation system at the plinth level of a brick masonry building.

2.2.2 Isolation Using Tyres

Recycled rubber was used as an isolation medium to retain backfills provided with granular rubber soil mixtures; as an underground layer, it is used to mitigate the phenomenon of liquefaction or even as an isolation layer for structures. The studies derived from the numerical analysis have demonstrated promising results in using recycled rubber (Tsang 2007) as seismic isolation material in the soil.

Sand/rubber mixtures (SRMs) and gravel/rubber mixtures (GRMs) provide potentially vibration-attenuation material for the mitigation of earthquake loads in infrastructures. The scrap tyres are used in different civil engineering applications like slope stabilization, vibration isolation, retaining structures, road construction, ground erosion control, etc. The combination of sand and tyre shreds helps strengthen the soil, both under static and dynamic loads. Further, rubber has been used as mats under railway embankment ballast for isolation (Nimbalkar and Indraratna 2016; Navaratnarajah and Indraratna 2017; Indraratna et al. 2019). It was revealed that due to its high damping efficiency, the mat of rubber would substantially absorb the vibration energy to protect the structure above it.

2.2.3 Isolation using Geofoms

Another soil reinforcement material used is geofom. Epoxy Polystyrene (EPS) is a kind of geofom having lightweight closed plastic cell foam used by Norweian engineers in 1965 as a thermally insulating material and was later used in 1972 to provide lightweight fill material for EPS blocks on the embankment built on soft soil. Plastic fibers and sheets are the major focus to improve and stabilize sandy soils, as fibre products are cost-competitive with other materials. The rigid plastic geofoms were used in the lightweight filling (Elragi 2006; Horvath 2008a, b) for soft-ground construction, slope stabilization, and wall or retaining walls isolation. Geofoms are also used for sub-grade isolation and foundational isolation for roads and runway applications. A thorough understanding of the compression and shear behavior of the geofom blocks, as well as the shear strength of the interface, is required for the successful design of composite systems like embankments and bridge approaches. At the New York State Route 23A site, using geofom to minimize the driving power of a slope was effective in stabilizing the slope (Jutkofsky et al. 2000). Since the treatment was completed in 1996, no slope movement has occurred. To allow for thermally-induced motions of the bridge superstructure without impacting the backfill, a thin compressible material was incorporated between the reinforced backfill and the integral bridge abutment wall. By January 2000, this construction was providing smooth

rides with no evidence of occurring normal bridge bump problem (Abu-Hejleh et al. 2000). The shear strength and sand ductility increased when waste HDPE strips added to subgrade soil (Choudhary et al. 2010; Shao et al. 2014). The effectiveness of the addition of high-density polyethylene strips to a subgrade soil of the pavement was examined. Waste HDPE strips added to soil in appropriate amounts significantly improved the strength and deformation behavior of subgrade soils. The angle of interface friction increases consistently as the density of geofabric material increased (Meguid and Khan 2019). Geofabric absorbs vibration energy and protects the structure when it was placed along with the sub-base fill materials (Aab et al. 2019; Moghaddas Tafreshi et al. 2021). However, the increased cost of these materials and the growing value of biodiversity led researchers to concentrate more on natural resources as an alternative to conventional products.

2.2.4 Isolation Using Coirs

Many natural materials in our surroundings can be used for seismic isolation purposes. Coir is a type of natural material in the form of fibers processed into mat forms. Coir is a fibrous coconut cover with a length of 50-350 mm approximately, and coir contains tannin, pectin, cellulose and a high amount of lignin. As the lignin content in the coir fibre is high, it is long-lasting compared to other fibers such as jute, sisal, etc. Coir is available in the form of fibers as well as a mat in industries. Even though geosynthetics can stabilize the soil, the coir fibre is used to do it because of various advantages; with a higher coefficient of friction between soil and coir fibre, it enhances soil reinforcement more efficiently than other reinforcement materials (Ghavami et al. 1999). Basic research in the application of coir as a reinforcement material began in the 1990s. Natural fibers such as coir were used in soil to increase their strength and decrease liquefaction (Boominathan and Hari. 2002; Keramatikerman et al. 2017). The coir fibre was more efficient at higher shear strains, where the shear modulus (G) is increased significantly by its contribution. However, the durability of the coir material is a concern. The durability can be improved by coating fibers with phenol and bitumen. Chemical treatment of reinforcement material is one method to enhance durability and mechanical

properties. Solani sand reinforced with a geogrid sheet, geosynthetic fibre, and natural coir fibre was tested for liquefaction resistance (Maheshwari et al. 2012). At 0.1g acceleration, a sand sample reinforced with 0.75 percent coir fibre increased its liquefaction resistance by 91%. The coconut fibre has been chemically treated with alkali and silane at different concentrations (Haque et al. 2012; Munirah Abdullah and Ahmad 2012; Kumar and Gupta 2016). They made composites of coir by reinforcing coir with polypropylene (PP) and polyethylene (PE). Chemical treatment increased the physical, mechanical, and thermal qualities of the manufactured components. Higher fibre loading resulted in improved mechanical properties of the resultant composites, while PP composites had better properties than PE composites. At the end of dynamic loading, there is a chance of stiffness degradation, but it is only about 30%, and stiffness remains the same after that (Perdana and Jamasri 2016). Coir fibre has 4-5 times the stiffness value of existing natural fibers such as sisal, bamboo, and so on. As a result, with this higher stiffness value already in place, the fibre can be used safely for seismic isolation in soil. The length of soil reinforced coir fibre is a factor studied because the long fibers have improved the resistance to liquefaction by limiting the interstitial pressures (Systra et al. 2016; Yang et al. 2016; Elif Orakoglu et al. 2017; Leng et al. 2017; Fardad Amini and Noorzad 2018; Karakan et al. 2018; Ziaie Moayed and Alibolandi 2018; Su et al. 2021; Talamkhani and Naeini 2021; Zwawi 2021). The inclusion of coir fibers increases the resistance to liquefaction in cohesive soils. The dynamic properties such as shear modulus and the damping efficiency of randomly distributed coir fiber-reinforced sand have been investigated (Talamkhani and Naeini 2021). The damping ratio increases as shear strain increases and decreased normalized shear modulus.

Furthermore, the location at which the isolation mats reinforce the soil, is a significant factor that affects the total efficiency to isolate the ground motion effects on structures. Studies on soil reinforcement using geosynthetic materials show that the different ways of reinforcing the same quantity of material cause different structural behavior. Researchers (Dash et al. 2004; Tafreshi and Dawson 2010; Piva et al. 2014; Srilatha et al. 2016; Solomon et al. 2017) indicated that the analysis of the placement

of geosynthetic materials in the soil is essential from the perspective of productivity and economy. The study on geocell enhanced soil reported a depth of placement of 1/10 times the base width, which shows the maximum performance to increase the bearing pressure of soil (Dash et al. 2004). From the experiment on circular footings, an optimum placement depth of geogrid was obtained as 1/20 times the foundation width. It is reported that the improvement factors were increased significantly for an embedment depth of $0-B/4$ from the foundation base (Piva et al. 2014) in geogrid reinforced soil. The variation in embedment depth values observed by different researchers may be due to the difference in soil form and the properties of reinforcing materials. The increased cost of geosynthetics and the growing value of biodiversity led researchers to concentrate more on natural resources as an alternative to conventional products. However, considering the amount of research in this area, very little evidence has been found in the parametric study of applying natural resources as soil isolation systems. The present research focuses on the parametric study on isolation mat in soil such as depth of placement, thickness and width and to obtain its optimum values for an effective reinforcement of soil.

2.2.5 Durability of Isolation Materials

In addition to the soil strengthening technique and the reinforcement location method mentioned above, the study of the durability of the material is also a significant factor to be considered. The experiments were conducted to study the effect of chemical treatment on fibers such as coconut, sisal, jute, and hibiscus cannabinus to analyze the tensile resistance and durability of natural fibers (Ramakrishna and Sundararajan 2005). Coconut fibers are 4-6 times more sustainable than other fibers and are used for; slope stabilization in railway embankments, protection of waterways, reinforcement of rural unpaved roads, sub-basis layer on highways, land reclamation, and the filtration in road drains, etc. (Ali 2010). Chemical treatment is a primary method for improving the longevity and mechanical characteristics of natural fibers. Coir was treated in a different medium such as alkalized, acidic, and neutral with benzene diazonium salt (Haque et al. 2012); as chemically processed, the hydrophilic groups in cellulose coir fibre were converted to

hydrophobic groups, which increases the durability of coir material. The water absorption capacity of coir fibre was between 130% and 180% better compared to other natural fibers and lasted for ten years (Hejazi et al. 2012). The earlier studies regarding the durability of coir fibre under dynamic load show that at the end of dynamic loading, there was a chance of degradation in the stiffness of the coir fibre, but that was around 30%, and after that stiffness remains the same (Perdana and Jamasri 2016). The coir fibre has 4-5 times the stiffness value compared to the existing natural fibers like sisal, bamboo, etc. Therefore, due to this higher value of stiffness, the fibre can be used safely for seismic isolation in soil. From these existing studies on the coir fibre, the idea of combining the coir material with other reinforcement-isolation material is developed. Geomembranes are good reinforcement materials that have proven higher isolation efficiency in earlier studies (Srilatha et al. 2016; Nguyen and Indraratna 2017; Moghaddas Tafreshi et al. 2021).

Also, polyethylene foam and rubber materials act as good isolation materials (Tatlisoz et al. 1998; Zarnani and Bathurst 2005; Elragi 2006; Tsang 2007). Therefore, the current work uses geomembrane, rubber and polyethylene foam as composite materials for the coir. The reinforced and unreinforced soil-structure models are developed by the finite element method; the seismic responses and the isolation efficiency of coir mat and coir composite mats are analyzed in detail.

2.2.6 Effects of Isolation Materials on Pore Water Pressure

An increase in excess pore water pressure causes liquefaction in soil. With its potential for damage, the high incidence of liquefaction during earthquakes is the main subject of earthquake engineering study. Some relevant papers summarized state-of-the-art discussions on liquefaction (Martin, P P; Seed 1982; Seed 1987; Sharma et al. 2018). The ASCE Specialist Session on "Liquefaction Problems in Geotechnical Engineering" addressed some of these articles. It is widely accepted that cyclic loading of the soil and the movement of seismic waves are the sources of the accumulation of pore water pressure in saturated sandy soil; when they are subjected to cyclic shear loading, the sandy soil compress and settles.

Pore pressures are the quantities that relate to the stress in the pores of the material. The pores in soil are usually filled with a mixture of water and air. Pore water pressure is the water pressure in pores of soil consisting of steady-state pore pressure and excess pore pressure. Excess pore water pressure results from undrained behavior and is affected by stress changes due to loading or unloading, sudden hydraulic condition changes, and consolidation. The shear stress on the soil would increase as there is an increase in the applied load until the maximum load at which the soil fails. This self-adjusting phenomenon is called stress mobilization. The amount of shear stress mobilized to resist the stress developed by the applied stress is called shear strength. Therefore, the term mobilized shear strength represents the stress that we use from the maximum available shear strength (mobilized shear strength=applied shear stress). From the analysis, mobilized shear strength is studied for unreinforced and reinforced soil cases. Soil reinforcement by isolation mats increase the mobilized shear strength since the shear stress passed to the soil-foundation interface reduces when a layer of isolation mats is placed at 1m below the foundation. Therefore, reduced shear stress/applied stress only reaches the soil-foundation interface.

2.2.7 Effects of Soil-Structure Interaction

The structural response to an earthquake is interconnected by three systems, such as; structure, foundation, and soil. Studying the soil-structure interaction is essential when seismic forces significantly impact the base movement compared with the free activity in the soil. Two fundamental approaches, namely direct method and substructure, are used to solve the soil-structure interaction (SSI) problems (Wolf and Song 2002). Many recent studies (Makris and Chang 2000) were utilized this method for the SSI analysis of complex structures using powerful computing efficiency in most modern computers. The direct SSI method is employed to model and analyze the entire soil structure in a single phase. In the substructure approach, the soil-structure system is divided into two substructures, the soil medium, and the structures. This method is based on the principle of superposition. One of the drawbacks of this method is that only linear systems can be analyzed. The main

advantage of the direct method also compared to the substructure method is that it can consider the nonlinear material behavior (Santoni et al. 2001; Majumder and Ghosh 2016). In this study, the SSI method was selected wherein the soil and structure are modeled together.

Many researchers have conducted raft foundation analysis by finite element methods (Shihada et al. 2012). The finite element method is found to be more accurate in the study of the design of raft foundations in loose sand (SaadEldin and El-Helloty 2014; Bhavikatti and Cholekar 2017). The type of soil in which the raft foundation rests has significance in its settlement behavior. Generally, there is a common design practice for dynamic loading, in which it is assumed that the building is fixed at its base. Still, in reality, the soil medium allows movement to some extent due to its property to deform. Buildings experience different earthquake loads and comply with diversity in the forms of soil conditions such as dense, medium, and soft soil.

Seismic waves can be affected by different soil properties when it passes the soil layer (Wang and Hao 2002). Lateral deflection in buildings varies with the change in soil property and zone increments (Bajaj et al. 2013). It was observed that the soil-structure interaction has an important effect on the structural responses due to flexibility in the soil. With the increase in soil flexibility, the importance of SSI becomes prominent. Therefore, in the current study the isolation efficiency of coir mat and coir composites are analyzed both in soft and stiff soil under different input motions. Three-dimensional finite element models of integrated building-raft-soil systems are developed and analyzed with and without a mechanism of soil isolation, incorporating the rigid and flexible bases of raft foundation. This study also aims to create a 3D-FE numerical model (in PLAXIS software) for simulating the performance of an isolation mat reinforced soil-structure system under different earthquake loading conditions to study the efficiency of coir mat, polymer foam, and rubber mat to isolate the pore water pressure generated in soil.

2.3 LITERATURE SUMMARY

From the literature survey, it is observed that different materials have been adopted for the soil reinforcement techniques in the previous studies. But the reinforcement materials that can act as isolation materials in soil for the absorption of earthquake energy for shallow foundations are not much discussed. Isolation materials were used in different civil engineering applications. The polymer materials especially epoxy polystyrene are used to strengthen the soil behind the retaining wall, slope stabilization, etc. When specified and properly installed, epoxy polystyrene is a long-lasting and permanent material. It will be effective for the period of any application, with no deficiency impacts expected over a 100-year life span. And since EPS is inert, it will not leach into underlying soil or underground water when buried. Another reason why EPS is an excellent material for construction is that it does not provide nutrients to insects, vermin, fungi, or bacteria. Because of the closed cell structure, the mechanical and thermal properties of EPS are unchanged by humidity and water absorption is kept to a minimum. EPS is simple to use, lightweight, waterproof, and has good cushioning properties. Lightweight construction materials have the advantage of being very easy to transport and are usually more environmental friendly than other heavier materials.

The application of polymer foams supports the shallow foundation for the structures, and its suitability as vibration absorbers has to be examined yet. The possibility of using low to high dense and stiff material is of great importance to study its effectiveness to act as isolation materials. From the previous studies on seismic soil isolation techniques it is realized that an analysis should be carried out using other forms of polymer foam, coir, and rubber materials. There are studies on the use of these materials, mainly in the form of fibers and strips. Since, the length of fibre helps to increase the isolation efficiency of the reinforcement materials, the current study proposes the application of reinforcing materials in their mat form. From the literature, it is observed that coir mats and coir composite mats are not used as the isolation material in soil for isolating the seismic response of multistorey structures and reducing the liquefaction in soil. There are so many studies existing to

increase the durability of fibers by treating them chemically. Combining the coir mat with other isolation mats is a novel technique introduced in the present study for better seismic response in RC buildings.

2.4 RESEARCH GAPS IDENTIFIED

- ❖ Some studies have reported the detrimental effect of SSI on buildings. But, limited research has been done on three-dimensional SSI analysis of buildings, including foundation-isolated soil systems.
- ❖ The increased cost of the conventional materials and the growing value of biodiversity open a way to concentrate more on natural resources as an alternative to conventional products.
- ❖ There are studies on the use of these materials, mainly in the form of fibers and strips. Since, the length of fibre helps increase the isolation efficiency of the reinforcement materials, there is a scope of doing research on effectiveness of isolation materials when those are applied in their mat form.
- ❖ There has been few research on the use of isolation materials to reduce pore water pressure development in soil under seismic loads.

2.5 OBJECTIVES

- (a) To study the seismic response of a building frame supported on raft foundation resting on a shallow depth of soil by numerical analysis and to investigate the parameters affecting the placement of isolation mat in soil
- (b) To analyse the effectiveness of coir mat, polymer foams, rubber mat and coir composites as a seismic vibration damper incorporating soil flexibility using linear and nonlinear analysis of reinforced soil-structure system.
- (c) To study the efficiency of coir mat, polymer foam and rubber mat to isolate the excess pore water pressure generated in soil under the earthquake loading.

Chapter 3

METHODOLOGY

3.1 DESCRIPTION OF THE PROBLEM

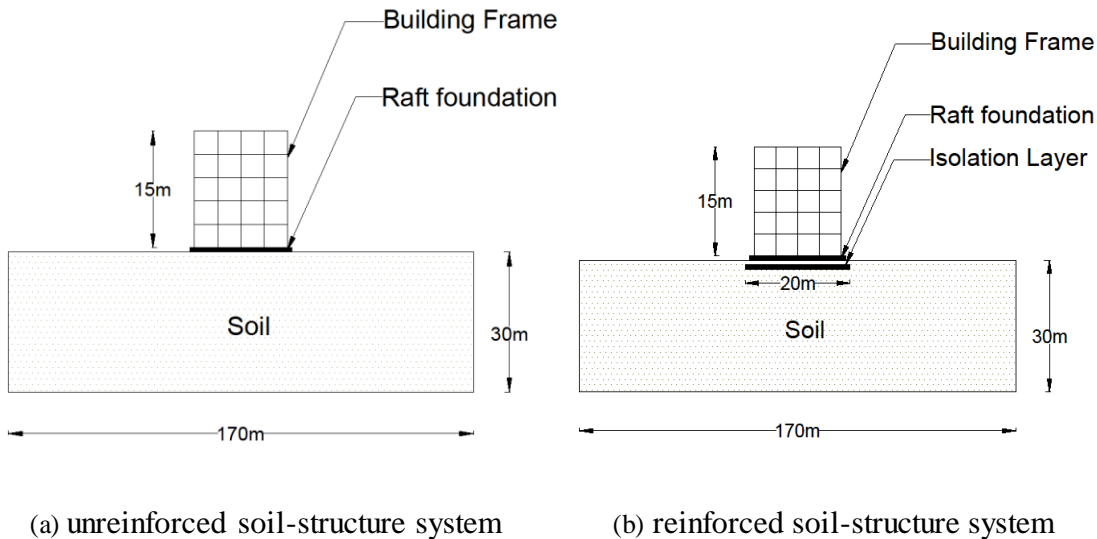
Studies on soil reinforcement with different materials are described in the literature (K.K.Babu 2007; Samia Sultana Mir et al. 2008; Tsang 2011; Aab *et al*, 2019; Moghaddas Tafreshi *et al*, 2021). The application of reinforcement materials for the soil isolation for shallow foundations is very few. Moreover, the application of reinforcement materials in their mat form for shallow foundations is not detailed in the literature. Studies (Talamkhani and Naeini 2021) reveal that the isolation efficiency of reinforcement fibers increases with the increase in the length of the fibre. Therefore, the concept of introducing the commonly available reinforcement materials in their mat form is addressed in this study. The current investigation consists of a response evaluation of multi-story buildings with raft foundations resting on different soil types and exposed to earthquake loads (Fig 3.1). The three-dimensional finite element model of the integrated building-foundation-soil system was analyzed based on the direct SSI method in which analysis of structure and soil is carried out in a single step. The seismic responses such as roof acceleration, roof deflection, interstorey drift, base shear ratio and shear force of building were assessed by incorporating the different base conditions for raft foundation. Also, the efficacy of soil isolation materials in reducing structural response was investigated.

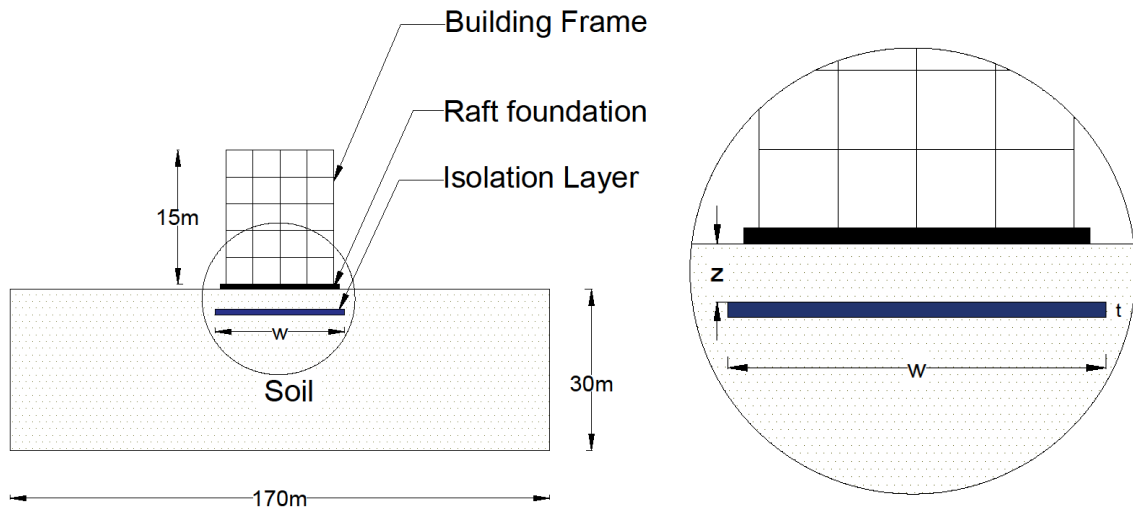
The efficacy of different isolation materials in the form of mats are identified based on various parameters. A detailed parametric analysis of coir mat was carried out. Coir mat was placed in the soil below the foundation for different widths, depths and thicknesses. The optimum values for the parameters were identified. PLAXIS 3D software was used to analyze the pore water pressure generated in the soil under the seismic loading. Different seismic responses were also analyzed for the soil reinforcement cases. The materials used

and how the finite element method was used to model and analyze different soil-structure systems for reinforced soil cases in different software are explained in this chapter.

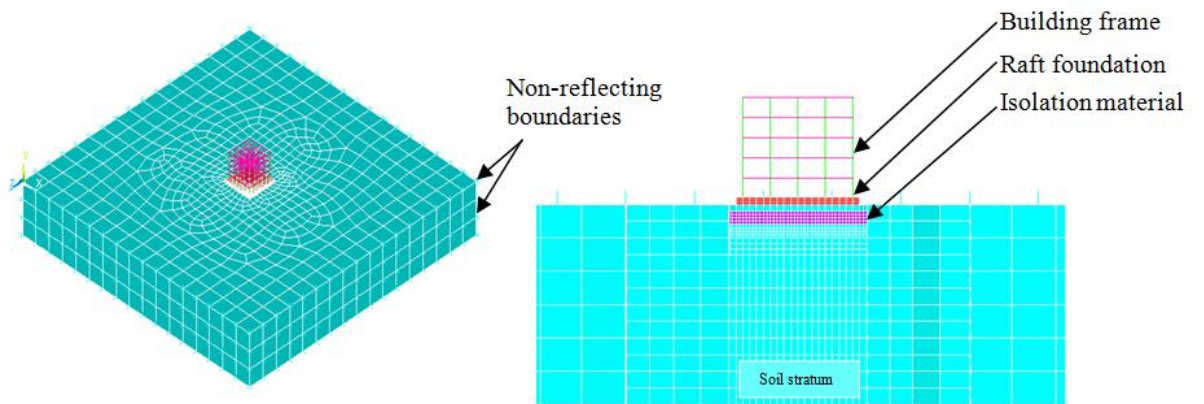
3.2 PARAMETRIC STUDIES ON PLACEMENT OF COIR MAT IN SOIL

The parametric analysis on the placement of coir in soil was carried out with a four bay five storey building and the parameters were standardized by considering the width of the raft foundation (B) as the reference (Fig. 3.1). Various parameters studied for coir mat reinforced soil-structure system are listed in Table 3.1. Dimensions and the properties of the materials of soil-structure system used for the numerical analysis are listed in Table 3.2, 3.3 and 3.4. The building-reinforced soil system was subjected to a dynamic seismic load corresponding to the recorded accelerogram of the EL Centro earthquake (1940) with a scaled-down PGA of 0.3g. Soft soil was considered for the parametric analysis. The properties of soft soil are shown in Table 3.2.



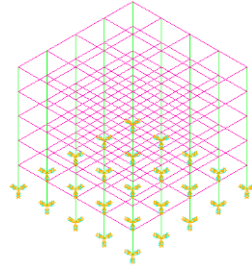


(c) parameters affecting the placement of isolation material



(d) finite element model

(e) cross section of finite element model



(g) rigid base structure model

Figure 3.1 Configuration of the soil-structure system

Table 3.1 Details of parametric study on placement of coir mat

Parameters	Dimension (B: Width of raft foundation)
Depth of embedment of coir mat (z)	$\frac{B}{18}$, $\frac{B}{9}$, $\frac{B}{4.5}$, $\frac{B}{2.25}$
Width of coir mat (w)	B , $\frac{B}{0.6}$, $\frac{B}{0.45}$, $\frac{B}{0.3}$
Thickness of coir mat (t)	$\frac{B}{36}$, $\frac{B}{18}$, $\frac{B}{12}$, $\frac{B}{9}$

3.3 LINEAR AND NONLINEAR ANALYSIS OF ISOLATED SOIL-STRUCTURE SYSTEM

Linear and nonlinear properties of soil and isolation materials were considered for the analysis of the soil-structure system.

3.3.1 Idealization of Structure

Four-bay five-storey RC framed buildings supported by the raft foundation resting on soft and stiff soil were considered for the analysis. The bay length of building frames was taken as 4m, and the storey height was taken as 3m. Based on structural requirements

in accordance with Indian standard codes for designing reinforced concrete structures, IS 456:2000 and IS 13920: 2016 (IS 1993, 2016), dimensioning of beams and columns of reinforced concrete structures were determined (Table 3.3). Raft size was taken as 18m x 18m with a thickness of 1m. The live load on floors was taken as 3kN/m² in addition to the dead load caused by the self-weight of the structural elements. M25-grade concrete and Fe 415-grade steel were selected as the building and raft materials. The modulus of elasticity (E_c) for building and raft foundation, 25GPa, was calculated corresponding to M25 grade concrete using the equation,

$$E_c = 5000\sqrt{f_{ck}} \quad (3.1)$$

where, f_{ck} is the characteristic compressive strength of concrete after 28 days

The unit weight and Poisson's ratio of concrete were taken as 25kN/m³ and 0.15 respectively, for both building and raft foundation.

The configuration of the soil-structure system is represented in Fig. 3.1(a) and Fig. 3.1(b). On these three-dimensional finite element models of field-scale models, transient analysis was performed with and without soil-isolation mechanism. The soil-structure system without isolation material is represented as 'UR.'

3.3.2 Idealization of Infinite Soil

To represent the soil, an inelastic continuum finite element model was assumed for the seismic analysis. Since soil is a semi-infinite medium, the boundary should be placed at a distance away from the foundation laterally, where the static responses of the system die out. The lateral edges of the finite soil stratum were placed about 4.5 times the width of raft from the center of the foundation. The bedrock was considered at a depth of 30m for all models considered so that a finite domain was considered for the analysis. Underneath the foundation, the soil was assumed as a single homogeneous stratum of size 170mx170m with a depth of 30m (Fig. 3.1(a)). Non-reflecting boundaries were assigned at lateral boundaries to represent an infinite soil stratum. The Young's modulus and

Poisson's ratio of the soil were adopted corresponding to the standards of NEHRP guidelines for the seismic rehabilitation of buildings from FEMA 274 (1997). The details of the various soil properties used for the linear analysis to study the effect of soil flexibility of soil-structure system are listed in Table 3.2. For the nonlinear analysis of isolated soil-structure system, only soft soil was considered as given in Table 3.4.

Table 3. 2 Properties of soil for linear analysis to study the effect of soil flexibility

Soil type	Description of soil	Shear wave velocity V_s (m/s)	Poisson's ratio	Unit weight(kN/m^3)
S_1	Soft soil	120	0.4	16
S_2	Stiff soil	270	0.35	18

In the viscous boundaries given, P-wave damping and shear wave damping are the two dash pots given per unit area of the boundary. Damping coefficients for the dashpots were given from the expressions below:

$$\left. \begin{aligned} C_p &= \rho V_p A \\ C_s &= \rho V_s A \end{aligned} \right\} \quad (3.2)$$

Where, V_s and V_p are the shear wave and perpendicular wave velocities, respectively. C_p is the damping coefficient for perpendicular wave, C_s is damping coefficient for shear wave, ρ - mass density of the soil system (Table 3.2). A is the area of the element on which the wave component acts.

Table 3. 3 Properties of building components and isolation materials for linear analysis

Specification	Dimension (m)	Modulus of Elasticity (MPa)	Poisson's ratio	Unit weight (kN/m³)
RC Beam (bxdxl)	0.3x0.3x4	25x10 ³	0.15	25
RC Column (bxdxl)	0.5x0.5x3	25x10 ³	0.15	25
Raft foundation (BxBxD)	18x18x1	25x10 ³	0.15	25
Rubber mat (WxW)	20x20	100	0.49	15
Coir mat(WxW)	20x20	4100	0.3	15
Polymer Foam _{PE1} (WxW)	20x20	150	0.2	4
Polymer Foam _{PE2} (WxW)	20x20	900	0.2	4
Polymer Foam _{PE3} (WxW)	20x20	22	0.1	0.22

3.3.4 Idealization of Isolation Layer

The effect of soil reinforcement materials as isolation medium in reducing the seismic response of the structure was evaluated in this study. Ground improvement with soil reinforcement is a standard method practiced. The addition of strengthening elements improves the engineering properties of soil stratum. The reinforcing materials absorb the tensile load and the shear stresses within the soil structure, preventing shear or excessive deformations. Suitable material must be chosen for the soil reinforcement so that seismic responses of the soil-structure system under the dynamic load should be minimum.

Table 3. 4 Properties of soil and reinforcement materials for nonlinear analysis

Specification	Dimension (BxW) (m)	Linear			Nonlinear (Isotropic hardening)		
		Young's Modulus of Elasticity (MPa)	Poisson's ratio	Unit weight (γ_d) (kN/m ³)	Yield stress (MPa)	Tangent modulus (MPa)	Damping ratio
Soft soil	170x170	65	0.4	16	0.3	30	0.05
Rubber mat	20x20	100	0.49	10	25	2	0.5
Coir mat	20x20	4100	0.3	15	30	500	0.093
Polymer foam (PE ₃)	20x20	22	0.1	0.22	0.3	5	0.7

The materials used for seismic isolation in the form of mats were coir mat, polymer foam, and rubber mat (Fig. 3.2). Three different polymer foams were used in which PE₁, PE₂ and PE₃ respectively are polyethylene with lower elastic modulus, polyethylene with higher elastic modulus and polystyrene foam. Polystyrene (Epoxy polystyrene) is selected for the nonlinear analysis as well as the pore water pressure analysis. The details of the properties of various isolation materials used in the analysis are listed in Table 3.4 (ASTM D7180; ASTM D6817 / D6817M-17, 2017; D5321, 2019; Fischer-Cripps, 2004). The depth of placement of reinforcement plays a vital role in reducing the seismic responses

under dynamic loads. An ideal depth helps to intercept the shear zone as much as possible and induces optimum lateral retention of the deformed zone under the raft foundation. The reinforcement mats were placed at an optimum depth of $B/18m$, which is obtained from the parametric study as per section 3.2. All the reinforcement mats provided were of a planar dimension of $20m \times 20m$ which covers the bottom area of the raft foundation with 1m extensions in all four sides.

3.3.5 Damping

Damping in soil happens under all types of vibrations. Damping plays an important role in the dynamic soil-structure interaction. The primary causes of material damping in soils are by two processes: (1) frictional damping among soil particles (known as internal damping) and (2) fluid-particle interaction and pore fluid motion. The viscous damping is frequency-dependent. There is frequency independent damping, i.e., constant material damping. The isolation mats used in this study were modeled by inputting their frequency-independent damping ratio (Table 3.4) (Rocco et al., 2012; Ge & Rice, 2018).

3.3.6 Finite Element Modeling of The Soil-Structure System in ANSYS

The integrated soil-structure system was analyzed by the finite element method using ANSYS software, assuming nonlinear inelastic behavior of soil and isolation materials (Table 3.4). The building frame was modeled using a two-node linear beam element, i.e., BEAM188. The soil stratum was discretized with eight-node linear brick reduced integration element, i.e., SOLID 185. It is a first-order element with linear interpolation for each direction that is suited for contact analysis convergence. Soil medium was discretized with solid elements of size in the order of 0.5m, 1m, 2.5m, 5m, and 10m along the lateral direction with fine mesh near the structure, which gradually increases to a coarser mesh away from the structure. Raft foundation also was discretized with SOLID 185 elements as soil with elements of size 1m. A 3D finite strain element, SOLSH190 element that has very low bending elastic modulus was employed to incorporate the bending of isolation materials under load. Soil isolation mats were meshed with 0.5m size. The

isolation materials were numerically modeled by creating a node-node connection between the soil and isolation material surfaces. The interface between the surrounding soil and the isolation materials was formulated with coefficients of friction values. The coefficient of friction between soil and rubber mat was assumed as 0.5, and the coefficient of polymer foam was taken as 0.3. The damping ratio of polymer foam is in the 0.6-0.7 range. The damping ratio of the rubber is in the range of 0.01 to 0.5, depending upon its structure (Thomas 2014). Non-reflective boundaries on the lateral boundary surfaces of the soil media were assigned to represent the infinite soil medium. COMBIN 14 elements were used for a viscous boundary, and proper damping and elastic modulus values corresponding to the soil were assigned.



(a)



(b)



(c)



(d)

Figure 3. 2 Photographic view of; (a) coir mat (b) rubber mat (c) polyethylene foam and (d) polystyrene foam

The soil stratum base was set as fixed so that any motion and moments would be prevented. The entire three dimensional building-raft-soil system was modelled using the ANSYS software and is shown in Fig. 3.1(b). Altogether 34299 nodes and 29409 elements which include 1600 solid shell reinforcement elements, were used for the model.

CONTACT and TARGET elements were used to model the interface of soil and isolation materials. The interface between the underneath soil and isolation materials is formulated with coefficient of friction values. The friction value of isolation material can be varied depending on the type of soil matrix in which it is reinforced and the internal angle of friction at the mat-soil interface. The current study uses the minimum value of friction at the coir mat interface and soil modeled using CONTA and TARGET elements. The coefficient of friction for coir mat (Rajeswari J S 2019, Babu K K 2007) and rubber mat were assumed as 0.5, and for polymer foam, it was assumed as 0.7.

3.3.7 Seismic Analysis

The time history analysis of the integrated soil-structure system was carried out with four different ground motions (corresponding to the elastic design spectrum for Zone III as per the Indian standard code (IS 1893 (Part 1): 2016), the Northridge earthquake on January in the San Fernando Valley (1994), the longitudinal component of the Imperial Valley earthquake at El-Centro (1940) and the Chi-Chi (Taiwan) earthquake (1999)) with modified peak ground acceleration (PGA) of 0.3g. The input motions corresponding to modified IS, Northridge, El Centro and Chi-Chi ground motions are designated as EQ-1, EQ-2, EQ-3, and EQ-4 input motions. The recorded accelerogram data were collected from PEER Strong Motion Database. The input ground motions were chosen based on the availability of peak amplitude-frequency content that matches the natural frequency of the soil-structure system. The resonance effect demonstrates the highest seismic response in the superstructure under the ground excitations. The FFT analysis shows that the peak value of Fourier amplitude occurs at a frequency range of 1.1Hz to 1.21Hz for the input motions. Fourier amplitude and specific energy density corresponding to the natural frequency of the reinforced soil-structure system are shown in Table 3.5. The total duration

of the ground motion was taken as 30sec for the El-Centro earthquake, bracketed duration of 17.81sec for IS input motion, 25sec for the Northridge input motion and 12.56 sec for Chi-Chi input motion. The acceleration time history plot of input ground motions is shown in Fig. 3.3. These four ground motions were applied in the global X direction of the soil-structure model in ANSYS.

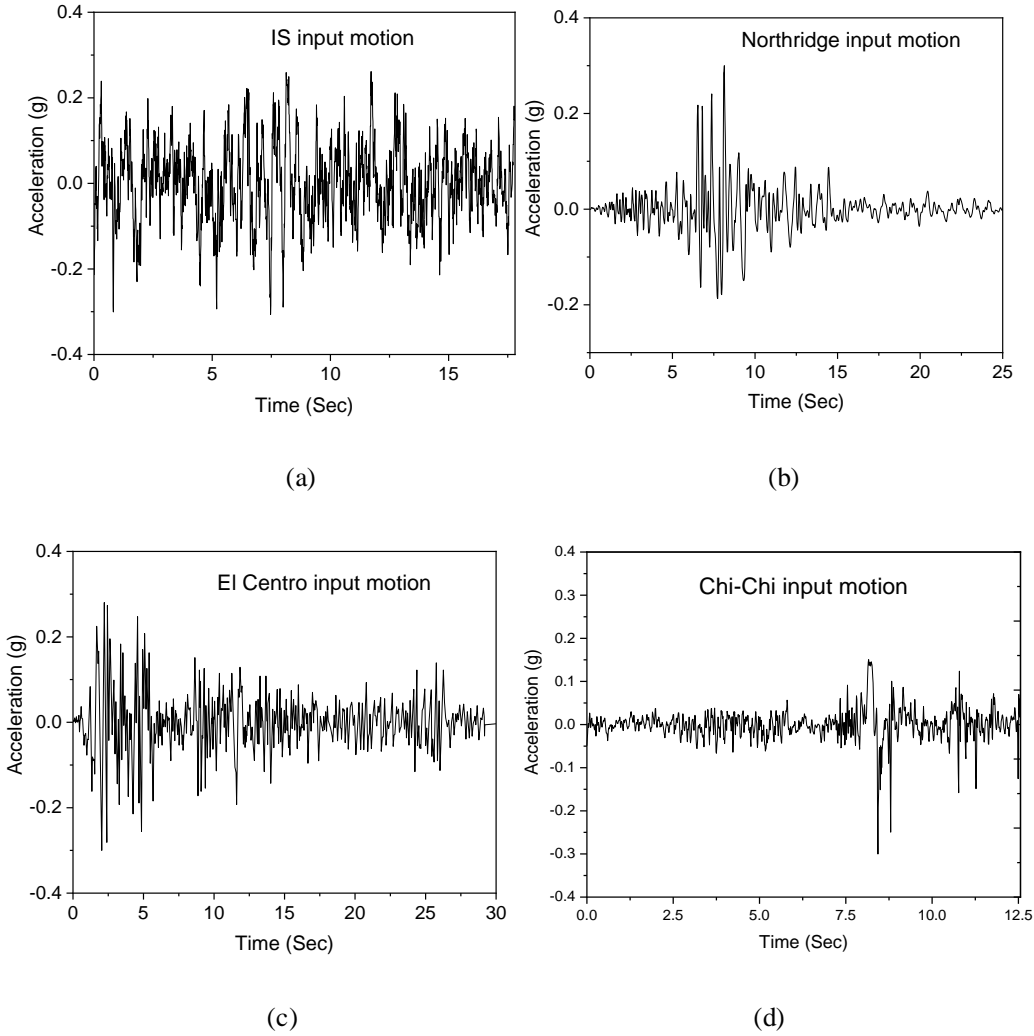


Figure 3.3 Input acceleration time history of (a) IS (EQ-1) (b) Northridge (EQ-2) (c) El Centro (EQ-3) and (d) Chi-chi (EQ-4) earthquake motions

Table 3. 5 Fourier amplitude and specific energy density of input motion

Input motion	Fourier amplitude	Specific energy density (m²/s)
Indian Standard (EQ-1)	0.252	0.4726
Northridge (EQ-2)	0.219	0.2110
El Centro (EQ-3)	0.11642	0.1805
Chi-chi (EQ-4)	0.0657	0.0522

The integrated building-soil system with and without soil isolation mechanism was analysed by incorporating the soil reinforcement with different isolation materials within the soil. Comparative analysis of seismic responses of buildings placed in isolated and conventional soil stratum would provide an idea of the isolation performance of the material.

The isolation efficiency of reinforced mats has been defined as follows;

Isolation efficiency of reinforced mats

$$= \frac{\text{seismic response (u)} - \text{seismic response (r)}}{\text{seismic response (u)}} \times 100$$

(3.3)

where,

Seismic response(u): Seismic response of the unreinforced soil-structure system

Seismic response(r): Seismic response of the reinforced soil-structure system

Thus, higher the reduction factor obtained in the results means a higher isolation effect and higher isolation efficiency (Eq. 3.3) for the particular reinforcement mat in the soil stratum.

Seismic building responses such as roof acceleration and base shear were evaluated to study the isolation performance of reinforcement materials in the soil. Seismic base shear is the highest lateral force exerted during the seismic event on the building at its base. Here, the seismic base shear of the building resting on soil reinforced with different isolation mats has been represented in terms of the total weight of the building as the base shear ratio (Eq. 3.4).

$$F' = \frac{F}{W} \quad (3.4)$$

where,

F': Base shear ratio of building

F : Shear force at the base of the building

W: Total weight of the building

A non-dimensional quantity, an improvement factor (IF) is introduced to quantify the isolation efficiency of reinforcement materials in reducing the seismic response of building (Eq. 3.5). It is identical to the bearing capacity ratio (BCR), which have previously clarified by Guido et al. (1986).

$$IF = \frac{SR_i}{SR_c} \quad (3.5)$$

where, SR_c , and SR_i are the seismic response of conventional and isolated soil-structure systems respectively.

3.4 FINITE ELEMENT MODELING OF THE SOIL-STRUCTURE SYSTEM IN PLAXIS 3D

The numerical simulation using the finite element method enables modeling the complicated nonlinear soil behavior and different interface conditions with varying geometries and soil characteristics. PLAXIS 3D was used for the numerical analysis of excess pore water pressure (P_{excess}) generation in the three-dimensional soil-structure system (Fig. 3.1(a,b)). The soil in the FE model was represented by the built-in 10-node tetrahedral elements used to incorporate the stress-strain behavior. This element type offers second-order displacement interpolation. Furthermore, built-in 10-node tetrahedral elements retains the geometry preferred in 3D mesh creation. Hardening soil model was used to model soil and isolation materials. Input parameters of soft soil used are shown in Table 3.2. To demonstrate correct load distribution and deflection patterns, the soil bed was extended 3.5 times raft width laterally and 1.5 times raft width downwards. The isolation mat was placed at the foundation and soil interface to function as absorbers and relieve the vibration energy transfer to the structure. Isolation mats were also modeled using the hardening soil model. Isolation mats are provided for a dimension of 20mx20mx0.5m which covers the bottom area of the raft foundation with 1m extensions in all four directions and placed at 1m below the raft foundation. Coir composites were modeled with each layer of composite materials having a thickness of 0.5m provided at the top and bottom sandwiched with 0.5m of coir mat in the middle to get an adequate total thickness of 1.5m. The base of the soil stratum was prevented from movement, while the lateral boundaries were absorbent boundaries. Coir and its composites such as coir mat (C), coir-polymer foam(C-PE₂), and coir-rubber (C-RU) mats were used as isolation materials in the pore water pressure analysis (Table 3.3).

A prescribed displacement at the bottom boundary was used to simulate the earthquake. To absorb outgoing waves, absorbent boundary conditions were imposed at the distant vertical limits. The typical absorbent boundaries for models were created at the left-edge, right-edge and bottom borders. While analyzing, the absorbent borders reduce

the box effect. The actual accelerogram of earthquakes in standard SMC format (Strong Motion CD-ROM) was used for the input motion and it was applied as a horizontal prescribed displacement to the bottom boundary. The peak ground acceleration in the accelerograms is 0.3g. Table 3.6 shows the Fourier amplitude and specific energy density corresponding to the natural frequency of the reinforced soil-structure system. The seismic study was done in two stages: first with the plastic analysis, followed by dynamic analysis. The dynamic analysis time interval was chosen as 15s.

3.4.1 Calculation of Pore Water Pressure

Total stresses (σ) are the sum of effective stresses (σ') and active pore pressures (P_{active})

$$\sigma = \sigma' + P_{\text{active}} \quad (3.6)$$

The active pore pressure is calculated by multiplying the effective saturation (S_{eff}) by the pore water pressure (P_w).

$$P_{\text{active}} = S_{\text{eff}} \cdot P_w \quad (3.7)$$

When the degree of saturation is less than unity, which is usually the case when the water level rises above the phreatic level, pore water pressure differs from active pressure. P_{active} and P_w are generally equal when the water level is below the phreatic level.

As an alternative to the pore water pressure (P_w), the groundwater head (h_w) can be viewed as:

$$h_w = z - P_w / \gamma_w \quad (3.8)$$

Where z is the vertical coordinate and γ_w is the unit weight of water. In the pore water pressure, a further distinction is made between steady-state pore pressure (P_{steady}) and excess pore pressure (P_{excess}).

$$P_w = P_{\text{steady}} + P_{\text{excess}} \quad (3.9)$$

Where, steady-state pore pressure is the steady-state or long-term part of pore pressure.

Excess pore pressure is the result of undrained behavior and is affected by stress changes due to loading or unloading, a sudden change in hydraulic conditions and consolidation.

Chapter 4

PARAMETRIC STUDIES ON THE PLACEMENT OF ISOLATION MATERIAL IN SOIL

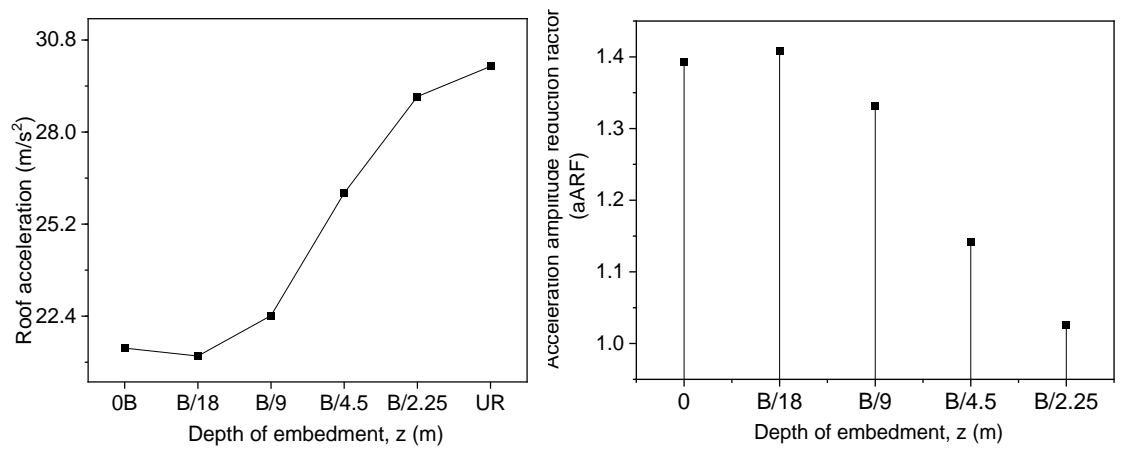
4.1 PARAMETRIC STUDY ON PLACEMENT OF COIR MAT

Different parameters regarding the placement of coir mat in soil are studied and discussed in the following section. Fig. 3.1(a) and Fig. 3.1(b) shows the finite element models simulated in ANSYS for the cases with and without the soil-isolation mechanism. Conventional and isolated soil cases are modelled and analyzed to study the effect of the soil-isolation mechanism to attenuate the seismic responses of buildings for varying parameters of placement of coir mat in soil. The optimum values of the parameters such as the depth of embedment, width and thickness of the coir mat for the effective reinforcement of soil have been analysed (Fig. 3.1(c,d)).

4.1.1 Depth of Embedment of Coir Mat

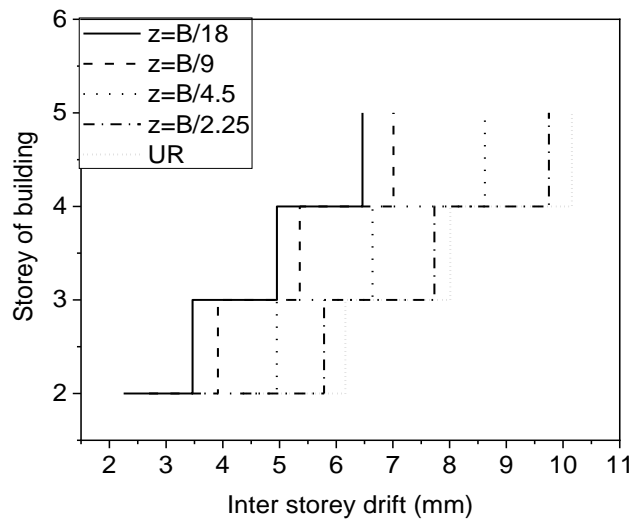
In the soil strengthening technique, the embedment depth of the reinforcement mat is observed as a key influencing parameter from the literature. It plays a significant role in reducing the seismic reactions of buildings. An appropriate depth is needed to intercept the shear zone and to maximize the lateral retention of the deformation zone underneath the raft foundation. The greater thickness of soil above the reinforcement layer results in increased settlement (Vinod et al. 2009). In this study, the coir mat with thickness of $B/9$ was positioned at various depths from the base of the raft foundation. For a range of $B/18$ to $B/2.25$ depth of embedment of coir mat below the foundation in soil, dynamic analysis of the soil-structure system was carried out to have a quantitative assessment of the extent of soil isolation, where 'B' is the width of the raft foundation. It is observed from the analysis that with an increase in the depth below the base of the raft foundation, the roof

acceleration responses of the building were reduced marginally. Fig. 4.1(a) indicates the variation in roof acceleration response of building resting on soft soil reinforced by coir mat. The reduction in roof acceleration amplitude is maximized when the material is located at B/18 depth from the base of the raft foundation. The coir mat positioned directly below the raft foundation shows a higher amplitude of roof acceleration than that placed at a level of B/18 depth. Adequate overload pressure obtained by an embedment depth of B/18 is required to improve the optimum frictional resistance at the coir mat and soil interface. By placing the coir mat at B/18 depth, around 30% reduction in the roof acceleration is obtained as compared to unreinforced soil. And, it is around 28% when the coir mat is placed directly below the foundation. The effectiveness of reinforcement as a vibration isolation mechanism is expressed by an acceleration amplitude reduction factor (aARF) (Fig. 4.1(b)). The acceleration amplitude reduction factor is defined as the ratio of the roof acceleration amplitude observed from the unreinforced soil to the reinforced soil. This reduction factor is the parameter used earlier to study about the analysis of the geogrid strengthened sand bed (Majumder and Ghosh 2015). The value of an amplitude reduction factor is maximum for effective vibration screening. The aARF value shown in Fig. 4.1(b) corresponding to the depth of coir mat such as B/18, B/9, B/4.5 and B/2.25 are 1.39, 1.41, 1.33, 1.14 and 1.03 respectively. This variation in aARF value with the depth of embedment indicates that the seismic response is dependent on the location at which the isolation materials are placed in the soil. The seismic response in the building resting on a strengthened soil bed decreases when the reinforcement depth increases from 0 to B/2.25 compared to the responses of the unreinforced soil system. It is observed that the isolation effect vanishes if the mat is placed below B/2.25 depth.



(a) roof acceleration

(b) acceleration amplitude reduction factor



(c) inter-storey drift

Figure 4.1 The effect of variation in the depth of embedment of coir mat

In addition to the roof acceleration, the inter-storey drift of the buildings corresponding to the change in depth of embedment of the coir mat below the foundation is also examined (Fig. 4.1(c)). The unreinforced soil-structure system shows an inter-storey drift of 4.4-10.2mm from top to bottom storey of the building. An inter-storey drift value of 2.2-6.4mm is observed with the coir mat placed at B/18 depth. The inter-storey drift in

the building is reduced around 57% to 4% from unreinforced soil when the depth of embedment value varied from $B/18$ - $B/2.25$. The inter-storey drift in buildings resting on reinforced soil decreases with the increase in embedment depth of coir mat from $B/18$ - $B/2.25$. An optimum depth of $B/18$ is needed to obtain a maximum reduced seismic response in buildings, which gives a minimum inter-storey drifts in the building. No beneficial effect in reducing the seismic response is observed at a depth of $B/2.25$ and further. From the seismic reactions in terms of roof acceleration and inter-storey drift value of the building analyzed, it is inferred that the depth of placement of the coir mat is needed at least $B/18$ from the raft foundation.

4.1.2 Width of Coir mat

The maximum roof acceleration response from the dynamic analysis of the soil-structure system is examined to study the effect of the width of the coir mat in the soil reinforcement technique. It is observed that peak roof acceleration decreases as the width of coir mat increase up to $B/0.45$ (Fig. 4.2(a)). But, no substantial decrease in acceleration is observed after a further rise in coir mat width beyond $B/0.45$. For roof acceleration, a percentage reduction of 12% is observed with a coir width of $B/0.6$ and 16% with a coir width of $B/0.45$ and $B/0.3$, compared to that with a coir mat of thickness B . The limiting value of the coir mat width, which gives the maximum reduced seismic response in the building, is obtained as $B/0.45$ in this analysis.

The interstorey drift between the floors of the buildings with variation in the width of the coir mat is studied (Fig. 4.2(b)). The drift value of 2.1- 6.3 mm from the top to bottom of the building was observed when the coir mat is reinforced in the soil for a width of B . For the cases of soil reinforced with coir mat of width B , $B/0.6$, $B/0.45$ and $B/0.3$, a maximum of 53% reduction in the inter-storey drift of building is observed with a coir mat of width $B/0.45$ as compared to unreinforced soil case. When the width is changed to $B/0.3$ from B , the drift in the building is not substantially varied. It is observed that the isolation effect vanishes if the mat is placed for a width beyond $B/0.45$.

It is inferred from the results that the effective frictional interaction of the coir mat with the soil is achieved with a portion of this mat that lies in the pressure zone, laterally beneath the foundation. Provision of coir mat laterally beyond this zone will not impart in the isolation mechanism. A previous study in the literature, shown an effective width $2.5B$ obtained from the experiments on sand bed reinforced with geotextiles (Guido et al. 1986). The bearing capacity obtained by the provision of geocells was not substantially enhanced beyond $4B$ (Dash et al. 2004). In the current analysis, the findings drawn from the seismic responses in the building show an optimum coir width of $B/0.45$ around the raft base.

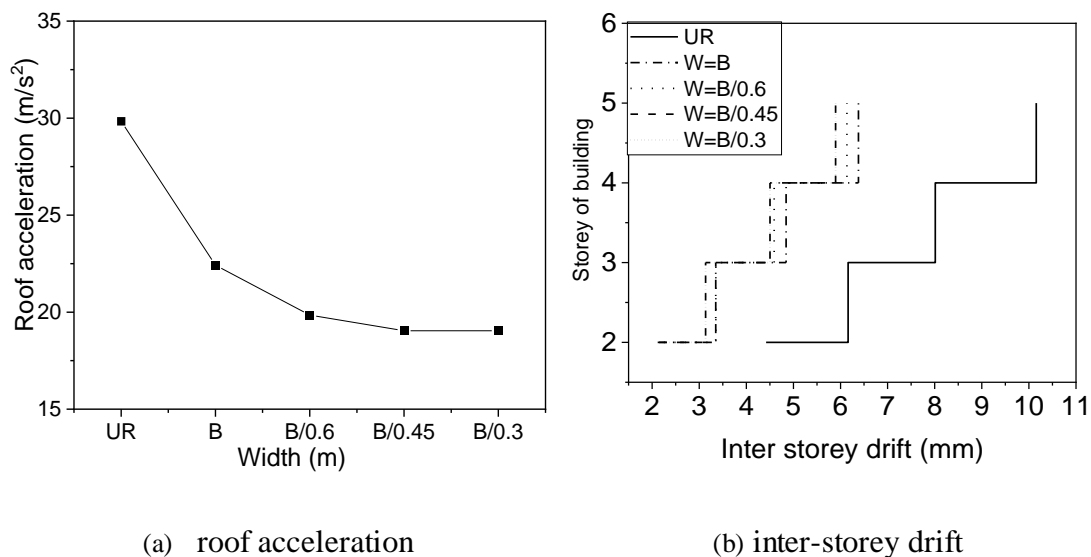


Figure 4.2 The effect of variation in the width of embedment of coir mat

4.1.3 Thickness of Coir Mat

The study on the effect of coir mat thickness on the seismic response was carried out on the isolated soil-structure system. The roof acceleration of the building is decreased with the increase in coir mat thickness. The acceleration response in building under seismic excitation is reduced with the coir mat thickness of $B/36$, $B/18$, $B/12$, and $B/9$, compared to the unreinforced soil base (Fig. 4.3(a)). A maximum of around 25% reduction in the

roof acceleration is achieved by reinforcing the coir mat in soft soil with a thickness of B/9 as compared to the unreinforced soil. Varying the thickness of the coir mat from B/36 to B/12 show only a slight change in the response of roof acceleration. The results demonstrate that the provision of coir mat having a thickness from B/12 to B/9 have an almost constant value of roof acceleration response in the building as shown in Fig. 4.3(a).

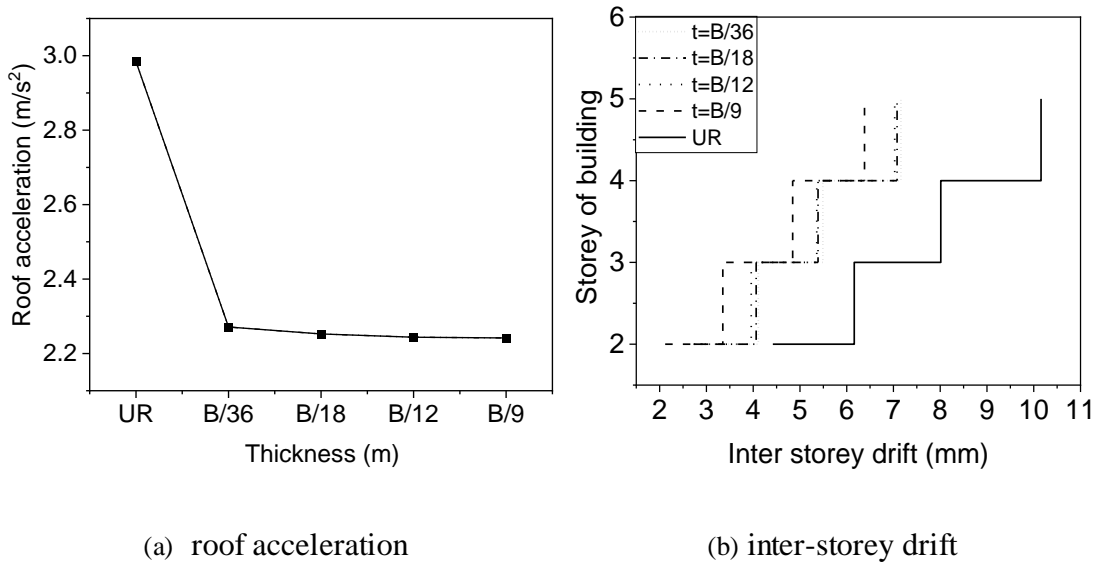


Figure 4.3 The effect of variation in the thickness of embedment of coir mat

The study on the effect of variation in the thickness of coir mat on inter-storey drift of building is carried out. The reinforcement of soil by the coir mat having thickness B/36 shows a building drift of 2.8-7.1mm, whereas, with the coir mat of thickness B/9, an inter-storey drift of 2.1-6.3mm is observed in the building (Fig. 4.3(b)). The reinforcement of the coir mat shows a maximum of around 37% reduction in the building drift for the thickness of B/9 in soil, and a reduction of 30% is observed with B/36 thick coir mat. An increase in thickness of the coir mat from B/36 does not show a considerable variation in reducing the inter-storey drift. i.e., the optimum thickness is observed as B/36, at which the seismic responses, including inter-storey drift, are reduced to a permissible limit. The buckling of the coir mat can probably be attributed to a certain thickness. Similar findings

in the studies of soil reinforcement with geosynthetics were reported (Dash et al. 2001; Tafreshi and Dawson 2010).

4.2 SUMMARY

The optimum values of the parameters such as the depth of embedment, width and thickness of the coir mat for the effective reinforcement of soil have been analysed. A minimum depth requirement of $B/18$ was identified for reinforcing the soft soil by the coir mat below the raft foundation. Also, it is observed that the isolation effect vanishes if the mat is placed below $B/2.25$ depth. The findings drawn from the seismic responses in the building show an optimum coir width of B and an optimum thickness of $B/36$ around the raft base, beyond which no significant change in seismic responses is noticed. Interstorey drift observed in the parametric analysis indicates that the drift value of an unreinforced soil model exceeds its code value limits. Hence, the reinforcement of soil by the coir mat can effectively reduce the inter-storey drift of unreinforced soil.

Chapter 5

EFFECT OF SOIL FLEXIBILITY ON ISOLATED SOIL- STRUCTURE SYSTEM

5.1 GENERAL

The seismic responses of the soil-structure system with and without isolation materials were analyzed and findings were compared for the selection of the best isolation material. Linear properties of soil as well as isolation materials were used for the analysis. Different seismic responses such as, roof acceleration, roof deflection, contact pressure at soil-raft interface, raft settlement and seismic base shear were studied. The linear behavior of soil-structure system under different earthquake motions incorporating the flexibility of soil is explained in this chapter.

5.2 EFFECT OF SOIL FLEXIBILITY

Soil-structure interaction effects on the seismic response of structures depend mainly on soil flexibility. Two types of soils, namely S_1 and S_2 representing soft soil and stiff soil, were considered to identify the effect of SSI (Table 3.2). It is observed from the modal analysis that the natural frequency of the SSI system is lower than the natural frequency of fixed base structure (1.96Hz) and about 43% reduction in natural frequency is noticed when the underlying soil is soft (Table 5.1).

For fixed-base models and buildings which rest on the soft and stiff soil stratum, the effect of SSI on seismic responses in terms of roof acceleration is analyzed. Fig. 5.1 indicates that seismic responses increase as soil flexibility increases. The roof acceleration of building is increased by about 70% and 33% respectively in soft and stiff soil base supported systems, compared to the fixed base system subjected to El Centro

input motion. SSI, therefore, has a significant role in the seismic behavior of structures. Since the seismic responses shown by buildings resting on soft and stiff soil are seen to be higher, seismic soil isolation is addressed. The following section compares the seismic responses of different mats reinforced soil-structure systems.

Table 5.1 Natural frequencies of the soil-structure system

Cases of Study	Isolation Mat	Natural frequency of soil-structure model (Hz)	
		Soft soil	Stiff soil
Case I	RU	1.1212	1.3529
	PE ₁	1.1212	1.3533
	PE ₂	1.1212	1.3621
	PE ₃	1.1212	1.3336
Case II	C	1.1212	1.3656
	C-RU	1.1212	1.3622
	C-PE ₂	1.1212	1.3617
	UR	1.1212	1.3590

5.2.1 Roof Acceleration of Building

Roof acceleration of the five-storey building is evaluated for the cases of unreinforced and reinforced soil base. The isolation capacity of case I and case II materials is compared by incorporating the soil flexibility. The percentage reduction in roof acceleration of buildings on soil reinforced by various isolation mats from that of unreinforced soil is evaluated.

From the study of soft soil strengthened with mats of Case I material, such as PE₃, RU, PE₁ and PE₂ mats respectively, subjected to El Centro input motion, a reduction of 2.6%, 9.8%, 15.1%, and 23% in the roof acceleration is observed (Fig. 5.2(a)). The roof acceleration does not reduce with the PE₃ mat reinforced soil base. Among the materials analyzed for its isolation efficiency in reducing roof acceleration, the rubber mat shows medium performance with a 9.8% reduction from unreinforced soil. In comparison with low stiff polyethylene (PE₁), a high stiff polyethylene mat (PE₂) reinforced soil system shows about 1.6 times higher percentage reduction in roof acceleration.

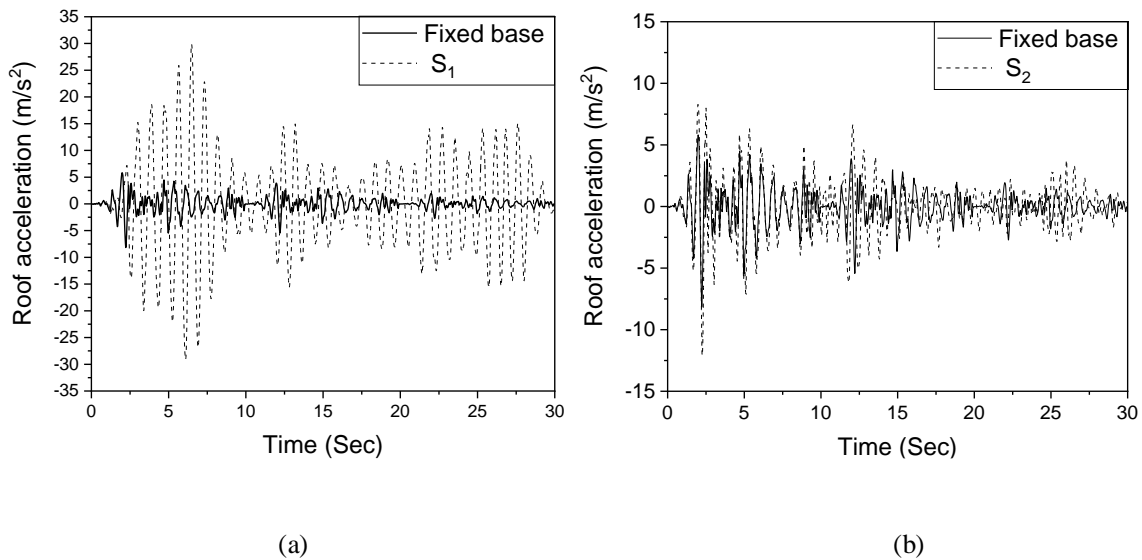


Figure 5.1 Time history of roof acceleration in building with fixed base and building on (a) soft soil (S₁) and (b) stiff soil (S₂)

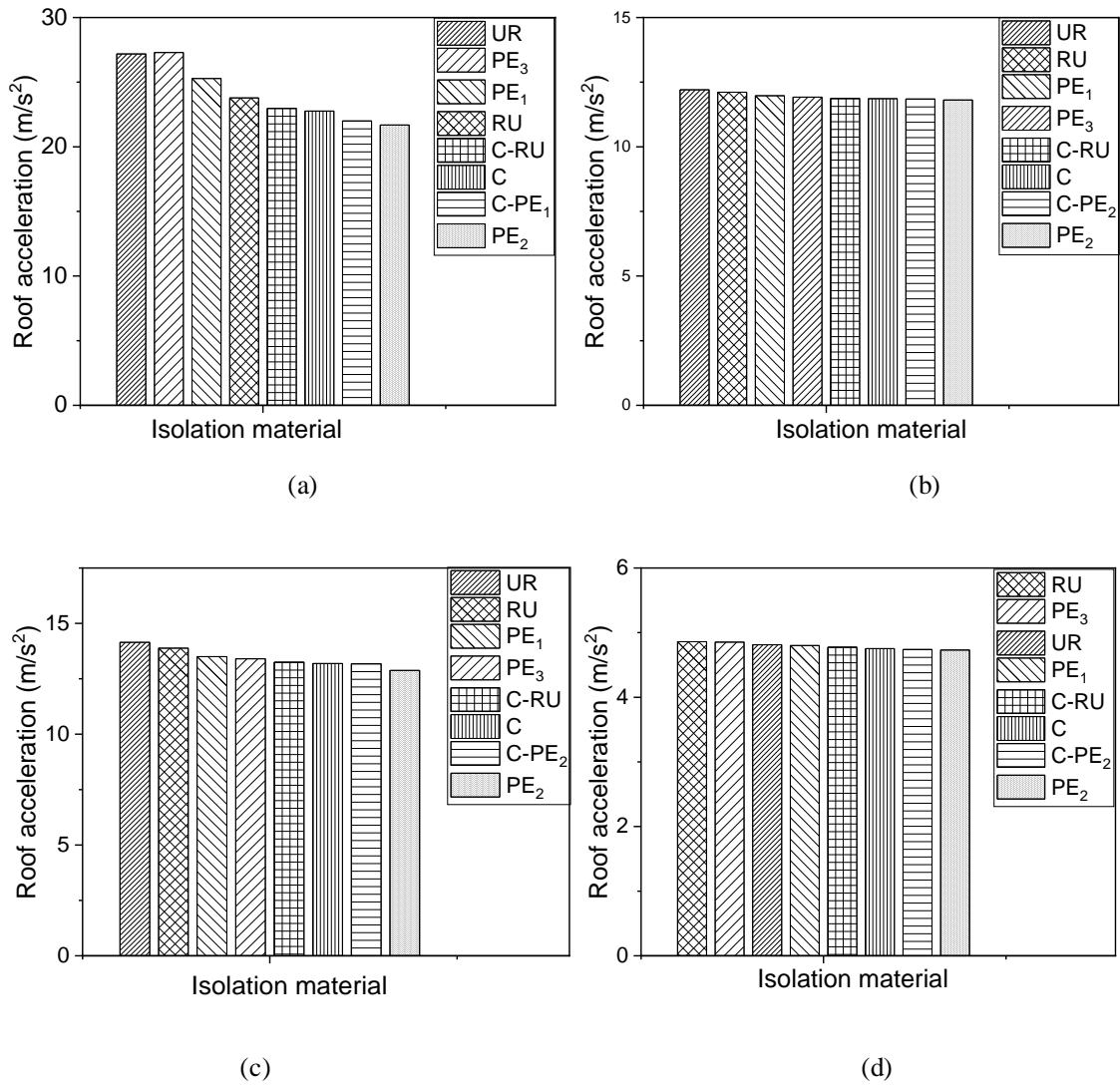


Figure 5.2 Roof acceleration for soil reinforced with different isolation mats (a) El Centro-soft soil (b) El Centro-stiff soil (c) IS-soft soil (d) IS-stiff soil

In stiff soil, the reinforced mats do not show a noticeable isolation efficiency in reducing the roof acceleration as compared to soft soil (Fig. 5.2(b)). The stiff soil reinforced by PE₃ mat exhibits improved performance. In the screening of the high-frequency dynamic source besides turbo generators, turbines, etc., continuous polystyrene foam (PE₃) is found more efficient (Keramatikerman et al. 2017). For comparatively more stiff soil deposition, PE₃ works well. In reducing roof acceleration of buildings resting on stiff soil, the efficacy of low stiff and high stiff polyethylene mat reinforcement does not vary significantly. The rubber mat does not contribute to the same at all.

The soil-structure system, in which the soil reinforced with mats of Case I materials, excited under IS input motion was analyzed. The reduction in building roof acceleration is achieved with all reinforcement mats. The percentage reduction in roof acceleration obtained for buildings resting on the soft soil is in the range of 2%-9% by the soil reinforcement with all the isolation mats (Fig. 5.2(c)). In comparison with low stiff polyethylene (PE₁), a high stiff polyethylene mat (PE₂) reinforced soil system shows about two times higher percentage reduction in roof acceleration. In stiff soil, the reduction in roof acceleration is observed with PE₁ and PE₂ mats only and which is about 5% (Fig. 5.2(d)).

From the analysis of soft soil reinforced with mats of Case II materials, it is observed that the roof acceleration is reduced by about two to eight times more compared to that observed from soft soil reinforced with the mats of Case I material such as mats of rubber and polymer foams. The combination of two materials having higher elastic modulus resulted in a better composite mat, C-PE₂, which reduces the seismic response significantly. The peak roof acceleration of the building on coir mat and C-PE₂ mat strengthened soil is decreased by 19% and 22% respectively as compared to the unreinforced soil. And this reduction is 18% with C-RU mat reinforcement. The coir mat reinforced soil stratum shows only 2.2% isolation efficiency to reduce roof acceleration in stiff soil.

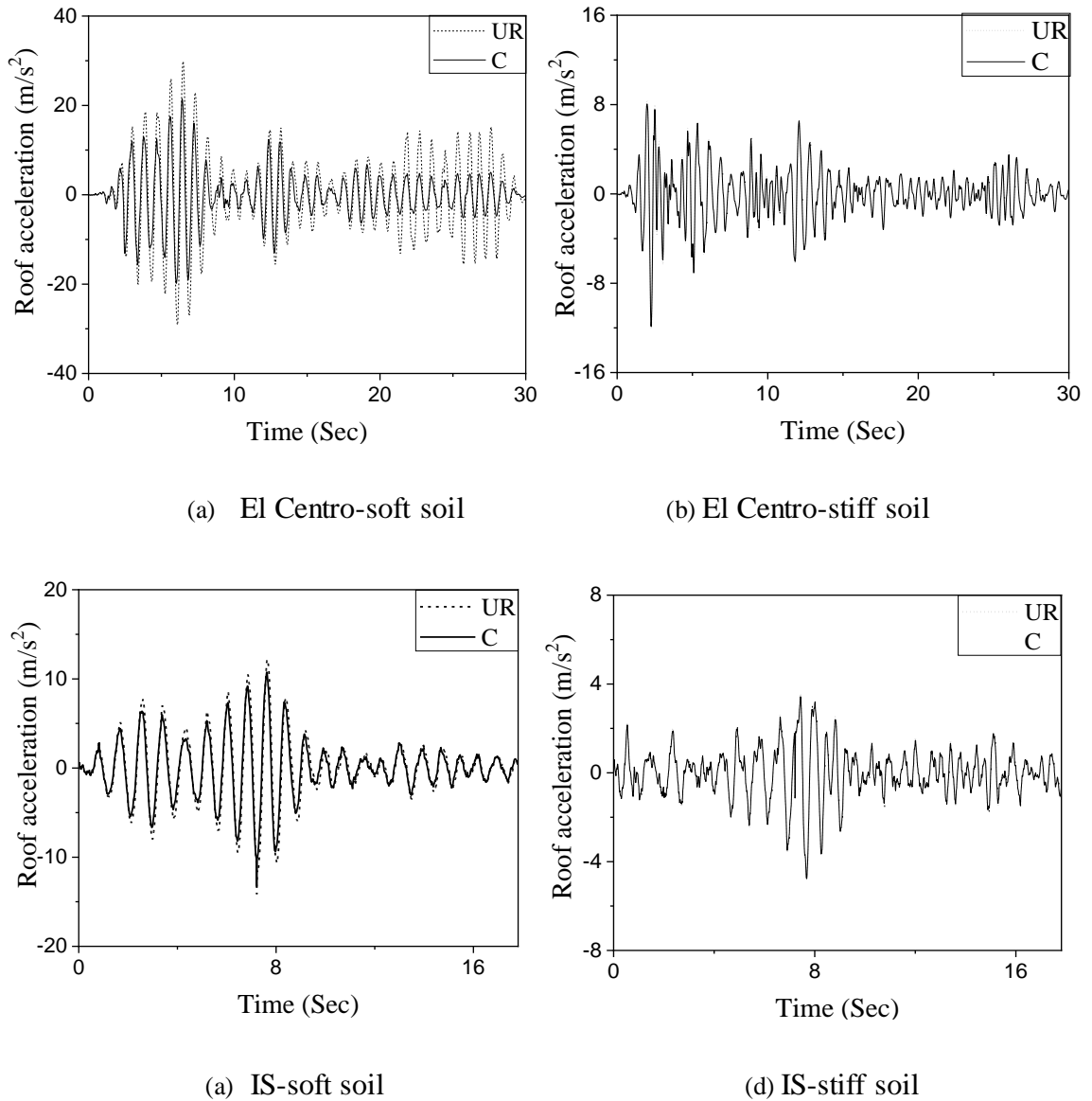


Figure 5.3 Roof acceleration time history plot of the soil-structure system for unreinforced and reinforced cases of S_1 and S_2 type soil with coir mat

Under the IS input motion, the roof acceleration response of the soil-structure system in which the soft soil is strengthened by mats of Case II materials was analyzed. The percentage reduction of 6.4%, 6.8%, and 6.9% respectively is observed in soil base enhanced by C-RU, C, and C-PE₂ mats (Fig. 5.2(c)). In stiff soil also, roof acceleration is

reduced with the reinforcement of all the Case II materials but, the reduction is not significant i.e., less than 5% (Fig. 5.2(d)). The roof acceleration time history plot of the soil-structure system for unreinforced and reinforced cases of S_1 and S_2 type soil reinforced with coir mat are shown in Fig. 5.3.

Roof acceleration response of five-storey building-isolated soil system excited under two different input motions, incorporating the soil flexibility is evaluated. The observed roof acceleration responses under input motions of El Centro are greater than that with IS input motion because, El Centro motions have high peak acceleration amplitudes in the frequency content in the FFT of earthquake motion which matches with the fundamental frequency of soil-structure system compared to IS input motion. It is also seen that isolation materials work better in soft soil than in stiff soil to mitigate seismic responses. A highly stiff polyethylene mat shows around 23%-33% more isolation efficiency than the coir mat in reducing the roof acceleration of the building. It is not technically feasible to have highly stiff polyethylene material as a soil reinforcement material for a 2m thickness, however composite of coir mat and polyethylene is practically possible. Not only for the isolation purpose, the composite of coir mat and polyethylene foam may also act as a good drainage medium. High stiff polyethylene has been chosen to make a composite with coir mat since the high stiff polyethylene mat shows around two times more isolation efficiency compared to low stiff polyethylene foam. The rubber mat gives better isolation efficiency and works as a good composite with the coir mat. It is a combination of synthetic and natural materials having lower and higher elastic modulus respectively. The acceleration response shown by the soil strengthened with coir mat is between that observed from the soil improved by C-RU and C-PE₂ mats (Fig. 5.2). Generally, isolation materials along with the pile foundations are practiced to mitigate the seismic response of multi storey buildings. For example, rubber mixed in the form of tyre chips in sand for 5m thickness along with piles to isolate seismic responses had shown an isolation efficiency of around 40% for roof acceleration in five-storey buildings (Munirah Abdullah and Ahmad 2012; Nanda et al. 2017). But in the current study, only the reinforcement of

isolation mats itself without pile reduces the roof acceleration response of the building significantly with a maximum percentage reduction of 23%.

5.2.2 Contact Pressure at Raft-Soil Interface

In the SSI system with soil reinforced by various mat cases, the contact pressure distribution below the raft foundation was analyzed by considering soil flexibility. From the response of the soil foundation interface on the application of dynamic load, it is noticed that the contact pressure distribution on the edge of the soil foundation is higher and decreasing towards the center.

Soil reinforcement reduces the contact pressure development under earthquake loads at the raft-soil interface. The decrease in contact pressure in terms of reduction factor is shown in Fig. 5.4 for reinforced soil from that of unreinforced soil system, where 'L' - length of the raft foundation.

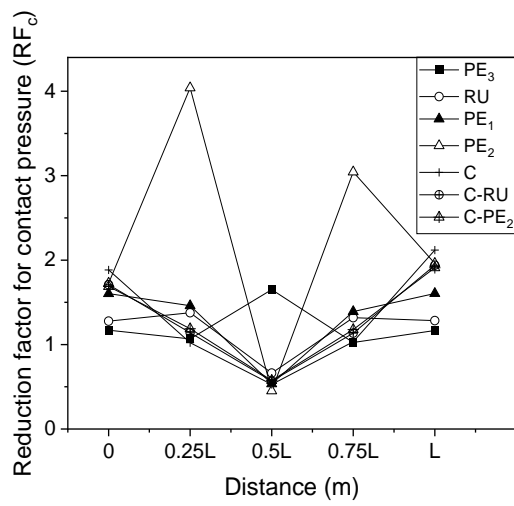
Among Case I materials, PE₁ and PE₂ in soft soil show 37.7%, and 42.2% isolation efficiency in reducing the contact pressure when subjected to El Centro input motion. PE₂ mat reinforcement in soft soil significantly reduced the contact pressure across the raft base with a maximum reduction factor of 1.73 (Fig. 5.4(a)). Rubber mat could act as good isolation material by reducing pressure distribution with a reduction factor of 1.3 i.e., about 22% reduction compared to unreinforced soft soil. PE₃ mat is found to be not efficient in reducing the differential settlement, but this reinforcement in soft soil reduces lateral slip as well as the contact pressure at the raft-soil interface. With PE₃ mat in soft soil, a 15% reduction in contact pressure from unreinforced soil is observed.

The pressure development under dynamic loads is influenced by soil flexibility. Stiff soil has high density and modulus of elasticity values. The findings show that the intensity of contact pressure is increased with an increase in the stiffness of the soil. Contact pressure developed beneath the raft base is 51.67% in the stiff soil than that of soft soil in the unreinforced soil-structure system. A contact pressure reduction factor (R_{Fc}) of 1.12 and 1.53 is seen in stiff soils, respectively when reinforced with PE₁ and PE₂ mats. A noticeable

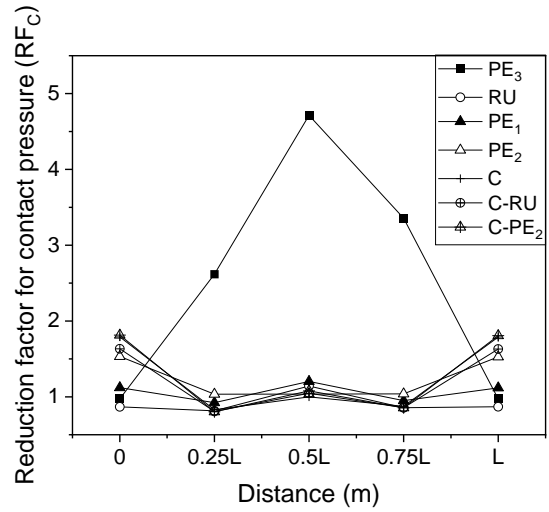
reduction in the pressure development below the raft foundation is not observed with the stiff soil enhanced by the RU mat.

Contact pressure developed below the raft foundation under IS input motion is examined. Under El Centro input motion, reinforced mats show higher isolation efficiency than under IS input motions. The maximum reduction in contact pressure is found to be with PE₂ mat in soft soil with an RFc of 1.2 and in stiff soil with an RFc of 1.4 (Fig. 5.4(c),(d)).

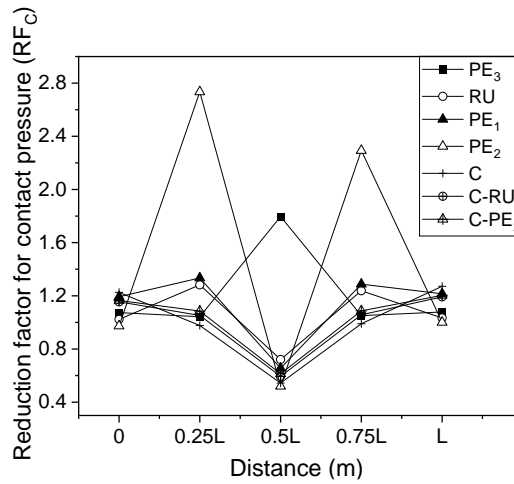
For soft soil reinforced with the mats of Case II materials, excited under El Centro input motion, soft soil strengthened by coir mat show a maximum RFc value among Case II materials, which is about 1.9 (Fig. 5.4(a)). The reduction factor of 1.71 and 1.72 is observed from C-RU and C-PE₂ mats enhanced soft soil. All the isolation mats impart their influence in efficiently reducing the seismic responses. The soil reinforcement by coir mat reduced the contact pressure nearly equally in both soft and stiff soils by about 46%.



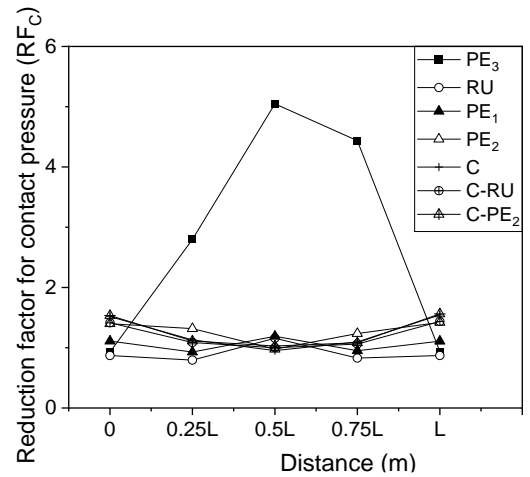
(a) El Centro-soft soil



(b) El Centro-stiff soil

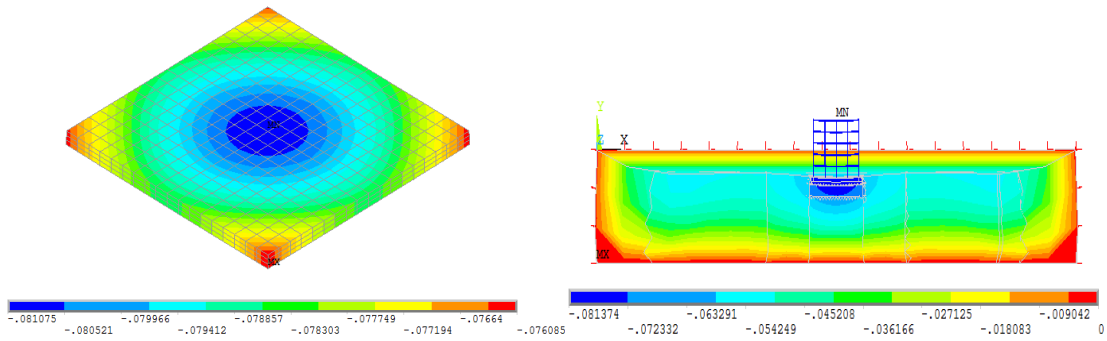


(c) IS-soft soil

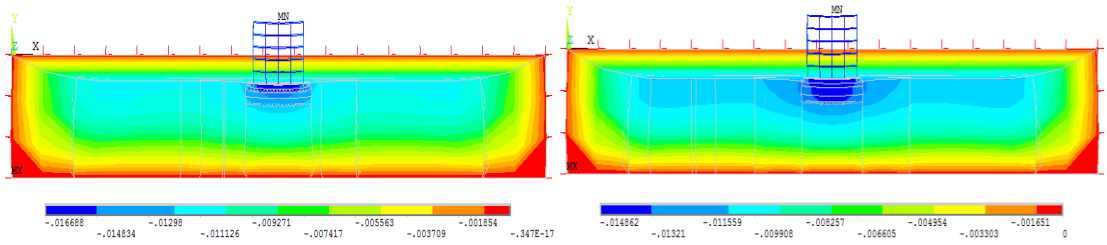


(d) IS-stiff soil

Figure 5.4 Reduction factor for contact pressure distribution along the length of raft foundation under different input motions



(a) raft foundation of the unreinforced soil (b) cross-section of the unreinforced soil-structure model



(c) soil reinforced with rubber mat (d) soil reinforced with coir mat

Figure 5.5 Vertical settlement along the length of raft foundation in soft soil

5.2.3 Total and Differential Settlement at Soil-Raft Foundation Interface

The settlement of the raft foundation should be as uniform as possible and it should be within permissible limits too. Therefore, it is important to avoid differential settlement rather than to maintain a uniform overall settlement of the structure. The settlement at the soil-raft foundation interface is noted and settlements are observed to differ over the length of the raft. In the middle, the vertical settlement is very small and increased to the edge of the raft foundation. Since the soil-structure system is laterally subjected to earthquake excitations, raft sliding is highly probable. The settlement is found to be dependent on soil flexibility. That is, the settlement of raft foundations decreases with the increase in soil flexibility. It is seen that soil deformation is very less in stiff soil since the raft foundation performs rigidly when interacts with stiff soil.

The permissible total settlement and differential settlement for raft foundation in the sand is 0.075m and 0.0021L for RCC structures according to IS 1904-1978 where, L is the center to center distance between columns in meters. It is found from the static analysis of the soft soil-structure system that the settlement (82mm) exceeds the permissible value given in the code and the soil must, therefore, be reinforced with a certain variety of isolation materials to enable the structures to resist the earthquake forces (Table 5.2). The raft-soil interface is an important area where energy is transferred from earthquake motions in the soil stratum to the superstructure. This makes the settlement at the interface a very critical parameter to be evaluated before and after the soil improvements.

Among Case I materials, the PE₂ mat shows 62.7% isolation efficiency to reduce the differential settlement in soft soil under El Centro input motion (Table 5.2). It marks the highest reduction in the differential settlement. PE₂ mat performs about two times better over PE₁ mat for the same. The isolation efficiency of reinforcement mats in reducing the settlement at the raft-soil interface is represented in terms of reduction factors (RFs) in Fig. 5.6. The deflection of the raft foundation is not significantly reduced by reinforcing with PE₃ mat in soft soil. The seismic response of the building is decreased by high-stiff reinforcement materials in the soil.

Table 5.2 Percentage reduction in differential settlement of raft foundation

Soil type	Input motion	Percentage reduction in differential settlement of raft foundation (%)						
		PE ₃	RU	PE ₁	PE ₂	C	C-RU	C-PE ₂
Soft	El Centro	12	27.2	35.8	62.7	46.6	44.1	50.1
	IS	5	25.2	32.6	58.5	40.7	39	39.9
Stiff	El Centro	10	16	30	43.2	42.1	41.1	42.5
	IS	4.5	11	20	37.4	37	36.6	30

Under IS input motion, a maximum reduction factor of 1.49 and 2.37 are obtained for the soft soil reinforced with PE₁ and PE₂ mats (Fig. 5.6(c)). In stiff soil, neither PE₃ nor RU mat reinforcement could reduce the settlement significantly when the SSI system is subjected to both the input motions.

From the study of soil strengthened with mats of Case II materials, the soft and stiff soil strengthened by C-PE₂ mat considerably reduces the differential settlement at the raft edges by about 50.1% and 42.5% respectively from unreinforced soil when it is excited under El Centro motions. The settlement is seen to be higher on the edges of the raft since the input motion has been applied to the soil structural system laterally.

From the analysis carried out to study the efficacy of isolation mats to reduce the differential settlement of raft foundations, it is concluded that differential settlement values seen for various isolated SSI systems analyzed under two different earthquake excitations are within permissible limits as per the code. The reinforcing mats show good RFs for soil-structure system excited under El Centro input motions compared to IS input motions. PE₂ and C-PE₂ mats are found to be more effective in reducing differential settlement of the raft foundation.

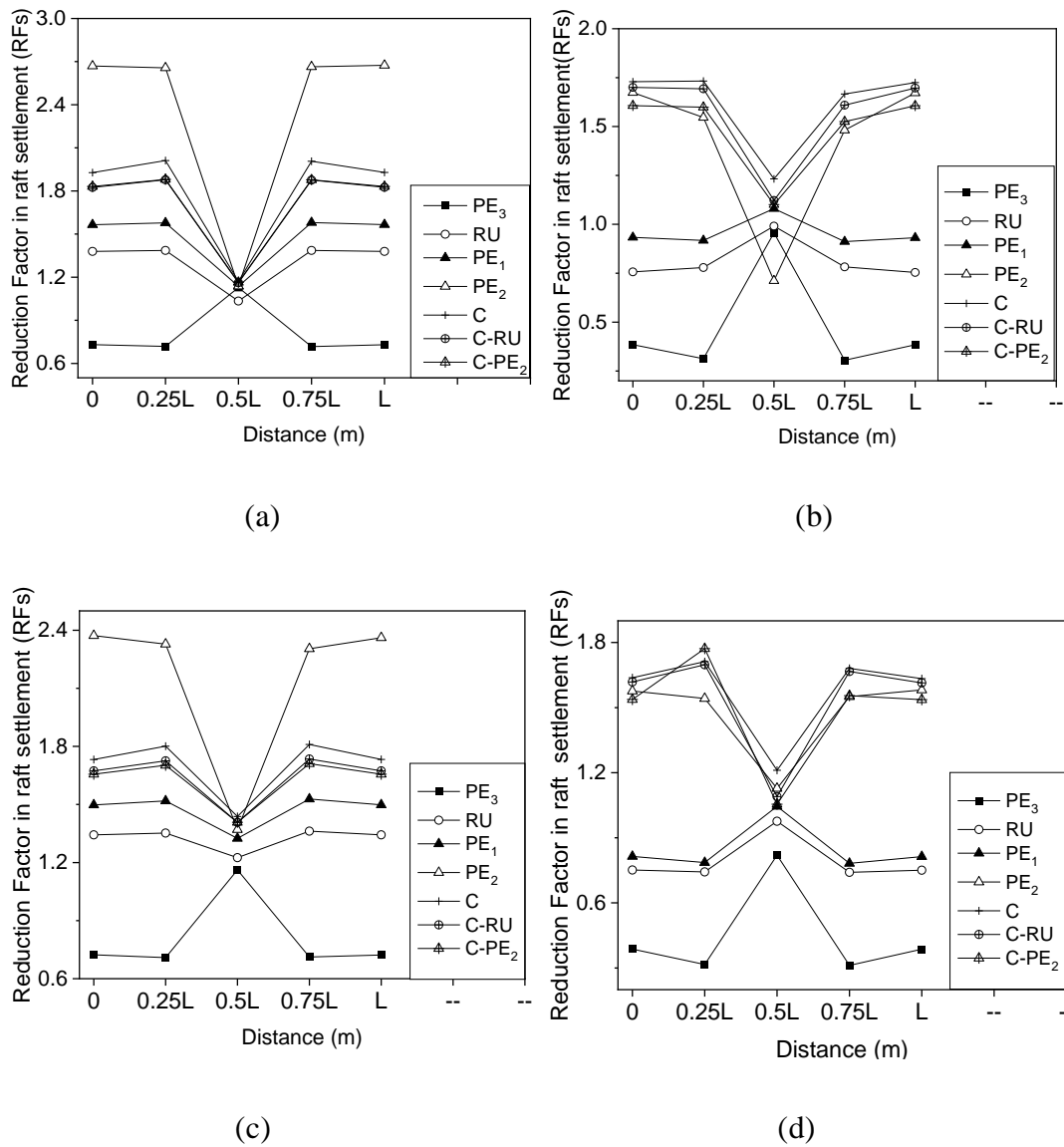


Figure 5.6 Reduction factor for total settlement along the length of raft foundation under (a) El Centro-soft soil (b) El Centro-stiff soil (c) IS-soft soil (d) IS-stiff soil.

5.2.4 Seismic Base Shear of Building

The variation in the base shear ratio (base shear divided by the weight of the building) is examined by considering the fixed base condition as well as incorporating the three-dimensional soil-structure interaction effect (Table 5.3). The isolated soil-

structure system is also analyzed and compared the isolation efficiency of reinforced mats to reduce the base shear of building. The base shear ratio is noted and represented in terms of the total weight of superstructure (Fig. 5.7). It is observed that the seismic base shear is more than the fixed base condition when the SSI effects are taken into consideration. With an increase in soil flexibility, the seismic base shear is increased. Isolation mats show a noticeable reduction in soft soil than in stiff soil.

It is seen that the soil condition has a pronounced effect on building base shear response. From the analysis of soil reinforced with isolation materials, a maximum of 23% and 22% reduction in the base shear value is observed with PE₂ mat and C-PE₂ mat reinforcement in soft soil. Stiff soil condition produces less base shear in buildings. Only below 10% reduction in base shear is observed while reinforcing stiff soil with all the isolation mats and excited under El Centro input motions (Fig. 5.7).

Table 5.3 Base shear ratio for buildings on a fixed base and flexible base

Earthquake	Base shear ratio (F')		
	Fixed base	Flexible base without isolation	
		Soft soil	Stiff soil
El Centro	0.046	0.18	0.06
IS	0.015	0.10	0.03

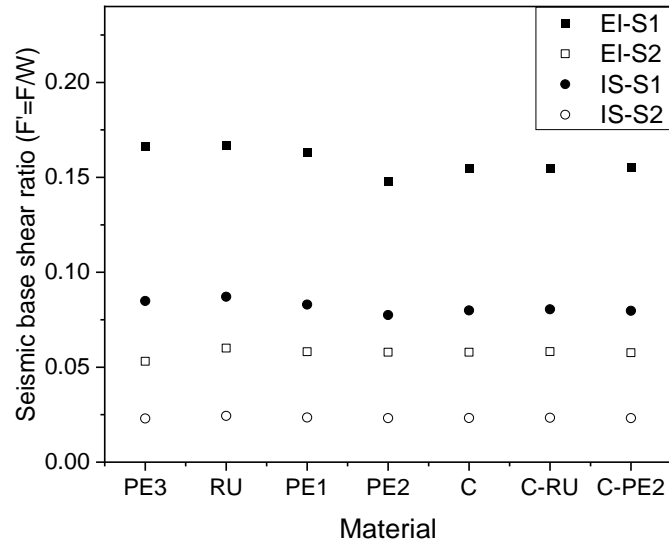


Figure 5.7 Seismic base shear of building on reinforced soil with various isolation mats

5.3 SUMMARY

The seismic response of buildings analysed from the linear analysis of SSI models is expressed in terms of roof acceleration and base shear, and that of raft foundation is represented in terms of total and differential settlement and contact pressure. Results show that as soil flexibility increases, seismic responses increase gradually. The natural frequency of the SSI system is lower than the natural frequency of the fixed base structure (1.96Hz), and about a 43% reduction in natural frequency is noticed when the underlying soil is soft. The roof acceleration of the building is increased in soft and stiff soil base supported systems by about 70% and 33% respectively, compared to the fixed base system subjected to El Centro input motion. The reinforcement of soft soil by the isolation mats effectively reduces seismic responses of building and raft foundations as compared with the reinforcement done in stiff soil. A maximum reduction in the building roof acceleration and base shear is observed as 22% and 23% by reinforcing soft soil with C-PE₂ and PE₂ mats. The PE₂ and C-PE₂ mats used as soil reinforcement materials effectively reduce the differential settlement of raft foundations compared to the other isolation materials. The PE₂ and C-PE₂ mats used resulted in an isolation efficiency of 62.7% and 50.1%, respectively. The maximum settlement reduction factor

(RFs) of 2.4 - 2.7 in soft soil is observed by reinforcing soil with PE₂ mat and about 1.8 in stiff soil by coir mat and its composites. The maximum reduction in contact pressure induced at the raft-soil interface is found to be 49% and 53% when the soft soil is reinforced with PE₂ mat and coir mat materials respectively.

Chapter 6

NONLINEAR ANALYSIS OF ISOLATED SOIL-STRUCTURE SYSTEM

6.1 GENERAL

The results from the soil-structure system (Fig. 3.4) analyzed by incorporating the linear properties of soil and isolation materials were discussed in the previous chapter. But, the soil and isolation materials can behave nonlinearly under dynamic loads. Therefore, it is important to conduct the nonlinear analysis also as a part of this research work. Rubber mat (RU), coir mat (C) and polymer foam (Epoxy polystyrene, PE₃) were considered for the nonlinear analysis of soil-structure system excited under EQ-1, EQ-2, EQ-3 and EQ-4 earthquake loads (Table 3.5). The seismic responses of the same soil-structure system (Fig. 3.4) were analyzed by incorporating the material nonlinearity and the findings were compared to select the best isolation material.

6.2 ROOF ACCELERATION AND ROOF DEFLECTION OF BUILDING

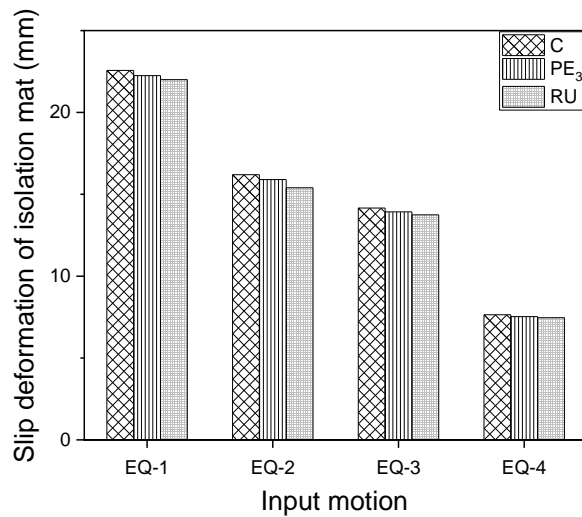
The roof acceleration response of the five-storey building was evaluated for the cases of unreinforced and reinforced soil base. Absolute roof acceleration was found to be reduced by the introduction of reinforcement materials in soil. Slip deformation of the isolation mats dissipates the energy of seismic excitations. The reduction in seismic response of building by this mechanism is expressed by comparing the slip deformation values of isolation materials (Fig. 6.1(a)). The coir mat shows higher deformation under all the input motions than other isolation mats, which means the seismic isolation by the slip deformation mechanism is found better by reinforcing soil with the coir mat. The isolation capacity of reinforcement materials is plotted (Fig. 6.1(b)). The percentage reduction in roof acceleration of buildings resting on soil reinforced with various mats compared to unreinforced soil was evaluated. Fig. 6.2 shows the time history of roof acceleration for coir reinforced soil-structure system excited under EQ-

1, EQ-2, EQ-3, and EQ-4 input motions. Maximum reduction in roof acceleration response is observed under EQ-3 input motion.

The study of soil strengthened with mats of coir, polymer foam and rubber respectively shows a maximum reduction of 34%, 30%, and 27% in the roof acceleration when subjected to EQ-3 input motion (Fig. 6.1(b)). Since the coir mat shows a considerable slip deformation among the isolation mats, roof acceleration is reduced by reinforcing the soil with the coir mat. The observed roof acceleration responses under input motion of EQ-1 are more significant than those with EQ-2, EQ-3 and EQ-4 input motions, as EQ-1 input motions have higher specific energy density than other input motions (Peak ground acceleration of all the input motions is 0.3g). Among the materials analyzed as the soil isolation material, it is found that the coir mat performs better over the rubber mat and polymer foam in reducing the roof acceleration response under dynamic loading. And the isolation efficiency of reinforcement materials is observed to be higher when the soil-structure system is subjected to El Centro input motion than other input motions. The main reason is that the frequency content of El Centro motions which matches with the fundamental frequency of soil-structure system is abundant.

Roof deflection response from the dynamic analysis of buildings is studied. It is observed that a maximum of 32% reduction in the roof deflection is observed by the reinforcement of soil with coir mat under EQ-3 input ground motion (Fig. 6.1(c)). Rubber mat and polymer foam show a maximum of 28% and 23% reduction under EQ-3 input motion. Performance-wise, isolation materials are suitable in the order of coir mat, polymer foam, and rubber mat to reduce the seismic responses. Building resting on fixed base conditions shows significantly fewer seismic responses in the building roof than when the soil-structure interaction is considered (Fig. 6.2, 6.3). Compared to the rigid base of the building, the roof acceleration and deflection of the structure are observed three times and ten times more in the building resting on an unreinforced soil bed. Therefore, it is clear from the results that the result of seismic responses in the building will be underestimated when the building is considered with rigid base conditions.

Generally, reinforcement materials and pile foundations are practiced to mitigate the seismic response of multi-storey buildings. For example, rubber was mixed in the form of tyre chips in the sand for 5m thick sand along with the piles to isolate seismic responses which showed an isolation efficiency of around 40% for roof acceleration in five-storey buildings. But in the current study, only the reinforcement of isolation mats with 0.5m thickness reduces the roof acceleration response of the building significantly with a maximum reduction of 34%.



(a)

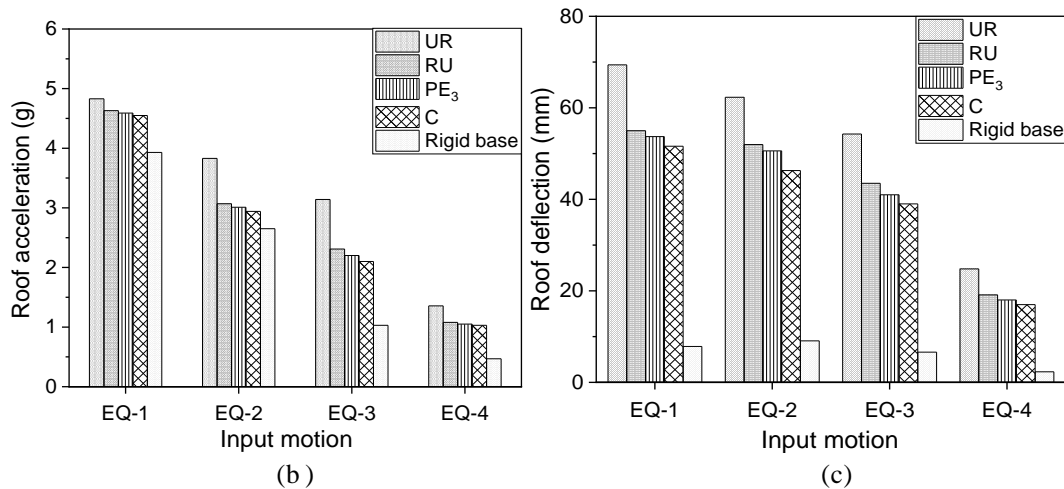


Figure 6.1 (a) Slip deformation of isolation mats under different earthquake input motions (b) roof acceleration (c) roof deflection (soil reinforced with different isolation mats) under different earthquake input motions

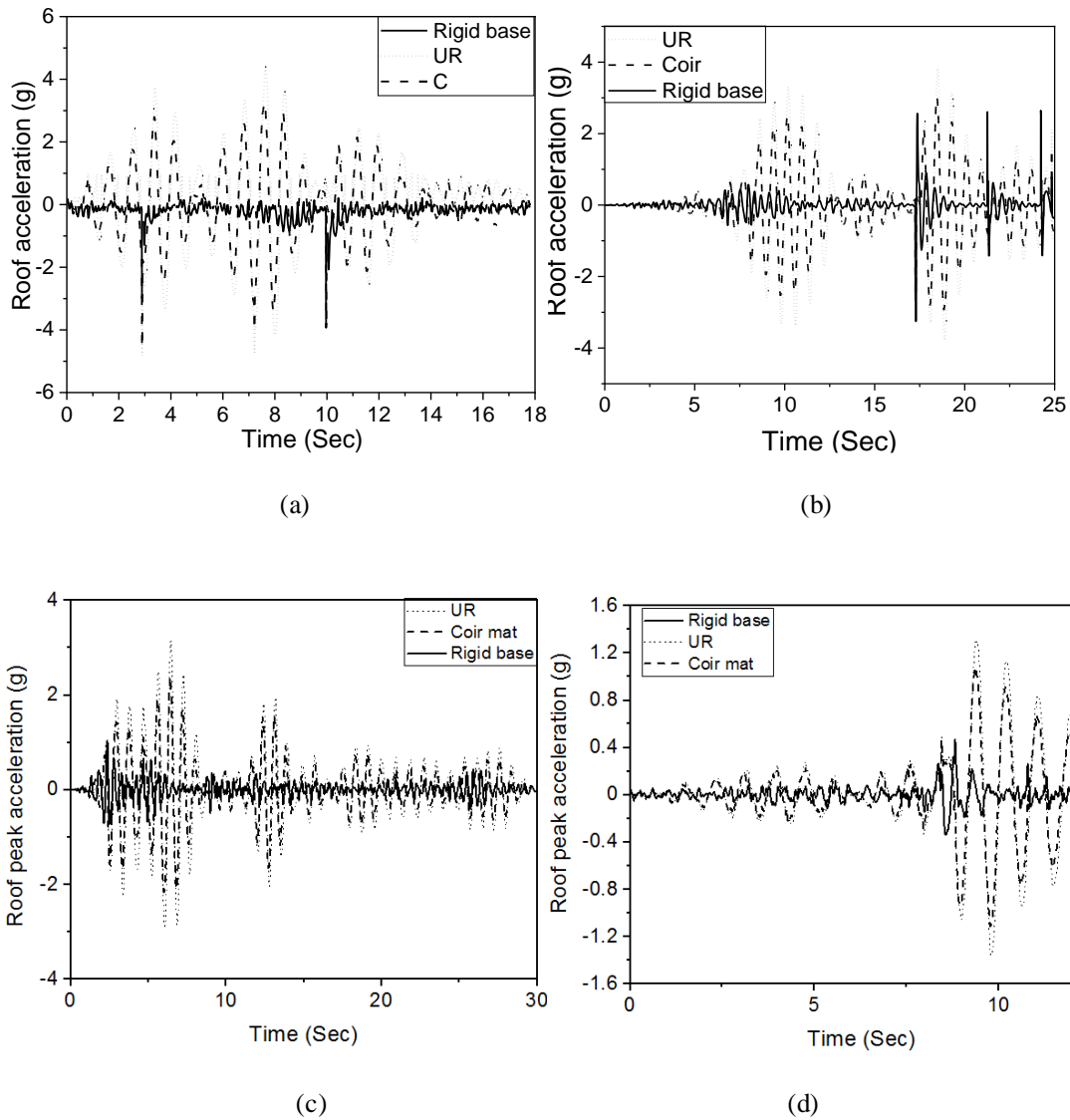


Figure 6.2 Roof acceleration time history plot of the soil-structure system for the rigid base, unreinforced and coir mat reinforced soil bases; (a) EQ-1 (b) EQ-2 (c) EQ-3 (d) EQ-4 input motions

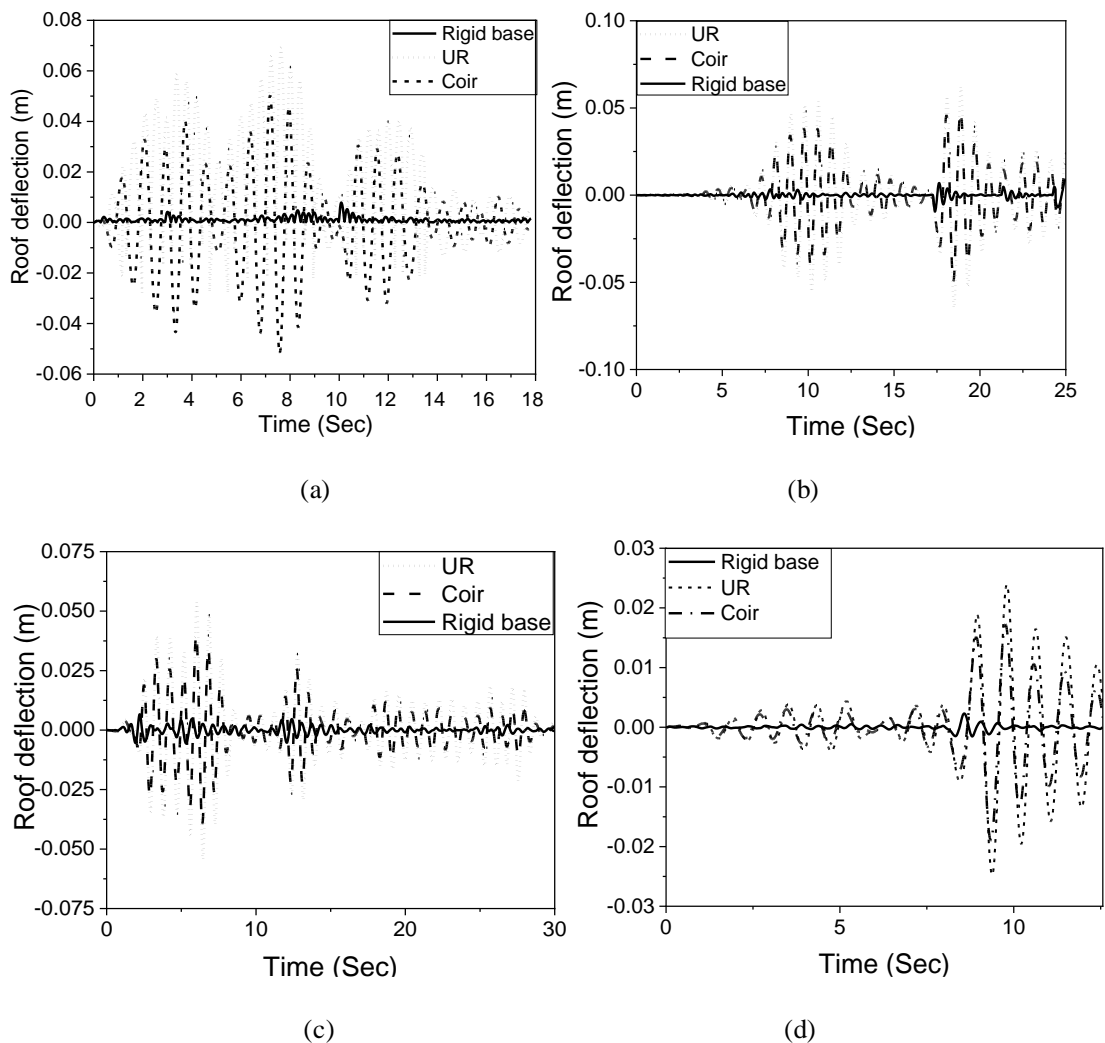


Figure 6.3 Roof deflection time history plot of the soil-structure system for the rigid base, unreinforced and coir mat reinforced soil base under (a) EQ-1 (a) EQ-2 (b) EQ-3 (c) EQ-4 input motions

6.3 INTERSTOREY DRIFT OF BUILDING

The interstorey drifts of the building resting on raft foundation having different base conditions were analysed under different earthquake motions (Fig. 6.4). Lateral deflection of the storey level increases with an increase in the height of the building, but the interstorey drift decreases with the height of the building i. e, the difference in lateral deflection of each nearest storey level decreases when the height of the building increases. Unreinforced soil shows an interstorey drift of 14, 5, 4 and 11 times more

compared to the rigid base case in the first storey level under EQ-1, EQ-2, EQ-3 and EQ-4 earthquakes respectively. While the reinforced and unreinforced cases of soil are compared, it is observed that soil reinforcement with isolation mats reduces the interstorey drifts in the building. Coir mat reinforced soil base shows a higher percentage reduction in interstorey drift among the isolation mats under all the earthquake motions. The maximum reduction observed is 40%, 43%, 50% and 44%, in the interstorey drift at the fifth storey level of the building under EQ-1, EQ-2, EQ-3 and EQ-4 earthquakes, respectively (Fig. 6.4).

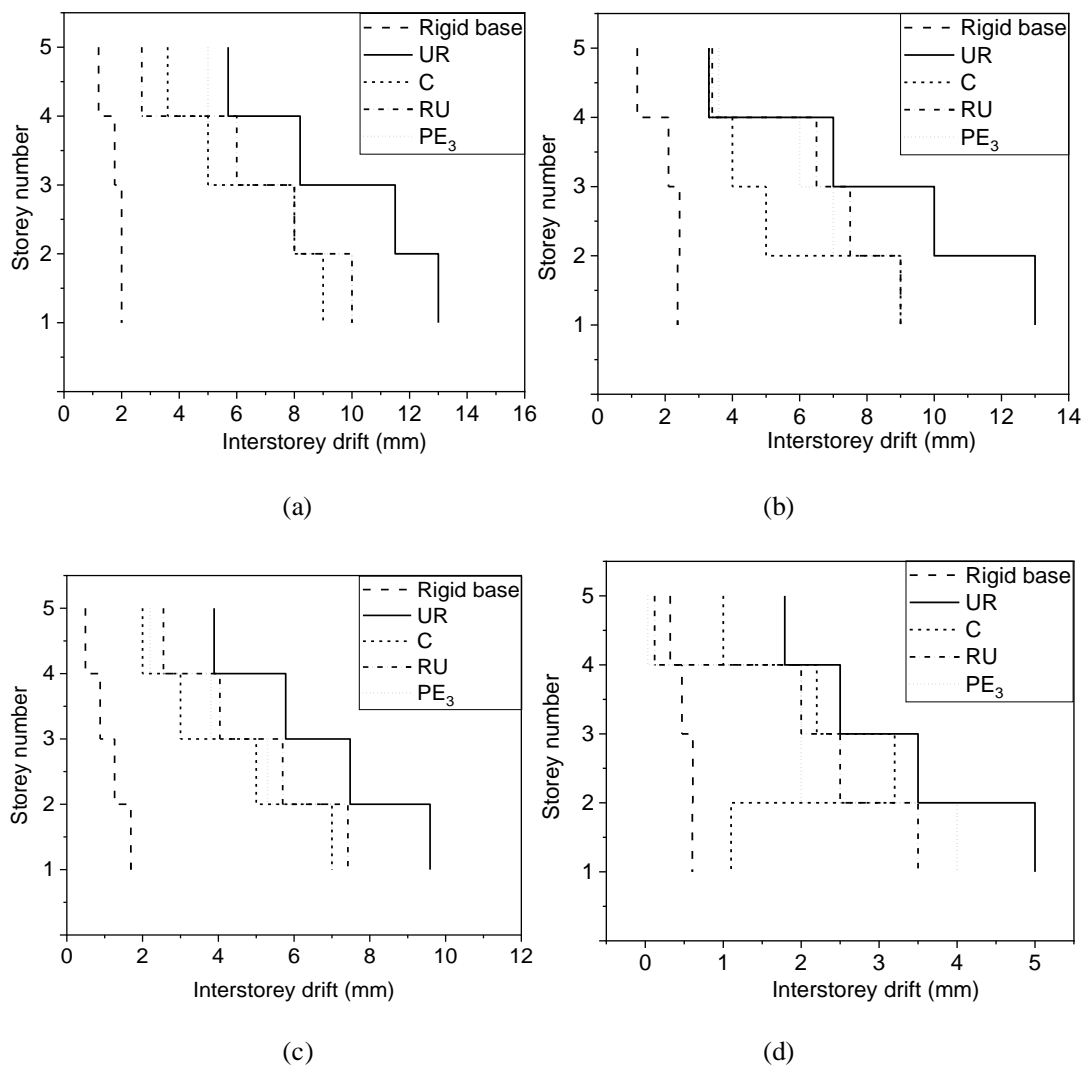


Figure 6.4 Interstorey drift of the building for the rigid, unreinforced and reinforced soil base under (a) EQ-1 (b) EQ-2 (c) EQ-3 (d) EQ-4 input motions

6.4 SEISMIC BASE SHEAR OF BUILDING

The variation in the base shear ratio (base shear divided by the weight of the building) obtained by considering the fixed base and incorporating the three-dimensional soil-structure interaction (SSI) effect was examined (Fig. 6.5).

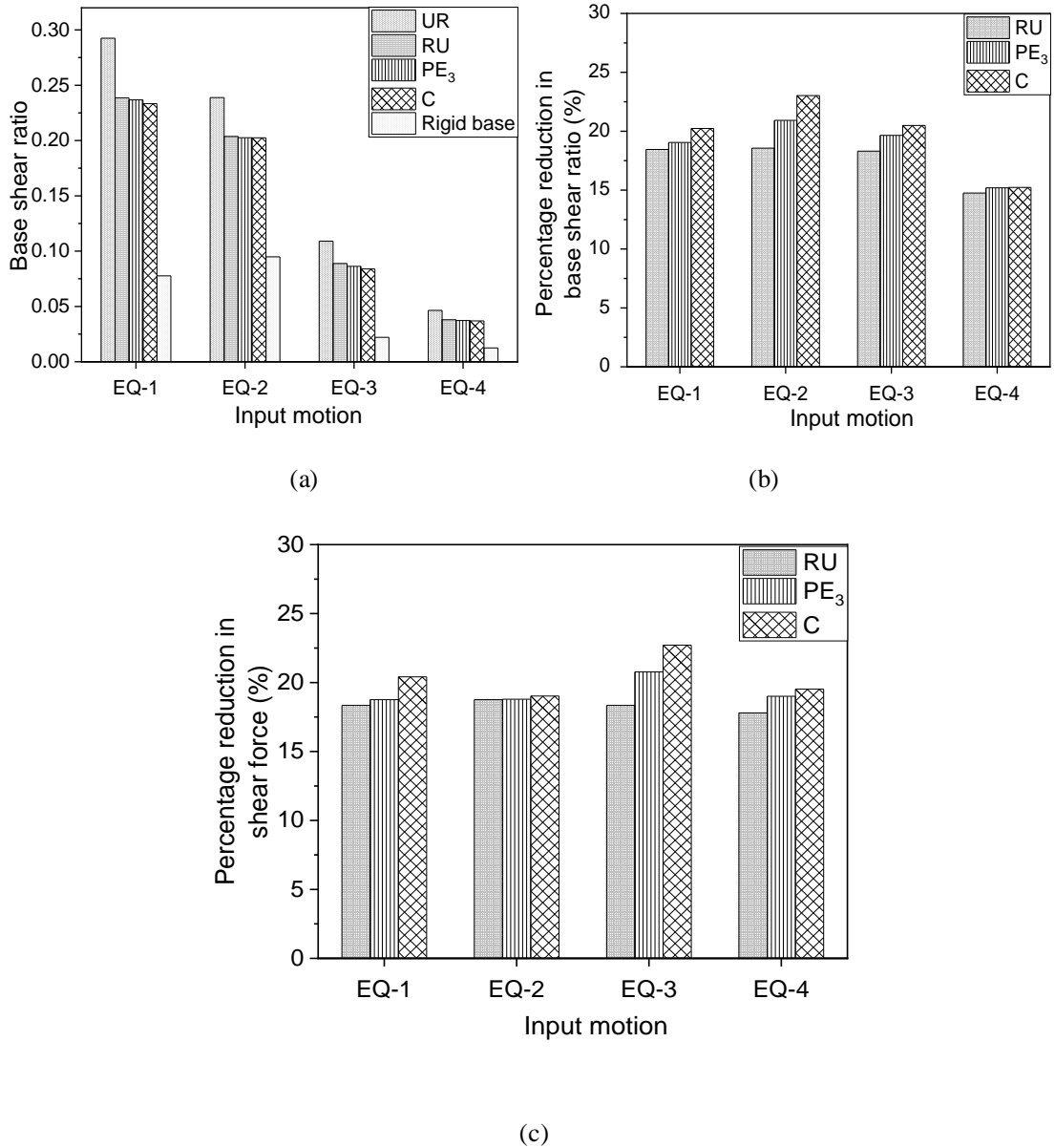


Figure 6.5 (a) Seismic base shear ratio of building on soil reinforced with various mats (b) Percentage reduction in the seismic base shear ratio (c) percentage reduction in seismic shear force of building on reinforced soil with various mats

The isolation efficiency of reinforcement mats to reduce the base shear in the isolated soil-structure system was also analyzed and compared. The base shear ratio is noted and represented in terms of total weight of the superstructure (Eq. 3.4) (Fig. 6.5(a)). It is observed that the seismic base shear is more than the fixed base condition when the SSI effects are taken into consideration (Fig. 6.5(a)).

It is seen from the analysis of soil reinforced with isolation mats that the reinforcement of soil by coir mat shows a maximum of 24% isolation efficiency when excited under EQ-3 input motion (Fig. 6.5(b)). The base shear observed in the soil-structure system subjected to EQ-1 input motions is higher than that observed with other input motions.

6.5 SHEAR FORCE OF BUILDING

In the SSI system for different cases of soil reinforcement, the shear force in the building was analyzed for different earthquake input motions. From the response of the structure by the application of dynamic load, the isolation efficiency of different reinforcement materials to reduce the seismic shear force is evaluated and represented in Fig. 6.5(c). The shear force in building at each storey level of building under rigid, unreinforced soil and isolation mat-reinforced soil base conditions are analysed and shown in Fig. 6.6. The shear force decreases with the increase in storey level for all the cases of the model considered. The importance of incorporating the soil-structure interaction and soil reinforcement by isolation mats is clear from the graph. It is observed that the seismic base shear is more than the fixed base condition when the SSI effects are taken into consideration and also the soil reinforcement reduces the seismic shear force in buildings under different earthquake loads.

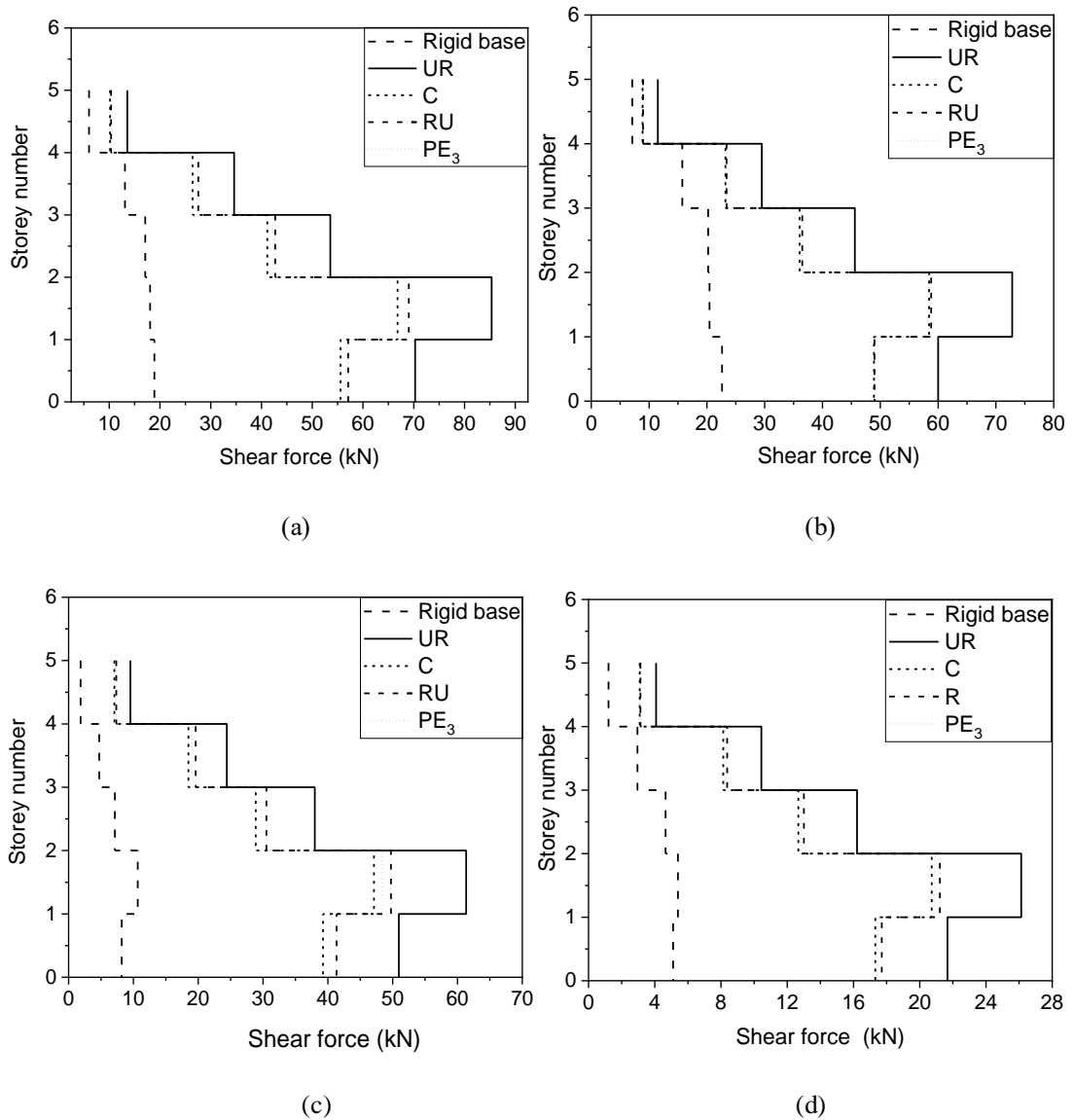


Figure 6.6 Storey shear force of the building for the rigid, unreinforced and reinforced soil base under (a) EQ-1 (b) EQ-2 (c) EQ-3 (d) EQ-4 input motions

The isolation efficiency of coir mat, polymer foam and rubber mat to reduce the seismic shear in building under EQ-3 input motion obtained at the fifth level of the building are 26%, 24%, 23% and that obtained at ground level are 23%, 21%, and 19% (Fig. 6.5(c)). Isolation mats show a good percentage reduction in seismic shear force under EQ-3 than other input motions since the low frequency contents of EQ-3 input motion is abundant, and the frequency of the SSI system is also low. The maximum reduction in shear force is obtained in the building by the reinforcement of soil with

coir mat. The maximum shear force observed in the building is higher under EQ-1 input motion (Fig. 6.6). The shear force-time history plot of the building for the unreinforced and coir mat reinforced soil base under various input motions is shown in Fig. 6.7.

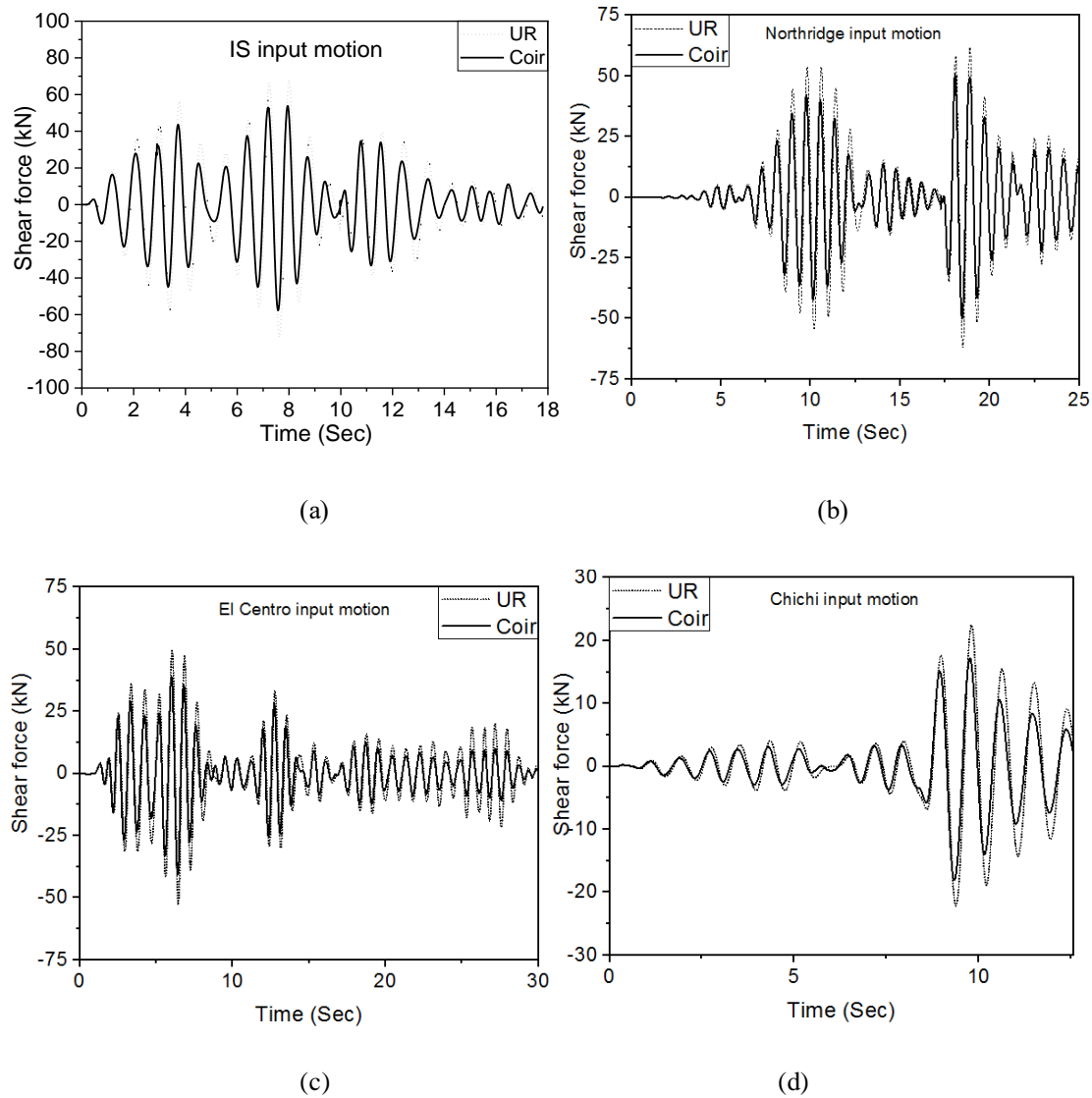


Figure 6.7 Shear force-time history plot of the building for the unreinforced and coir mat reinforced soil base under (a) EQ-1 (b) EQ-2 (c) EQ-3 (d) EQ-4 input motions

6.6 SUMMARY

The seismic responses such as roof acceleration, roof deflection, interstorey drift, base shear and shear force in building are studied from the nonlinear analysis of the isolated soil-structure system. A maximum reduction in the building roof acceleration is obtained as 34% by reinforcing soft soil with a coir mat when subjected to El Centro input motions and is 32% in reducing the roof deflection. A 50% reduction in the interstorey drift is obtained by the reinforcement of soil with the coir mat under the El Centro input motion. Base shear is higher for buildings resting on a flexible base compared to fixed base conditions. Seismic base shear is best reduced with coir mat reinforcement in soft soil, which is 23%. The maximum isolation efficiency of the coir mat obtained is 26% to reduce the seismic shear in the building and which is under EQ-3 input motion. The peak amplitudes are more in IS input motion than other ground motions. Therefore, seismic responses such as roof acceleration, roof deflection, interstorey drift, seismic base shear, and shear force in the building are found higher under IS input motions compared to other input motions. From the analysis of different input motions to the soil-structure system, it can be seen that with the increase in the specific energy density of earthquake motion, the soil-structure responses increase. But, due to the abundant lower frequencies available in the El Centro input motion compared to other input motions, the isolation efficiency of reinforcement materials is higher when the soil-structure system is subjected to El Centro input motion.

Chapter 7

PORE WATER PRESSURE ANALYSIS

7.1 GENERAL

Soil and structures are frequently exposed to both static and dynamic stresses. If the loads are high, they cause significant damage to soil and superstructures during earthquakes. The dynamic analysis allows the investigation of the impacts of vibrations in the soil. Vibrations in soil causes liquefaction when the excess pore water pressure in soil increases. Therefore, the reinforced cases of soil were analyzed by studying the excess pore pressure developed in soil and compared it with the unreinforced soil to understand the efficiency of isolation materials in reducing the liquefying tendency of soil. One-dimensional FEM software Cyclic 1D and three-dimensional FEM software PLAXIS 3D were used to investigate the development of pore water pressure. The natural material, coir mat (C) and its composites with, polystyrene (C-PE₃) and rubber mat (C-RU) were used as the isolation materials to study the isolation efficiency in effectively reducing the excess pore water pressure in soil under earthquake loads.

7.2 MODELLING IN CYCLIC 1D

The modeling of soil for liquefaction analysis was performed using FEM. Cyclic 1D is a nonlinear Finite Element program for one-dimensional (1D) lateral dynamic site-response simulations. The program works in the time domain, allowing for linear and nonlinear studies of soil (Hughes 1987). Incremental plasticity models simulate nonlinearity to qualify for permanent modeling deformation and generation of hysteretic damping.

The depth of the soil bed modeled was 30m. Input parameters were assigned corresponding to the engineering properties of soft soil and isolation materials as shown in Table 3.3. In Cyclic 1D, a finite element mesh composed of elements of 0.25m size was used to discretize the soil domain. The coir mat was modeled by assigning coir

material properties for 0.5 m thick elements at 1 m below ground level. Coir composites are modeled with 0.5m thick coir mat sandwiched by 0.5m thick polystyrene foam/ rubber mat to form C-PE₃ and C-RU composites. A simple model of soft soil with and without isolation mat inclusion was analyzed. At a depth of 30 m below ground level, rigid bedrock has been defined. Earthquake motion corresponding to El Centro (1940) and Northridge (1994) earthquakes were used as the input motion for seismic analysis.

7.2.2 Pore Water Pressure Analysis in Cyclic 1D

Dynamic analysis of soil model was carried out in Cyclic 1D software by using in-built earthquake acceleration data, El Centro (1940) and Northridge (1994) input motions. From the study, change in excess pore water pressure was analyzed for various soil depths below the ground. The soil becomes liquefiable when the excess pore pressure increases beyond a threshold necessitating the importance of mitigation of liquefaction. For this the natural material coir and its composites such as C-PE₃ and C-RU mats were considered as the isolation materials in soil to reduce the excess pore water pressure. The change in pore water pressure by the soil reinforcement with coir mat for the entire depth of soil is studied and shown in Fig. 7.1. Among the isolation materials analyzed, C-PE₃ performs with excellent features by significantly reducing the excess pore water pressure generated beneath the foundation. A maximum of 93% reduction is obtained by the reinforcement of soil with C-PE₃ mat under El Centro input motion and it is 88% under Northridge motion. Since, the polystyrene material is impermeable and provided at the top and bottom of the coir mat in C-PE₃ composite, the composite material shows very good efficiency in reducing the pore water pressure development in soil compared to the coir mat alone. Excess pore water pressure increased with an increase in soil depth below the foundation. For both reinforced and unreinforced soil cases, the excess pore water pressure-time history obtained under El Centro and Northridge earthquake motions is shown in Fig. 7.2 and Fig. 7.3. Fig. 7.4 shows the percentage reduction in excess pore pressure in the soil domain near the ground surface for unreinforced and reinforced soil (soil reinforcement with C, C-PE₃ and C-RU) under El Centro and Northridge input motion. The excess pore water pressure near the ground surface is noted both for reinforced and unreinforced cases of soil conditions and the percentage reduction is obtained by using Eqn 3.3. The excess

pore water pressure increases when the duration of earthquake increases. But, after a particular duration, pore water pressure becomes constant.

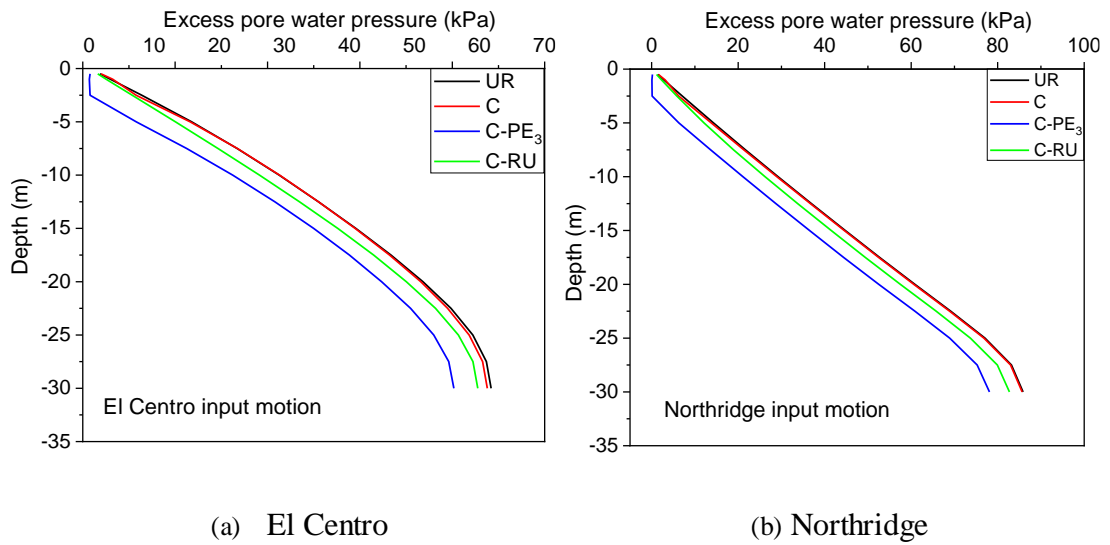
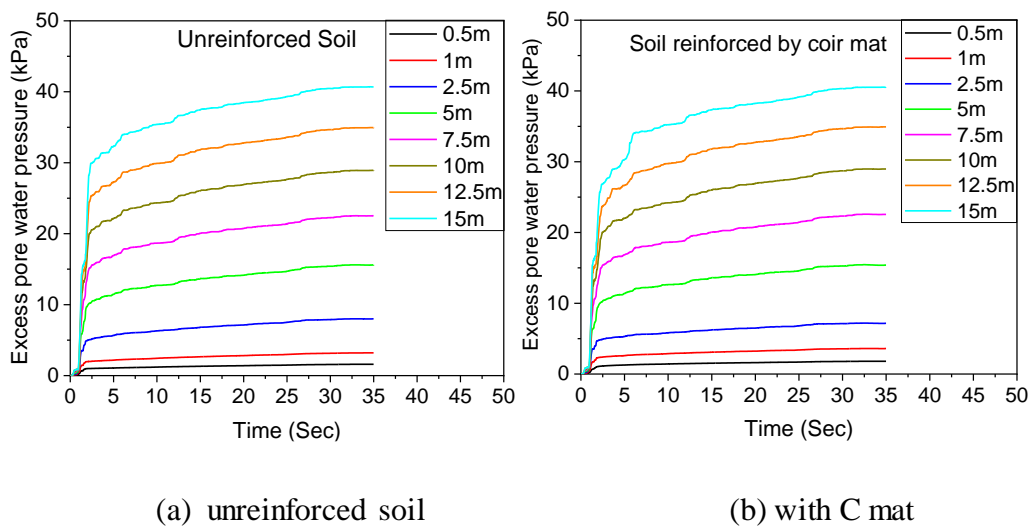
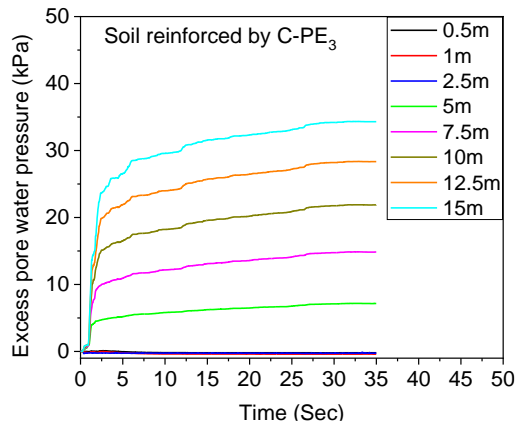
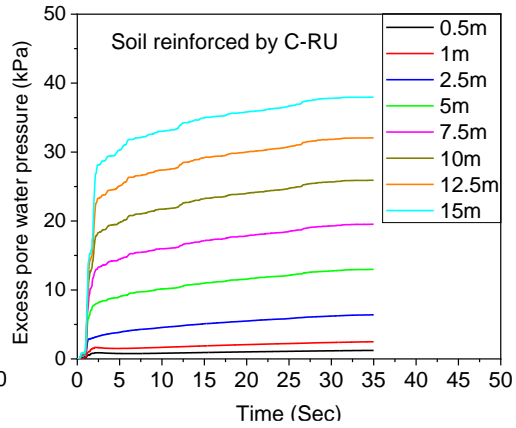


Figure 7.1 Variation in excess pore water pressure with the depth of soil domain for unreinforced (UR) and soil reinforcement with C, C-PE₃ and C-RU mats



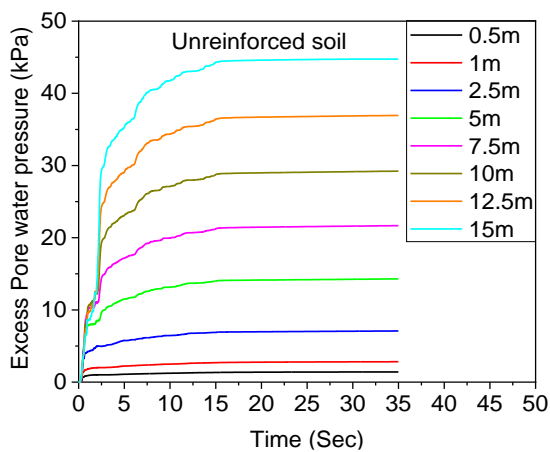


(c) with C-PE₃

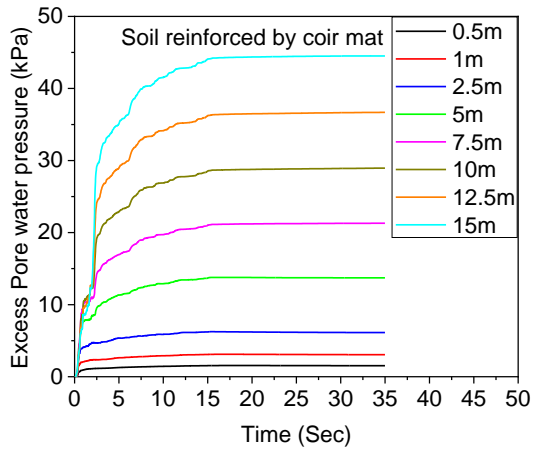


(d) with C-RU

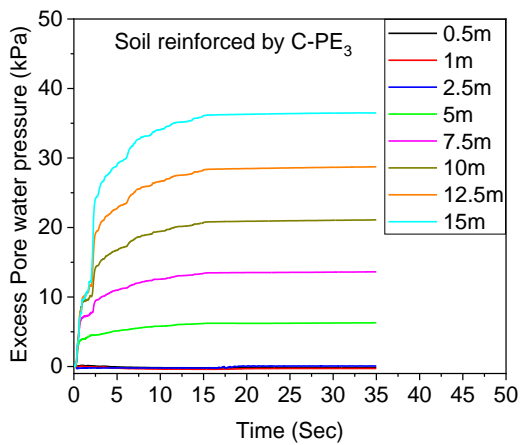
Figure 7.2 Excess pore pressure-time history plot of the soil domain at different depths below the ground level under El Centro input motion



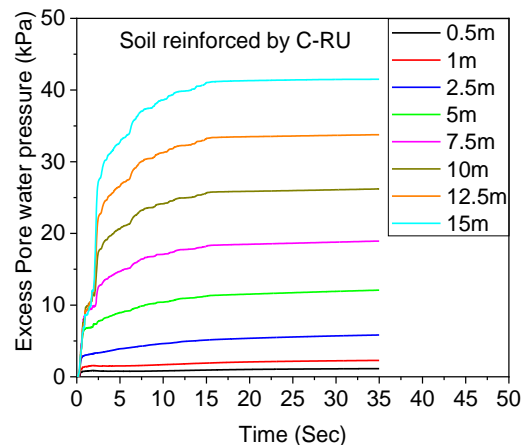
(a) unreinforced soil



(b) with C mat



(c) with C-PE₃



(d) with C-RU

Figure 7.3 Excess pore pressure-time history plot of the soil domain at different depths below the ground level under Northridge input motion

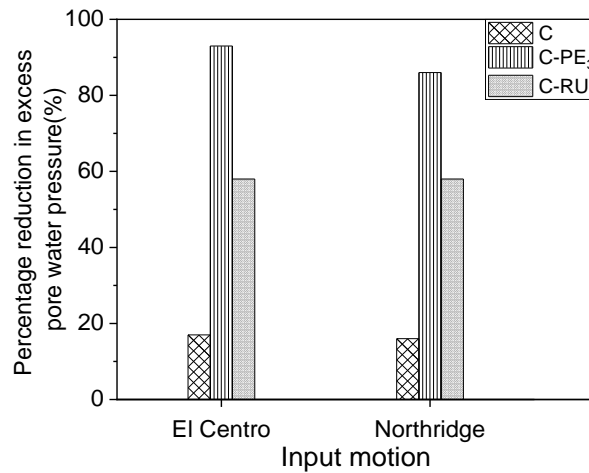


Figure 7.4 Percentage reduction in excess pore pressure in the soil domain near the ground surface for isolated soil base under El Centro and Northridge input motion

7.3 PORE WATER PRESSURE ANALYSIS IN PLAXIS 3D

The pore water pressure generated, mobilised shear strength, shear strain and effective stress in soil under the seismic motions of the soil-structure system were analysed. The efficacy of isolation materials to reduce this excess pore water pressure generated in soil was also investigated.

7.3.1 Excess Pore Water Pressure in Soil (P_{excess})

The soil in which significant pore water pressure is generated on a change in load is the most likely to liquefy. Excess pore water pressure in soil for both reinforced and unreinforced cases of soil was analyzed for different input motions. P_{excess} was noted beneath the raft foundation for unreinforced and reinforced soil. With the increase in time, pore pressure is observed to be increased for all reinforced cases of soil. The reduction in P_{excess} in soil under EQ-1, EQ-2, EQ-3, and EQ-4 earthquake motions

obtained with the reinforcement by C mat is 76%, 75%, 82% & 81.5%, respectively, by C-PE₃ mat is 72%, 71%, 77% & 79.3% respectively and by C-RU mat is 67%, 70%, 72% & 72% respectively (Fig. 7.5). Among the isolation mats reinforced in soil, the coir mat reduces the P_{excess} in soil considerably. Since, there is a chance for water to flow through the entire length of the coir mat when the coir mat is solely placed in the soil, the coir mat absorbs the water through its entire surfaces and reduces the further flow to the topsoil, near the foundation. When the C-PE₃ and C-RU are implemented in the soil, the impermeable materials such as polymer foam and rubber mat do not absorb the water; therefore, there is a chance for water to pass through the sidewise of isolation material to reach the foundation level. It's observed from the results that there is not much difference in pore water pressure generated in soil when it was reinforced with C, C-PE₃ and C-RU composites. Since coir is a natural material, there is a chance of degradation in the material as time goes on. Therefore, the provision of coir-polymer and coir-rubber composite mats are recommended. And, especially coir-polymer mat shows much more isolation efficiency in reducing the P_{excess} compared to coir-rubber. The variation in P_{excess} with the increase in depth of soil below the foundation was also analyzed. Fig. 7.5 shows the excess pore water pressure-time history in soil for reinforced and unreinforced cases under different earthquake input motions. The excess pore water pressure distribution in the soil at its central portion covering the superstructure for reinforced and unreinforced cases of soil was also analyzed and shown in Fig. 7.6. It is clear from the contour plot that the intensity of pore water pressure reduced at the soil-foundation interface when the coir reinforcement was incorporated in the soil.

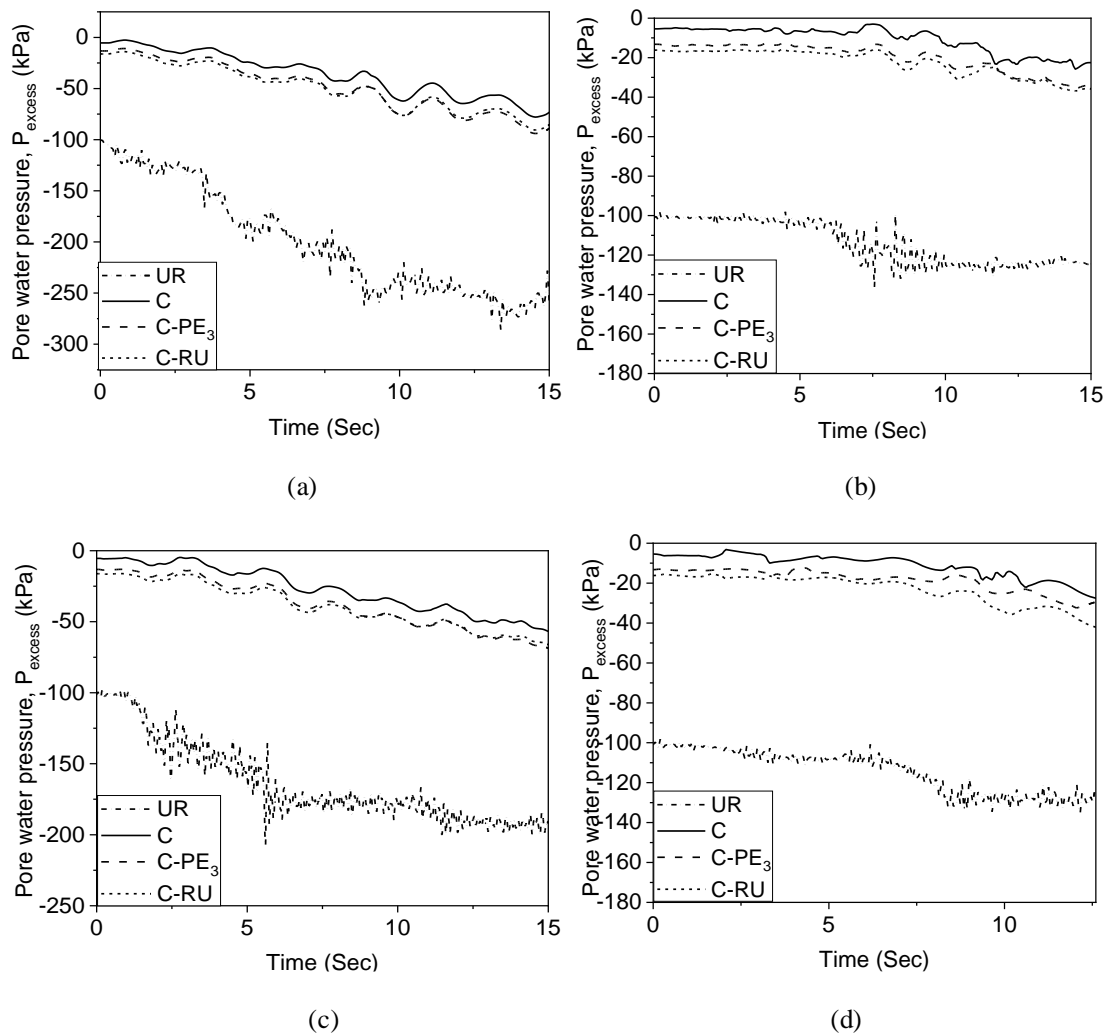
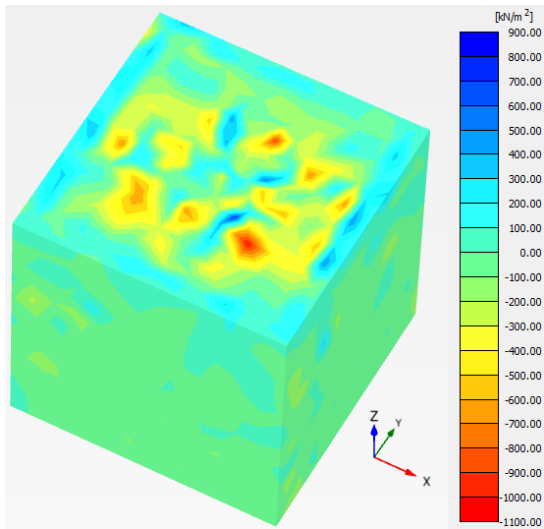
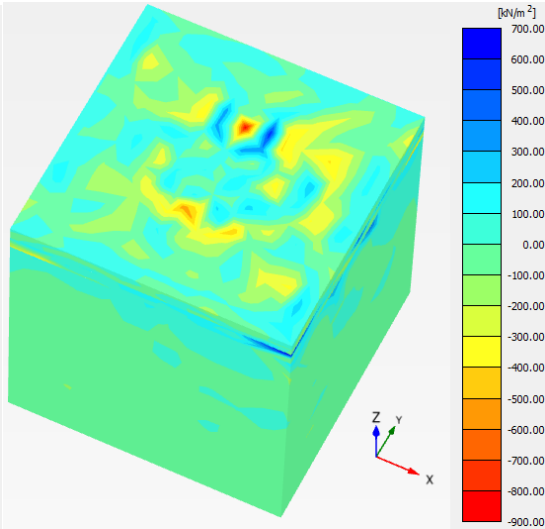


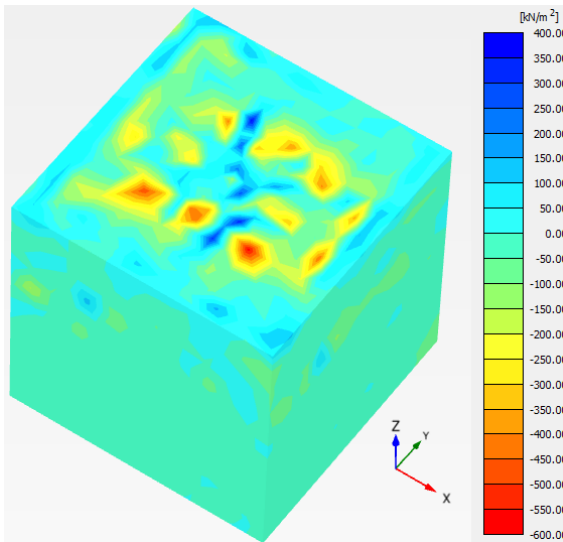
Figure 7.5 Excess pore water pressure-time history in soil for reinforced and unreinforced cases under different earthquake input motions; (a) EQ-1, (b) EQ-2, (c) EQ-3, (d) EQ-4



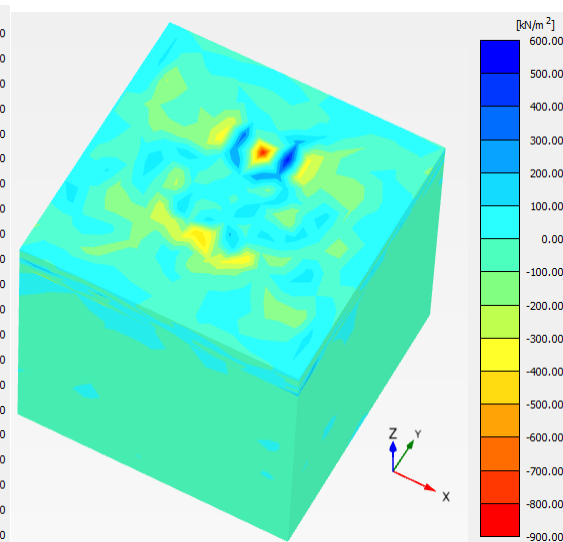
(a) Unreinforced soil



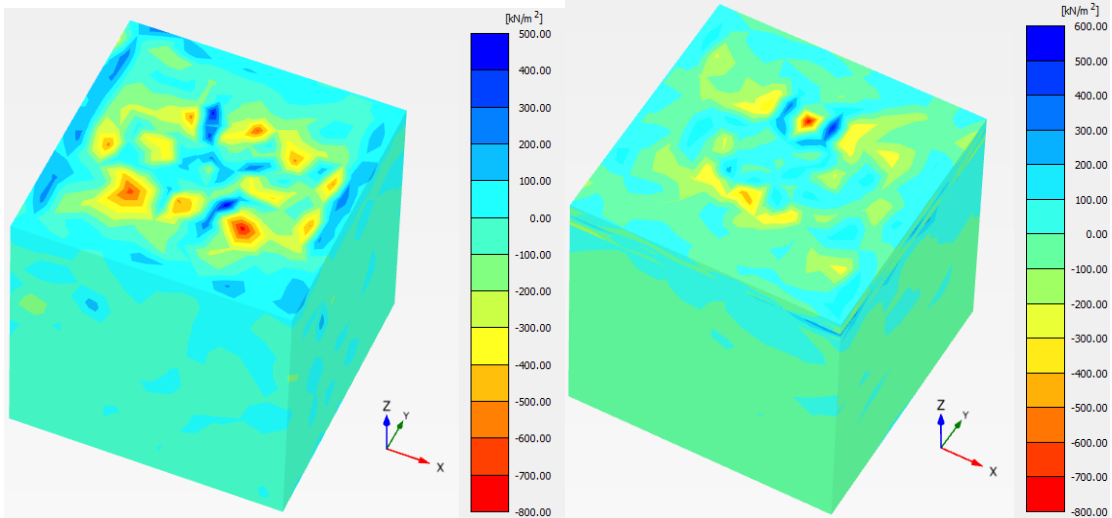
(b) Reinforced soil



(c) Unreinforced soil

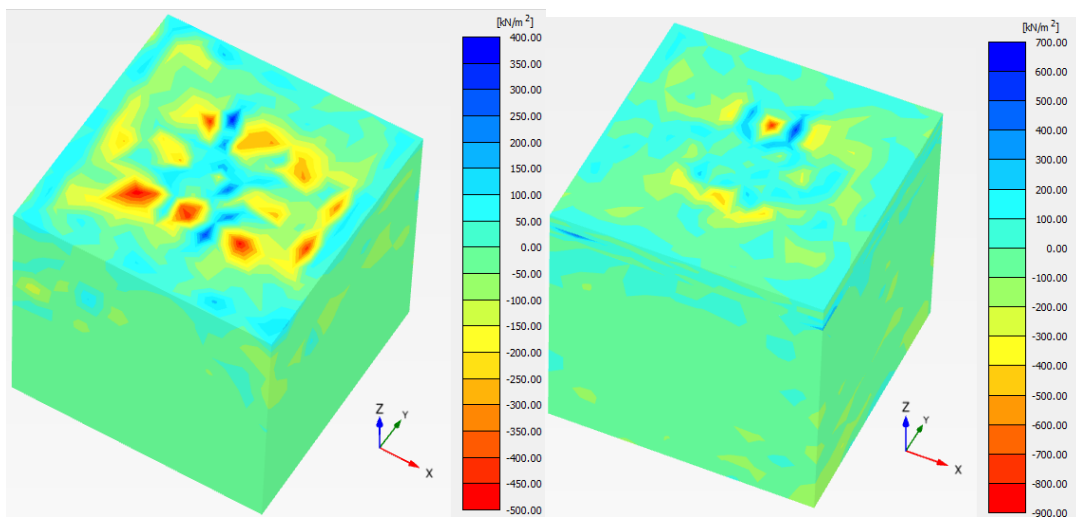


(d) Reinforced soil



(e) Unreinforced soil

(f) Reinforced soil



(g) Unreinforced soil

(h) Reinforced soil

Figure 7.6 Excess pore water pressure distribution in the soil at its central portion below the superstructure for coir mat reinforced and unreinforced cases of soil excited under; (a)-(b) EQ-1 (c)-(d) EQ-2 (e)-(f) EQ-3 (g)-(h) EQ-4

7.3.2 Shear Strain and Mobilized Shear Strength

The increase in seismic-induced soil shear strain and reduction in shear strength are major concern for the overall stability of structures. With the reinforcement of isolation mats in the soil, the shear strain of soil decreases by the increase in the mobilized shear strength. The shear strain and shear strength of soil beneath the foundation were analyzed for different models under various earthquake motions. Reinforcement reduces the shear strain in the soil since the isolation materials modify the shear strength of soil. Dynamic analysis was performed on the soil-structure system for soil without reinforcement and soil with C, C-PE₃ and C-RU mats placed horizontally below the raft foundation. Fig. 7.7 shows shear strain in reinforced and unreinforced soil. With the increase in the duration of earthquake motion, shear strain in the soil also increases. Shear strain is reduced for soil reinforced by isolation mats. The reduction in shear strain in soil under EQ-1, EQ-2, EQ-3, and EQ-4 earthquake motions obtained by the reinforcement of soil with C mat is 5%, 26.13%, 43.4% & 16% respectively, with C-PE₃ mat is 19%, 81%, 51% & 72% respectively and with C-RU mat is 21.46%, 83.1%, 57% & 20% respectively (Fig. 7.7). This is because the isolation mats act as the reinforcement layer in the soil, strengthening the soil and reducing the shear strain by increasing its shear strength. C-RU material does not show a proportionate shear strain development in soil under different input motions. Under EQ-4 input motion, the shear strain developed in soil by the reinforcement of C-RU material is found to be higher than C-PE₃ composite. But under all other input motions, C-PE₃ performs better over C-RU in the shear strain reduction in soil. The frequency content of EQ-4 does not match with the natural frequency of the soil reinforced with C-RU mat. Therefore, the complete efficiency of material to reduce the shear strain in soil couldn't be attained. The change in mobilized shear strength in reinforced soil compared to the unreinforced soil under different input motions is shown by the contour diagram in Figs. 7.8, 7.9, 7.10 and 7.11. The mobilized shear strength at the top and bottom interfaces of isolation materials is analyzed. The results show that compared to the bottom interface of polymer/rubber-coir mats, the top interface shows higher mobilized shear strength which means the additional layer of isolation material helps in improving the shear mobilization in soil.

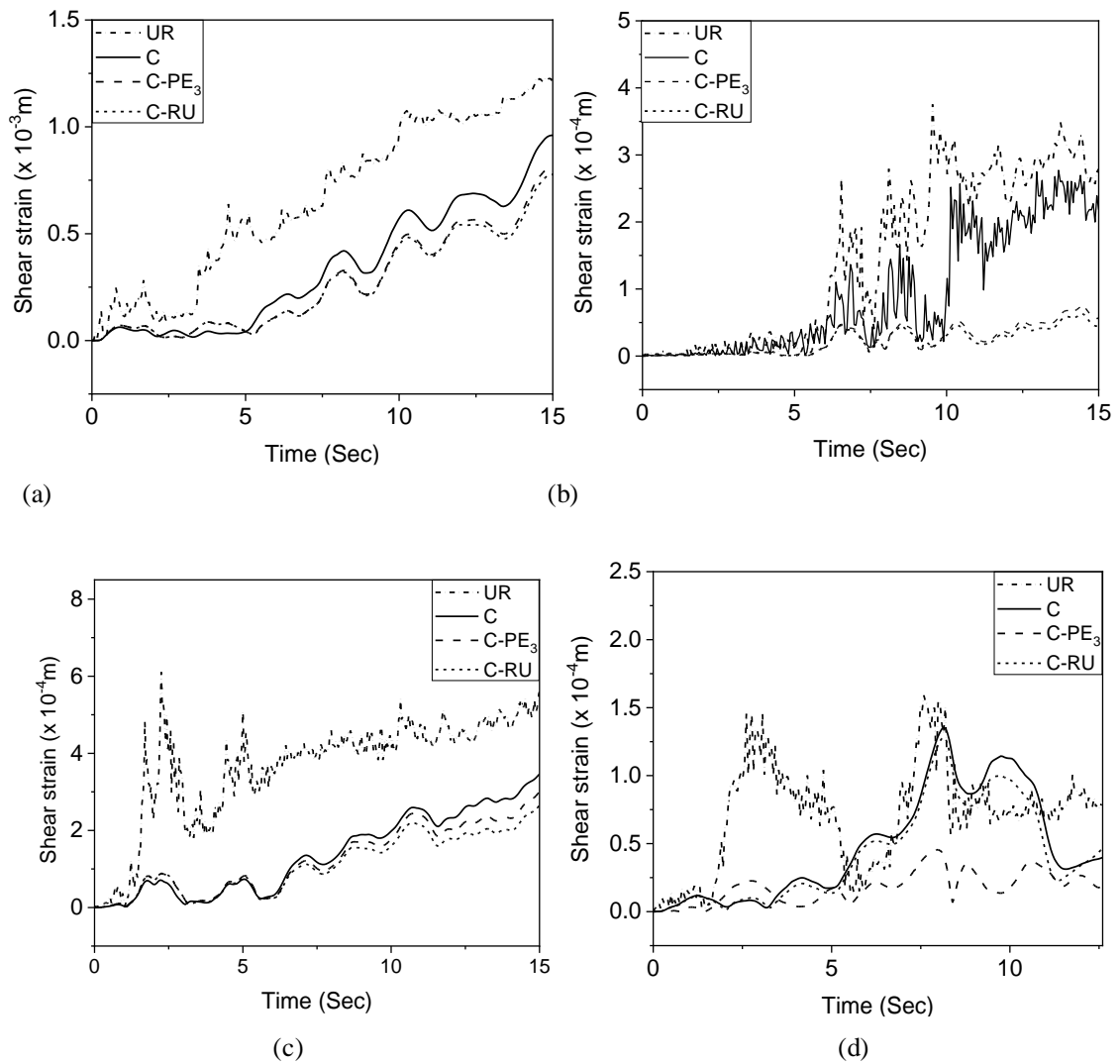
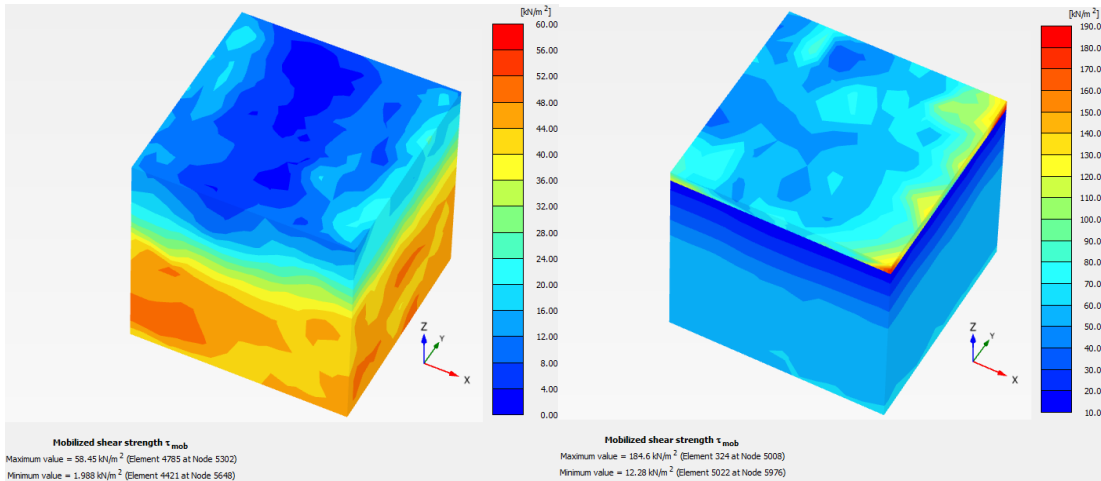
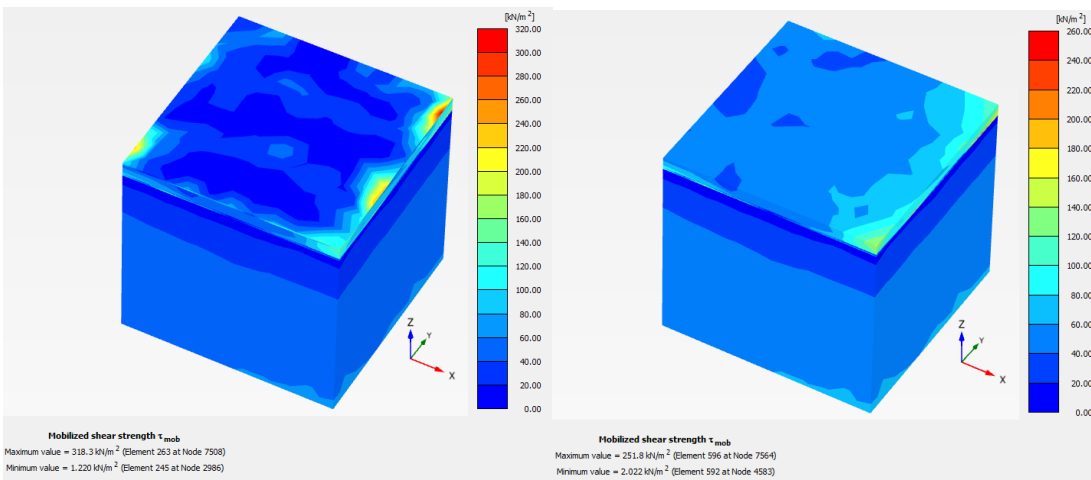


Figure 7.7 Shear strain time history in the soil for reinforced and unreinforced cases under different earthquake input motions; (a) EQ-1, (b) EQ-2, (c) EQ-3, (d) EQ-4.



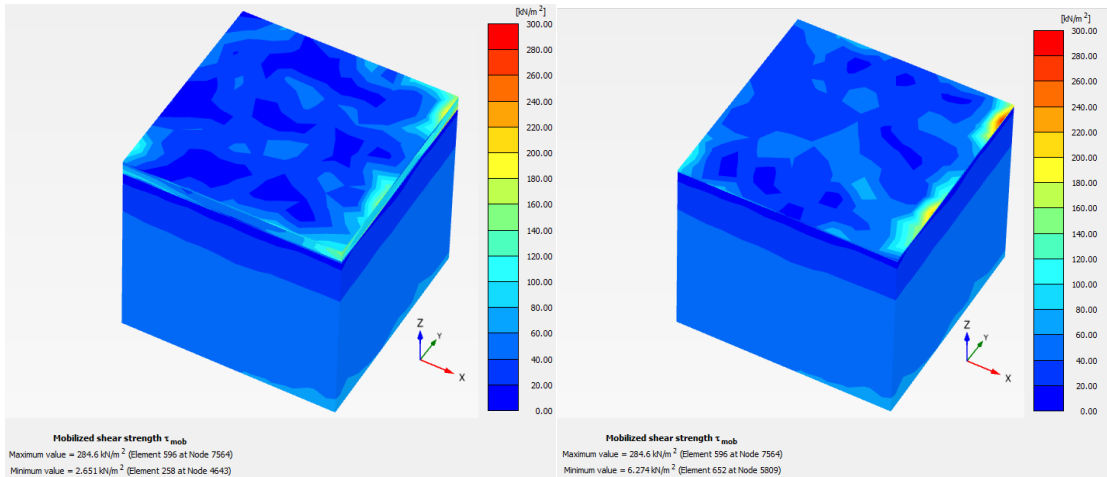
(a) unreinforced soil

(b) soil reinforced with coir mat



(c) at top coir-polymer interface

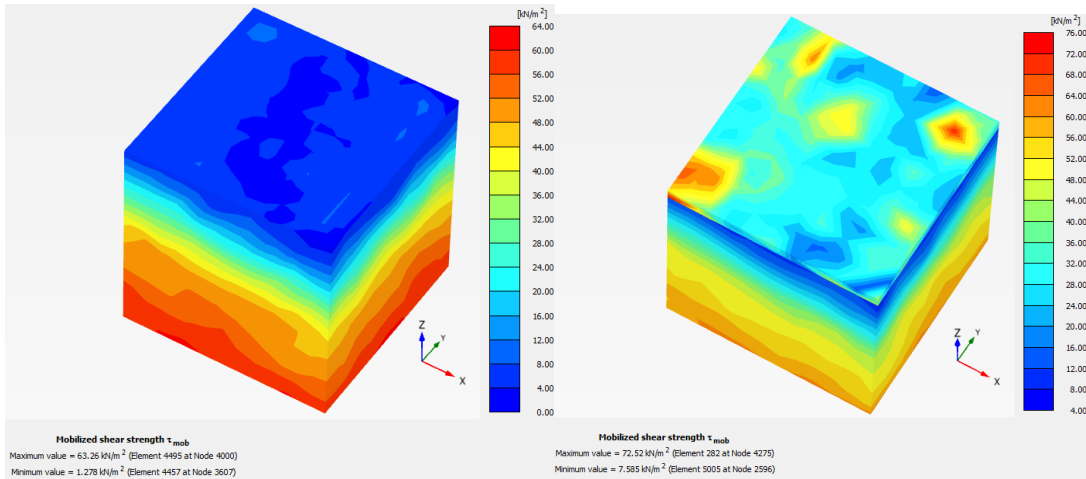
(d) at bottom coir-polymer interface



(e) at top coir-rubber interface

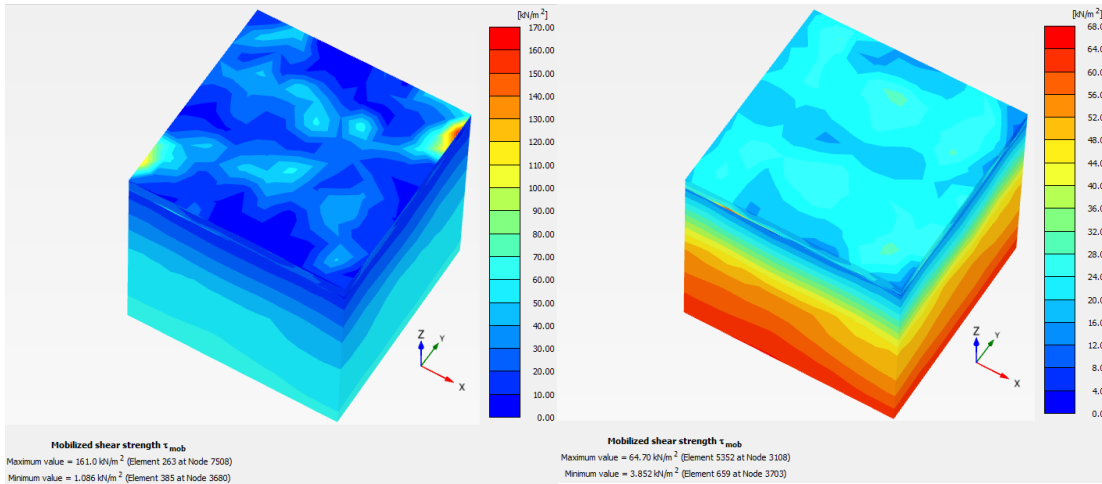
(f) at bottom coir-rubber interface

Figure 7.8 Mobilized shear strength in the soil at its central portion below the superstructure excited under EQ-1 input motion



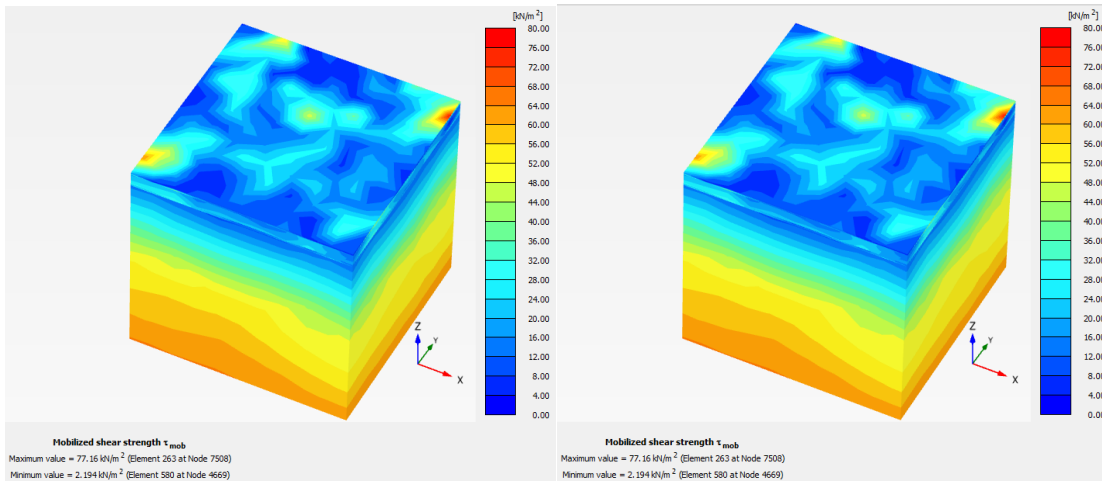
(a) unreinforced soil

(b) soil reinforced with coir mat



(c) at top coir-polymer interface

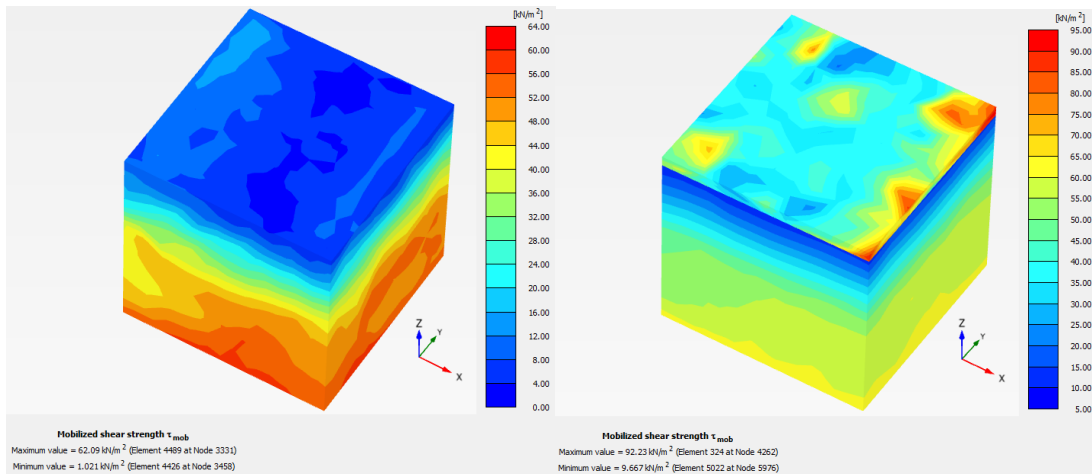
(d) at bottom coir-polymer interface



(e) at top coir-rubber interface

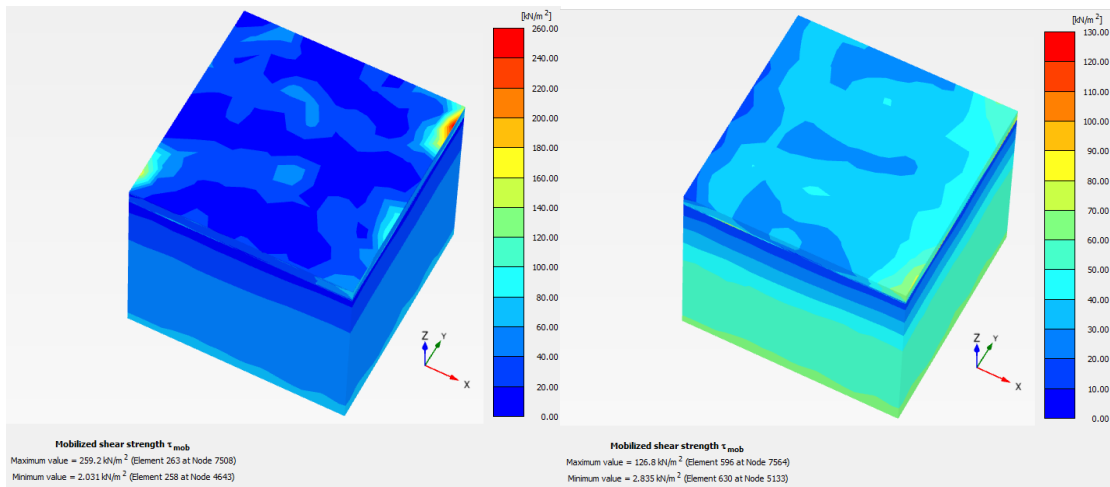
(f) at bottom coir-rubber interface

Figure 7.9 Mobilized shear strength in the soil at its central portion below the superstructure excited under EQ-2 input motion



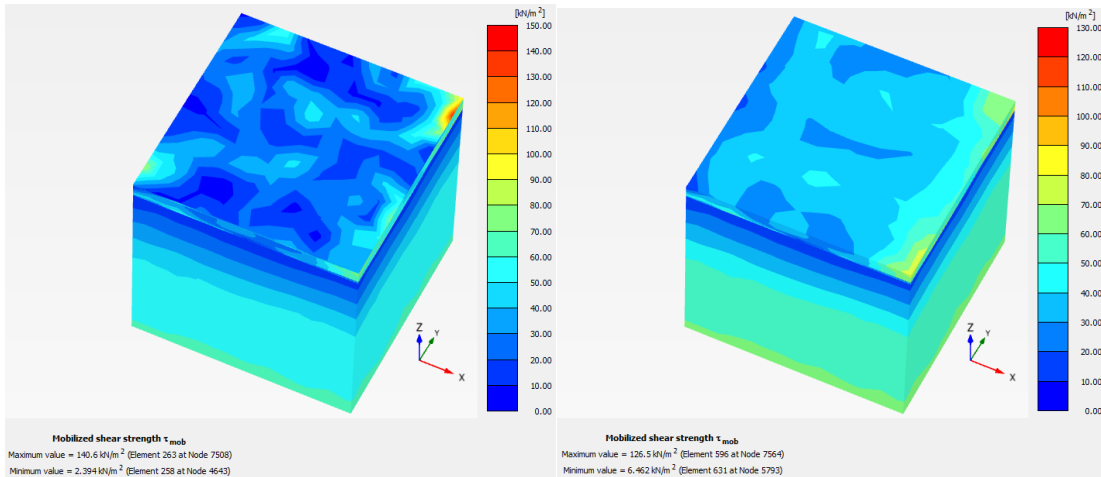
(a) unreinforced soil

(b) soil reinforced with coir mat



(c) at top coir-polymer interface

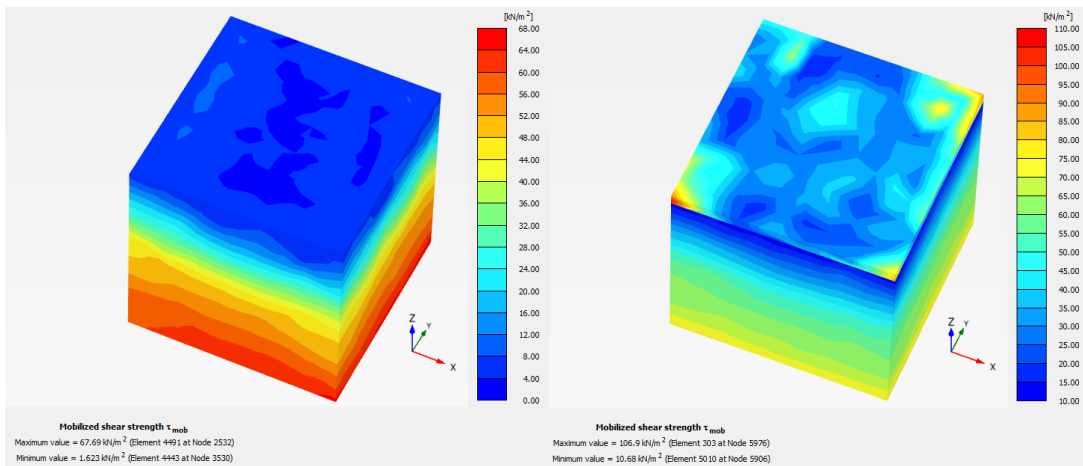
(d) at bottom coir-polymer interface



(e) at top coir-rubber interface

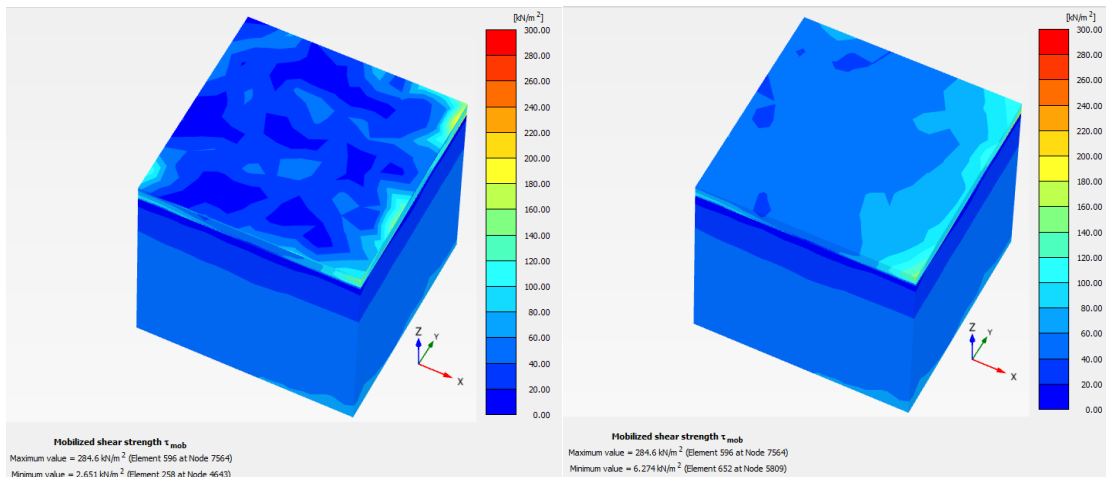
(f) at bottom coir-rubber interface

Figure 7.10 Mobilised shear strength in the soil at its central portion below the superstructure excited under EQ-3 input motion



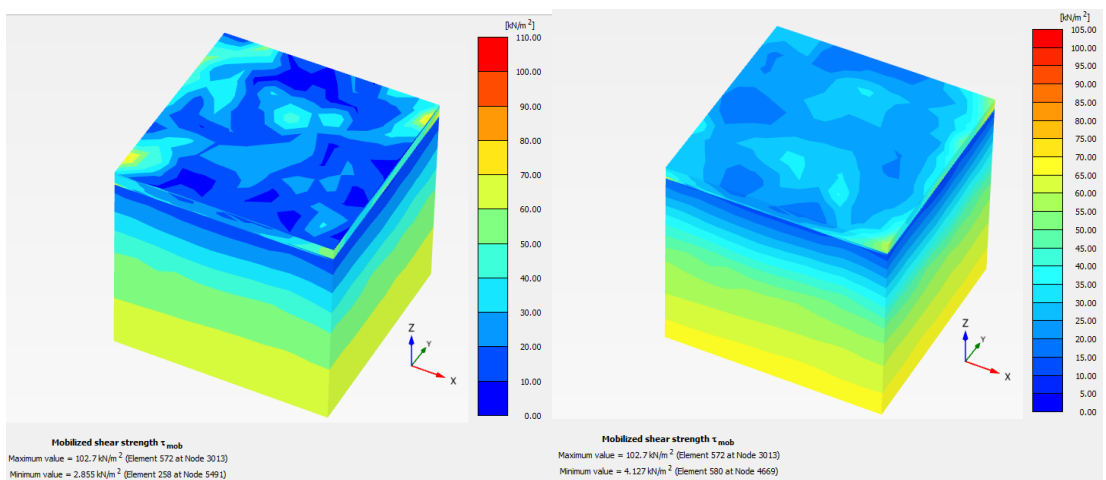
(a) unreinforced soil

(b) soil reinforced with coir mat



(c) at top coir-polymer interface

(d) at bottom coir-polymer interface



(e) at top coir-rubber interface

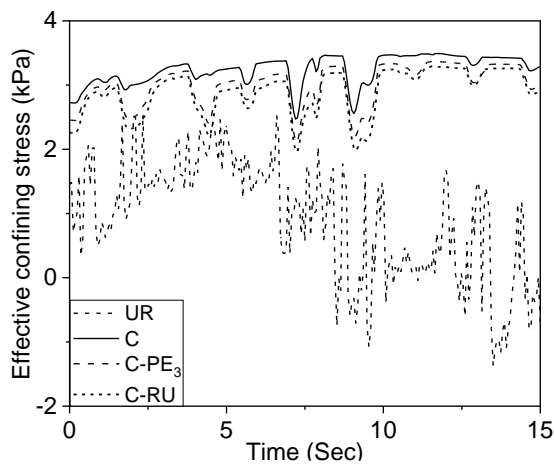
(f) at bottom coir-rubber interface

Figure 7.11 Mobilized shear strength in the soil at its central portion below the superstructure excited under EQ-4 input motion

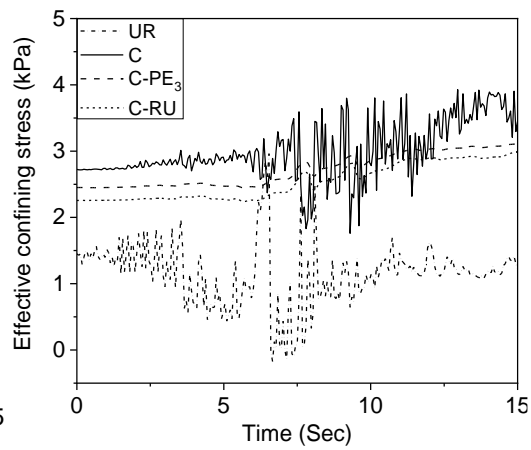
7.3.3 Effective Confining Stress

The inclusion of a basal reinforcement mat adds confining stress to the reinforced soil system and foundation. This increases the bearing capacity in traditional soft foundation soil while reducing the plastic failure zone, resulting in a more stable platform. Coir mat considerably improved the effective stress in soil (Fig. 7.12). The effective stress is observed to be decreasing with the increase in the duration of

earthquakes for unreinforced soil cases. But, for reinforced soil, effective confining stress increases with the time of the earthquake and becomes constant after a particular time. An increase in effective stress makes the supporting soil for the superstructure strong, so liquefaction reduces in the soil. In a previous study, it is observed that the stress in the fiber-reinforced soil increased rapidly as the load increases, and the confining pressure had a significant effect on the strength of the fiber-reinforced soil (Zhao et al. 2020). That is, the greater the confining pressure, the greater the reinforcement effect.



(a)



(b)

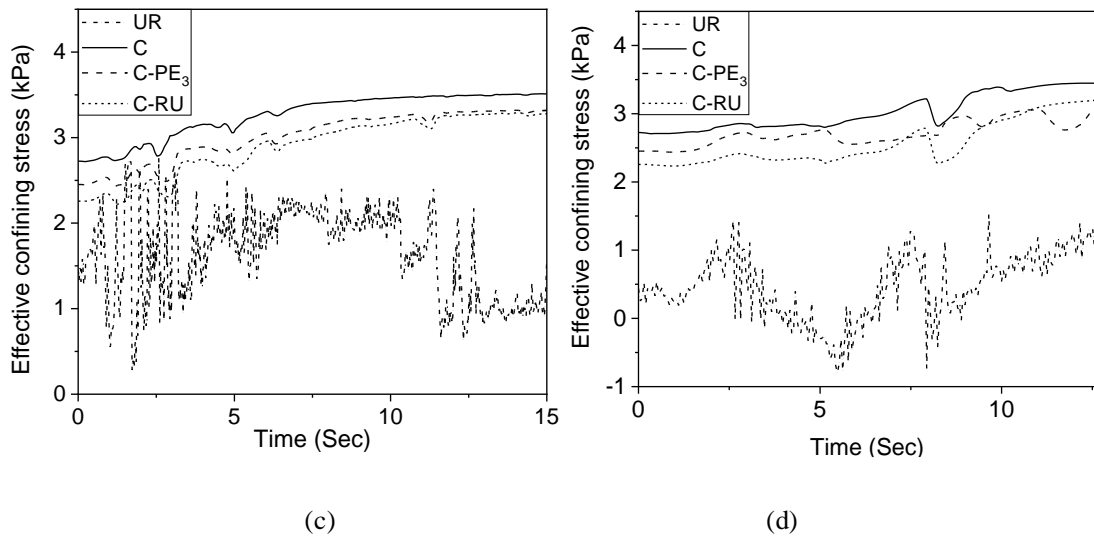


Figure 7.12 Effective confining stress time history in the soil for reinforced and unreinforced cases under; (a) EQ-1, (b) EQ-2, (c) EQ-3, (d) EQ-4

7.4 SUMMARY

The isolation efficiency of reinforcement materials, C, C-PE₃, and C-RU mats to reduce the excess pore water pressure under different earthquake motions obtained are 75-82%, 71-80%, and 67-72% respectively. Coir-polymer shows much more isolation efficiency in reducing the P_{excess} compared to coir-rubber. The P_{excess} increased with the increase in depth of soil below the foundation. The resulting shear strain for soil reinforced by isolation mats is lower than that obtained from unreinforced soil since the isolation mats strengthen the soil. The shear strength and effective stress of the soil reinforced with coir and coir composites are improved compared to the unreinforced soil. The reduction in roof acceleration and raft acceleration of building resting on soil reinforced with coir mat excited under EQ-1, EQ-2, EQ-3, and EQ-4 earthquake motions respectively are obtained as 62%, 51%, 53%, 62%; 54%, 48.5%, 47.23%, 33%. Seismic responses such as excess pore water pressure, shear strain, shear strength, and effective stress in soil and roof acceleration in the building are observed to be increased with an increase in specific energy density of earthquake motion considered (Table 3.5). But as a conflict to this conclusion, the seismic responses under El Centro input motion (specific energy density = 0.18m²/s) show higher seismic responses than that under

Northridge earthquake motion (specific energy density = $0.211\text{m}^2/\text{s}$). This may be due to the abundant frequency content available in the El Centro earthquake data which matches with the natural frequency of soil-structure system causing maximum resonance response.

Chapter 8

CONCLUSION

Detailed numerical investigations have been carried out to study the effects of seismic isolation of sustainable materials on the dynamic response of low-rise RC buildings. The major conclusions are summarized below:

- From parametric analysis of coir mat isolated soil-structure system, the optimum values of width, depth of embedment and thickness of coir mat were identified as B, B/18 and B/36 based on the width of foundation, B.
- As soil flexibility increases, seismic responses increase gradually. The isolation efficiency of reinforcement materials in effectively reducing the seismic responses is more when the materials are placed on soft soil as compared with those reinforced in stiff soil.
- Reinforcing soft soil with C-PE₂ and PE₂ mats show a maximum reduction in the building roof acceleration and base shear (i.e. 22% and 23% respectively). The coir mat causes the maximum reduction in building roof acceleration, roof deflection and inter-storey drift under El Centro input motions (i.e. 34%, 32% and 50% respectively). Seismic base shear was best reduced (24%) in soft soil by reinforcing soil with coir and C-PE₂ mats.
- The reinforcement of soil with C-PE₃ mat causes a maximum of 93% reduction in excess pore water pressure under El Centro input motion and it is 88% under Northridge motion from the one dimensional analysis. The isolation efficiency of reinforcement materials, C, C-PE₃ and C-RU mats to reduce the excess pore water pressure under different earthquake motions are 75-82%, 71-80%, and 67-72% respectively from the three dimensional pore water pressure analysis.
- The seismic isolation systems considered here has an advantage of lightweight and compressible properties of polymer foam to reduce the induced seismic responses in soil and superstructures from the earthquake loading. The durability of the isolation material is a factor to be considered while selecting the proper

material. Polymer foam has a good lifespan. Chemically, polystyrene foam is a very stable compound, and no material decay should be expected when it is placed in the ground.

It is inferred from the study that coir and its composites can act as good isolation material, especially in soft soil. The coir mat composited with other materials can effectively improve the durability of the coir mat by protecting it from biodegradation and can also act as a suitable drainage medium. The use of the coir material as an isolation medium in the soil will be economically feasible as coir is a readily available natural material than standard isolation materials. From the detailed transient analysis of integrated soil-structure system with various isolation materials, coir mat and coir-polymer foam composite mat are recommended as the efficient soil isolation medium, especially at soft soil sites.

PUBLICATIONS

JOURNALS

1. Sreya M V., B R Jayalekshmi., and Katta Venkataramana (2021). “Effect of Coir Reinforced Soil on the Seismic Response of RC framed Buildings”, *Indian Geotechnical Journal*. doi :10.1007/s40098-021-00593-w.
2. Sreya M V., B R Jayalekshmi., and Katta Venkataramana (2021). “Seismic Response of Buildings Resting on Soil Isolated with EPS Geofoam Buffer”, *International Journal of Geotechnical Earthquake Engineering* doi: 10.4018/IJGEE.298987.
3. Sreya M V., B R Jayalekshmi., and Katta Venkataramana (2021). “Pore Water Pressure Analysis in Coir Mat-Reinforced Soil Incorporating Soil-Structure Interaction”, *International Journal of Geosynthetics and Ground Engineering* doi: 10.1007/s40891-022-00354-6.
4. Sreya M V., B R Jayalekshmi., and Katta Venkataramana. “Seismic Response Analysis of RC Framed Buildings on Geo-Reinforced Soil”, *Innovative infrastructure solutions* (Under review).
5. Sreya M V., B R Jayalekshmi., and Katta Venkataramana. "Dynamic Response Analysis of Geo-Reinforced Soil-Structure System", *Earthquake Engineering and engineering Vibration* (Under review).

CONFERENCE PROCEEDINGS

1. Sreya, M. V., Jayalekshmi, B. R., and Venkataramana, K. (2021, March). A Study on Seismic Response of Buildings on Coir Mat Reinforced Sand Bed. *In IOP Conference Series: Materials Science and Engineering* (Vol. 1114, No. 1, p. 012018) doi:10.1088/1757-899X/1114/1/012018. IOP Publishing.
2. Sreya M V., B R Jayalekshmi., and Katta Venkataramana (2021), "Seismic Response of Buildings Resting on Raft Foundation with EPS Geofoam Buffer", *7th International Conference on Recent Advances in Geotechnical Earthquake Engineering and Soil Dynamics (7ICRAGEE)*, July 12-15, 2021, IISc Bangalore, India. doi.org/10.1007/978-981-33-4001-5.
3. Sreya, M. V., Jayalekshmi, B. R., and Venkataramana, K. (2023). “Seismic Response of Buildings Resting on Geosynthetics Reinforced Sand Bed”. In *International Conference on Advances in Structural Mechanics and Applications*. Springer, Cham. NIT Silchar (Full paper accepted).
4. Sreya M V., B R Jayalekshmi., and Katta Venkataramana. (2019), "A review of experimental studies on geosynthetic reinforced pile supported railway embankments", *Proceedings of the 8th International Engineering Symposium*

- *IES* 2019, March 13-15, 2019, Kumamoto University, Japan, pp. C6-6-1.

REFERENCES

- Aab R, Bartlett SF, Du M, et al (2019) 5th International Conference on Geofoam Blocks in Construction Applications
- Abu-Hejleh N, Wang T, Zornberg JG (2000) Performance of geosynthetic-reinforced walls supporting bridge and approaching roadway structures. Proc Sess Geo-Denver 2000 - Adv Transp Geoenvironmental Syst Using Geosynth GSP 103 291:218–243. [https://doi.org/10.1061/40515\(291\)15](https://doi.org/10.1061/40515(291)15)
- Ali M (2010) Coconut fibre - A versatile material and its applications in engineering. 2nd Int Conf Sustain Constr Mater Technol 1441–1454
- ASTM D6817 / D6817M-17 (2017) Standard Specification for Rigid Cellular Polystyrene Geofoam. ASTM Int 1–8. <https://doi.org/10.1520/D6817>
- ASTM D7180 Expanded Polystyrene Geofoam Applications & Technical Data
Geofoam Applications & Technical Data
- Babu K K (2007) Utilisation of Coir Geotextiles for UnpaVed Roads and Embankments. Thesis Work CUSAT
- Bajaj K, Chavda J, Vyas BM (2013) Seismic Behaviour of Buildings on Different Types of. 1–6
- Bhavikatti Q, Cholekar SB (2017) Soil structure interaction effect for a building resting on sloping ground including infill subjected to seismic analysis . Int Res J Eng Technol 4:1547–1551
- Bledzki AK, Gassan J (1999) Composites reinforced with cellulose_Bledzki_1999.pdf. Prog Polym Sci 24:221–274
- Bolarinwa O WA (2008) Mechanical Property Evaluation of Coconut Fibre. BioResources 7:923–932

- Boominathan A, Hari. S (2002) Liquefaction strength of fly ash reinforced with randomly distributed fibers. *Soil Dyn Earthq Eng* 22:1027–1033. [https://doi.org/10.1016/S0267-7261\(02\)00127-6](https://doi.org/10.1016/S0267-7261(02)00127-6)
- Choudhary AK, Jha JN, Gill KS (2010) a Study on Cbr Behavior of Waste Plastic Strip Reinforced Soil. *Emirates J Eng Res* 15:51–57
- D5321 A (2019) Geosynthetic Interface Shear Testing. 1–59
- Dash SK, Krishnaswamy NR, Rajagopal K (2001) Bearing capacity of strip footings supported on. *Geotext Geomembranes* 19:235–256
- Dash SK, Rajagopal K, Krishnaswamy NR (2004) Performance of different geosynthetic reinforcement materials in sand foundations. *Geosynth Int* 11:35–42. <https://doi.org/10.1680/gein.2004.11.1.35>
- Dicker MPM, Duckworth PF, Baker AB, et al (2014) Green composites: A review of material attributes and complementary applications. *Compos Part A Appl Sci Manuf* 56:280–289. <https://doi.org/10.1016/j.compositesa.2013.10.014>
- Duškov M (1997) Measurements on a flexible pavement structure with an EPS geofoam sub-base. *Geotext Geomembranes* 15:5–27. [https://doi.org/10.1016/s0266-1144\(97\)00004-6](https://doi.org/10.1016/s0266-1144(97)00004-6)
- Elif Orakoglu M, Liu J, Niu F (2017) Dynamic behavior of fiber-reinforced soil under freeze-thaw cycles. *Soil Dyn Earthq Eng* 101:269–284. <https://doi.org/10.1016/j.soildyn.2017.07.022>
- Elragi AF (2006) Selected Engineering Properties and Applications of EPS Geofoam. *State Univ New York Coll Environ Sci For* 39
- Fardad Amini P, Noorzad R (2018) Energy-based evaluation of liquefaction of fiber-reinforced sand using cyclic triaxial testing. *Soil Dyn Earthq Eng* 104:45–53. <https://doi.org/10.1016/j.soildyn.2017.09.026>
- Fema 274-1997 NEHRP Commentary on the Guidelines for the Seismic Rehabilitation

of Buildings. Fed Emerg Manag Agency, Washington, DC, Dev by Appl Technol Counc

Fischer-Cripps AC (2004) Materials data. Phys Companion. <https://doi.org/10.1887/0750309539/b1258b1>

Ge C, Rice B (2018) Impact damping ratio of a nonlinear viscoelastic foam. *Polym Test* 72:187–195. <https://doi.org/10.1016/j.polymertesting.2018.10.023>

Ghavami K, Toledo Filho RD, Barbosa NP (1999) Behaviour of composite soil reinforced with natural fibres. *Cem Concr Compos* 21:39–48. [https://doi.org/10.1016/S0958-9465\(98\)00033-X](https://doi.org/10.1016/S0958-9465(98)00033-X)

Guido VA, Chang DK, Sweeney MA (1986) Comparison of Geogrid and Geotextile Reinforced Earth Slabs. *Can Geotech J* 23:435–440. <https://doi.org/10.1139/t86-073>

Guler E, Enunlu AK (2009) Investigation of dynamic behavior of geosynthetic reinforced soil retaining structures under earthquake loads. *Bull Earthq Eng* 7:737–777. <https://doi.org/10.1007/s10518-009-9106-9>

Haque MM, Ali ME, Hasan M, et al (2012) Chemical treatment of coir fiber reinforced polypropylene composites. *Ind Eng Chem Res* 51:3958–3965. <https://doi.org/10.1021/ie200693v>

Hejazi SM, Sheikhzadeh M, Abtahi SM, Zadhoush A (2012) A simple review of soil reinforcement by using natural and synthetic fibers. *Constr Build Mater* 30:100–116. <https://doi.org/10.1016/j.conbuildmat.2011.11.045>

Ho TH (2011) Geotechnical seismic isolation. *Earthq Eng New Res* 55–87

Horvath JS (2008a) Extended Veletsos-Younan Model for Geofoam Compressible Inclusions behind Rigid, Non-Yielding Earth-Retaining Structures. 1–10. [https://doi.org/10.1061/40975\(318\)151](https://doi.org/10.1061/40975(318)151)

Horvath JS (2008b) Seismic Lateral Earth Pressure Reduction on Earth-Retaining

Structures Using Geofoams. 1–10. [https://doi.org/10.1061/40975\(318\)155](https://doi.org/10.1061/40975(318)155)

Hughes DW (1987) Finite-amplitude solutions for interchange instabilities driven by magnetic buoyancy

Indraratna B, Ionescu D, Christie HD (1998) Shear Behavior of Railway Ballast Based on Large-Scale Triaxial Tests. *J Geotech Geoenvironmental Eng* 124:439–449. [https://doi.org/10.1061/\(asce\)1090-0241\(1998\)124:5\(439\)](https://doi.org/10.1061/(asce)1090-0241(1998)124:5(439))

Indraratna B, Qi Y, Ngo TN, et al (2019) Use of geogrids and recycled rubber in railroad infrastructure for enhanced performance. *Geosci* 9:. <https://doi.org/10.3390/geosciences9010030>

IS 13920: (1993) Ductile Detailing of Reinforced Concrete Structures Subjected To Seismic Forces -Code of Practice. Bur Indian Stand New Delhi 13920:1–16

IS 456: (2000) IS 456:2000 Indian Standard Plain and Reinforced Concrete - Code of Practice. Bur Indian Stand New Delhi, India New Delhi,India

Jutkofsky WS, Teh Sung J, Negussey D (2000) Stabilization of embankment slope with geofoam. *Transp Res Rec* 94–102. <https://doi.org/10.3141/1736-12>

Karakan E, Eskişar T, Altun S (2018) The liquefaction behavior of poorly graded sands reinforced with fibers. *Adv Civ Eng* 2018:.. <https://doi.org/10.1155/2018/4738628>

Keramatikerman M, Chegenizadeh A, Nikraz H (2017) Experimental study on effect of fly ash on liquefaction resistance of sand. *Soil Dyn Earthq Eng* 93:1–6. <https://doi.org/10.1016/j.soildyn.2016.11.012>

Kolathayar S (2019) Vibration Isolation of Foundation Using Hdpe and Natural Geocells - A Review : Proceedings of the 2nd GeoMEast International Congress and Exhibition on Sustainable Civil Infrastruct ... Vibration Isolation of Foundation Using Hdpe and Natural Geocells - A. Springer International Publishing

Kou Y, Shukla SK (2019) Analytical Investigation of Load Over Pipe Covered with

- Geosynthetic-Reinforced Sandy Soil. *Int J Geosynth Gr Eng* 5:0.
<https://doi.org/10.1007/s40891-019-0156-z>
- Kumar A, Gupta D (2016) Behavior of cement-stabilized fiber-reinforced pond ash, rice husk ash-soil mixtures. *Geotext Geomembranes* 44:466–474.
<https://doi.org/10.1016/j.geotexmem.2015.07.010>
- Leng W, Xiao Y, Nie R, et al (2017) Investigating Strength and Deformation Characteristics of Heavy-Haul Railway Embankment Materials Using Large-Scale Undrained Cyclic Triaxial Tests. *Int J Geomech* 17:04017074.
[https://doi.org/10.1061/\(asce\)gm.1943-5622.0000956](https://doi.org/10.1061/(asce)gm.1943-5622.0000956)
- Maheshwari BK, Singh HP, Saran S (2012) Effects of Reinforcement on Liquefaction Resistance of Solani Sand. *J Geotech Geoenvironmental Eng* 138:831–840.
[https://doi.org/10.1061/\(asce\)gt.1943-5606.0000645](https://doi.org/10.1061/(asce)gt.1943-5606.0000645)
- Majumder M, Ghosh P (2015) Finite element analysis of vibration screening techniques using EPS geofoam. *Comput Methods Recent Adv Geomech - Proc 14th Int Conf Int Assoc Comput Methods Recent Adv Geomech IACMAG 2014* 649–654.
<https://doi.org/10.1201/b17435-112>
- Majumder M, Ghosh P (2016) Intermittent geofoam in-filled trench for vibration screening considering soil non-linearity. *KSCE J Civ Eng* 20:2308–2318.
<https://doi.org/10.1007/s12205-015-0267-6>
- Makris N, Chang SP (2000) Effect of viscous, viscoplastic and friction damping on the response of seismic isolated structures. *Earthq Eng Struct Dyn* 29:85–107.
[https://doi.org/10.1002/\(SICI\)1096-9845\(200001\)29:1<85::AID-EQE902>3.0.CO;2-N](https://doi.org/10.1002/(SICI)1096-9845(200001)29:1<85::AID-EQE902>3.0.CO;2-N)
- Martin, P P; Seed HB (1982) *Rock and Soil Improvement Techniques*. 836288
- Meguid MA, Khan MI (2019) On the role of geofoam density on the interface shear behavior of composite geosystems. *Int J Geo-Engineering* 10:12–22.
<https://doi.org/10.1186/s40703-019-0103-9>

- Moghaddas Tafreshi SN, Ghotbi Siabil SMA, Azizian M (2021) EPS Geofom Pavement Foundations Overlaid by Geocell-Reinforced Soil under Static Loading: Large-Scale Tests and Numerical Modeling. *J Mater Civ Eng* 33:04021014. [https://doi.org/10.1061/\(asce\)mt.1943-5533.0003615](https://doi.org/10.1061/(asce)mt.1943-5533.0003615)
- Munirah Abdullah N, Ahmad I (2012) Effect of Chemical Treatment on Mechanical and Water-Sorption Properties Coconut Fiber-Unsaturated Polyester from Recycled PET. *ISRN Mater Sci* 2012:1–8. <https://doi.org/10.5402/2012/134683>
- Nanda RP, Agarwal P, Shrikhande M (2012) Base isolation by geosynthetic for brick masonry buildings. *JVC/Journal Vib Control* 18:903–910. <https://doi.org/10.1177/1077546311412411>
- Nanda RP, Dutta S, Das A, Khan HA (2017) Geosynthetic Liner as Foundation Isolation for Seismic Protection. *Int J Geosynth Gr Eng* 3:0. <https://doi.org/10.1007/s40891-017-0098-2>
- Narjabadifam P, Chavoshi M (2018) Modern Aseismic Applications of Geosynthetic Materials. *Int J Sci Eng Appl* 7:034–038. <https://doi.org/10.7753/ijsea0703.1002>
- Navaratnarajah SK, Indraratna B (2017) Use of Rubber Mats to Improve the Deformation and Degradation Behavior of Rail Ballast under Cyclic Loading. *J Geotech Geoenvironmental Eng* 143:04017015. [https://doi.org/10.1061/\(asce\)gt.1943-5606.0001669](https://doi.org/10.1061/(asce)gt.1943-5606.0001669)
- Negusseyo D (2008) Design parameters for EPS geofom. *Soils Found* 48:861. <https://doi.org/10.3208/sandf.48.861>
- Nguyen TT, Indraratna B (2017) The permeability of natural fibre drains, capturing their micro-features. *Proc Inst Civ Eng Gr Improv* 170:123–136. <https://doi.org/10.1680/jgrim.16.00032>
- Nimbalkar S, Indraratna B (2016) Improved Performance of Ballasted Rail Track Using Geosynthetics and Rubber Shockmat. *J Geotech Geoenvironmental Eng* 142:04016031. [https://doi.org/10.1061/\(asce\)gt.1943-5606.0001491](https://doi.org/10.1061/(asce)gt.1943-5606.0001491)

- Orman HDPEBME (1994) Interface Shear Strength Properties of Roughened HDPE. 120:758–761
- Patil, Reddy G (2012) State Of Art Review - Base isolation systems for structures. *Int J Emerg Technol Adv Eng* 2:438–453
- Perdana M, Jamasri J (2016) Effect of Moisture Content and Dynamic Loading Cyclic On Stiffness of Fiberglass and Coir Fiber-Based Hybrid Composit. 27–31. <https://doi.org/10.21063/ictis.2016.1005>
- Pincus H, Edil T, Bosscher P (1994) Engineering Properties of Tire Chips and Soil Mixtures. *Geotech Test J* 17:453. <https://doi.org/10.1520/gtj10306j>
- Piva P, Bauman P, von Kármán T, et al (2014) Federal Guidelines for Dam Safety. *Soil Dyn Earthq Eng* 2:1–10
- Ramakrishna G, Sundararajan T (2005) Impact strength of a few natural fibre reinforced cement mortar slabs: A comparative study. *Cem Concr Compos* 27:547–553. <https://doi.org/10.1016/j.cemconcomp.2004.09.006>
- Rocco NT, Luna R, Stephenson R, Rogers JD (2012) Characterization of Expanded Polystyrene (EPS) Presented to the Faculty of the Graduate School of the In Partial Fulfillment of the Requirements for the Degree
- SaadEldin M, El-Helloty A (2014) Effect of Opening on Behavior of Raft Foundations Resting On Different Types of Sand Soil. *Int J Comput Appl* 94:34–40. <https://doi.org/10.5120/16358-5744>
- Samia Sultana Mir, Mahbub Hasan, Syed M.N. Hasan, Md. Jahangir Hossain NN (2008) Flame-Retardancy Properties of Intumescent Ammonium Poly(Phosphate) and Mineral Filler Magnesium Hydroxide in Combination with Graphene. *Polym Polym Compos* 16:101–113. <https://doi.org/10.1002/pc>
- Santoni BRL, Tingle JS, Members A, Webster SL (2001) for Road Construction. 127:258–268

- Seed HB (1987) Design problems in soil liquefaction. *J Geotech Eng* 113:827–845. [https://doi.org/10.1061/\(ASCE\)0733-9410\(1987\)113:8\(827\)](https://doi.org/10.1061/(ASCE)0733-9410(1987)113:8(827))
- Shao W, Cetin B, Li Y, et al (2014) Experimental Investigation of Mechanical Properties of Sands Reinforced with Discrete Randomly Distributed Fiber. *Geotech Geol Eng* 32:901–910. <https://doi.org/10.1007/s10706-014-9766-3>
- Sharma N, Dasgupta K, Dey A (2018) A state-of-the-art review on seismic SSI studies on building structures. *Innov Infrastruct Solut* 3:. <https://doi.org/10.1007/s41062-017-0118-z>
- Shihada S, Hamad J, Alshorafa M (2012) Suggested Modifications of the Conventional Rigid Method for Mat Foundation Design. 2:418–428
- Solomon A, Latha H, Solomon AA, Hemalatha G (2017) Article ID: IJCIET_08_01_022 Cite this Article: A. Arun Solomon and G. Hemalatha. Inspection of Properties of Expanded Polystyrene (EPS), Compressive Behaviour, Bond and Analytical Examination of Insulated Concrete Form (ICF) Blocks Using Different Densit. *Int J Civ Eng Technol* 8:209–221
- Srilatha N, Latha GM, Puttappa CG (2016) Seismic Response of Soil Slopes in Shaking Table Tests: Effect of Type and Quantity of Reinforcement. *Int J Geosynth Gr Eng* 2:1–13. <https://doi.org/10.1007/s40891-016-0074-2>
- Su L, Zhou L, Liu X, et al (2021) Numerical investigation for liquefaction mitigation of saturated sand stratum reinforced by fiber. 2021 7th International Conference on Hydraulic and Civil Engineering and Smart Water Conservancy and Intelligent Disaster Reduction Forum, ICHCE SWIDR 2021 440–446. <https://doi.org/10.1109/ICHCESWIDR54323.2021.9656361>
- Systra AS, Singh Y, Sarkar A, Ahmad A (2016) Seismic Design of Expanded Polystyrene Core Panel Based Building Systems Seismic Strengthening with FRP and Wire Mesh View project Slope Building Interaction View project Seismic Design of Expanded Polystyrene Core Panel Based Building Systems

- Tafreshi SNM, Dawson AR (2010) Behaviour of footings on reinforced sand subjected to repeated loading - Comparing use of 3D and planar geotextile. *Geotext Geomembranes* 28:434–447. <https://doi.org/10.1016/j.geotexmem.2009.12.007>
- Talamkhani S, Naeini SA (2021) The Undrained Shear Behavior of Reinforced Clayey Sand. *Geotech Geol Eng* 39:265–283. <https://doi.org/10.1007/s10706-020-01490-4>
- Tatlisoiz N, Edil TB, Benson CH (1998) Interaction between Reinforcing Geosynthetics and Soil-Tire Chip Mixtures. *J Geotech Geoenvironmental Eng* 124:1109–1119. [https://doi.org/10.1061/\(asce\)1090-0241\(1998\)124:11\(1109\)](https://doi.org/10.1061/(asce)1090-0241(1998)124:11(1109))
- Thomas S (2014) Vibration and sound damping in polymers. *Resonance* 19:821–833. <https://doi.org/10.1007/s12045-014-0091-1>
- Tsang HH (2011) Geotechnical seismic isolation. *Earthq Eng New Res* 55–87
- Tsang HH (2007) Seismic isolation for low-to-medium-rise buildings using granulated rubber–soil mixtures: numerical study Hing-Ho. *Pacific Conf Earthq Eng* 1–6. <https://doi.org/10.1002/eqe>
- Vinod P, Bhaskar AB, Sreehari S (2009) Behaviour of a square model footing on loose sand reinforced with braided coir rope. *Geotext Geomembranes* 27:464–474. <https://doi.org/10.1016/j.geotexmem.2009.08.001>
- Wang S, Hao H (2002) Effects of random variations of soil properties on site amplification of seismic ground motions. *Soil Dyn Earthq Eng* 22:551–564. [https://doi.org/10.1016/S0267-7261\(02\)00038-6](https://doi.org/10.1016/S0267-7261(02)00038-6)
- Wolf JP, Song C (2002) Some cornerstones of dynamic soil-structure interaction. *Eng Struct* 24:13–28. [https://doi.org/10.1016/S0141-0296\(01\)00082-7](https://doi.org/10.1016/S0141-0296(01)00082-7)
- Yang KH, Nguyen MD, Yalaw WM, et al (2016) Behavior of geotextile-reinforced clay in consolidated-undrained tests: Reinterpretation of porewater pressure parameters. *J Geoenviron* 11:45–57. [https://doi.org/10.6310/jog.2016.11\(2\).1](https://doi.org/10.6310/jog.2016.11(2).1)

- Yegian MK, Catan M (2004) Soil Isolation for Seismic Protection Using a Smooth Synthetic Liner. *J Geotech Geoenvironmental Eng* 130:1131–1139. [https://doi.org/10.1061/\(asce\)1090-0241\(2004\)130:11\(1131\)](https://doi.org/10.1061/(asce)1090-0241(2004)130:11(1131))
- Yegian MK, Kadakal U (2004) Foundation isolation for seismic protection using a smooth synthetic liner. *J Geotech Geoenvironmental Eng* 130:1121–1130. [https://doi.org/10.1061/\(ASCE\)1090-0241\(2004\)130:11\(1121\)](https://doi.org/10.1061/(ASCE)1090-0241(2004)130:11(1121))
- Yegian MK, Lahlaf AM (1994) Dynamic interface shear strength properties of geomembranes and geotextiles. *J Geotech Eng* 120:465. [https://doi.org/10.1061/\(ASCE\)0733-9410\(1994\)120:2\(465\)](https://doi.org/10.1061/(ASCE)0733-9410(1994)120:2(465))
- Yegian MK, Yee ZY, Harb JN (1995) Response of Geosynthetics Under Earthquake Excitations. *Geosynth.* 1995 677–689
- Zarnani S, Bathurst RJ (2005) Numerical investigation of geofoam seismic buffers using FLAC. *Proc North Am Geosynth Soc (NAGS)/GRI19 Conf Las Vegas, Nev* 14–16
- Zhao Y, Ling X, Gong W, et al (2020) Mechanical properties of fiber-reinforced soil under triaxial compression and parameter determination based on the duncan-chang model. *Appl Sci* 10:1–16. <https://doi.org/10.3390/app10249043>
- Ziaie Moayed R, Alibolandi M (2018) Effect of geotextile reinforcement on cyclic undrained behavior of sand. *Soil Dyn Earthq Eng* 104:395–402. <https://doi.org/10.1016/j.soildyn.2017.11.013>
- Zwawi M (2021) A review on natural fiber bio-composites, surface modifications and applications. *Molecules* 26:. <https://doi.org/10.3390/molecules26020404>